VOLUME 33 | SUPPLEMENT 2 | MARCH 2020

MODERN PATHOLOGY

ABSTRACTS

BONE AND SOFT TISSUE PATHOLOGY (37-109)

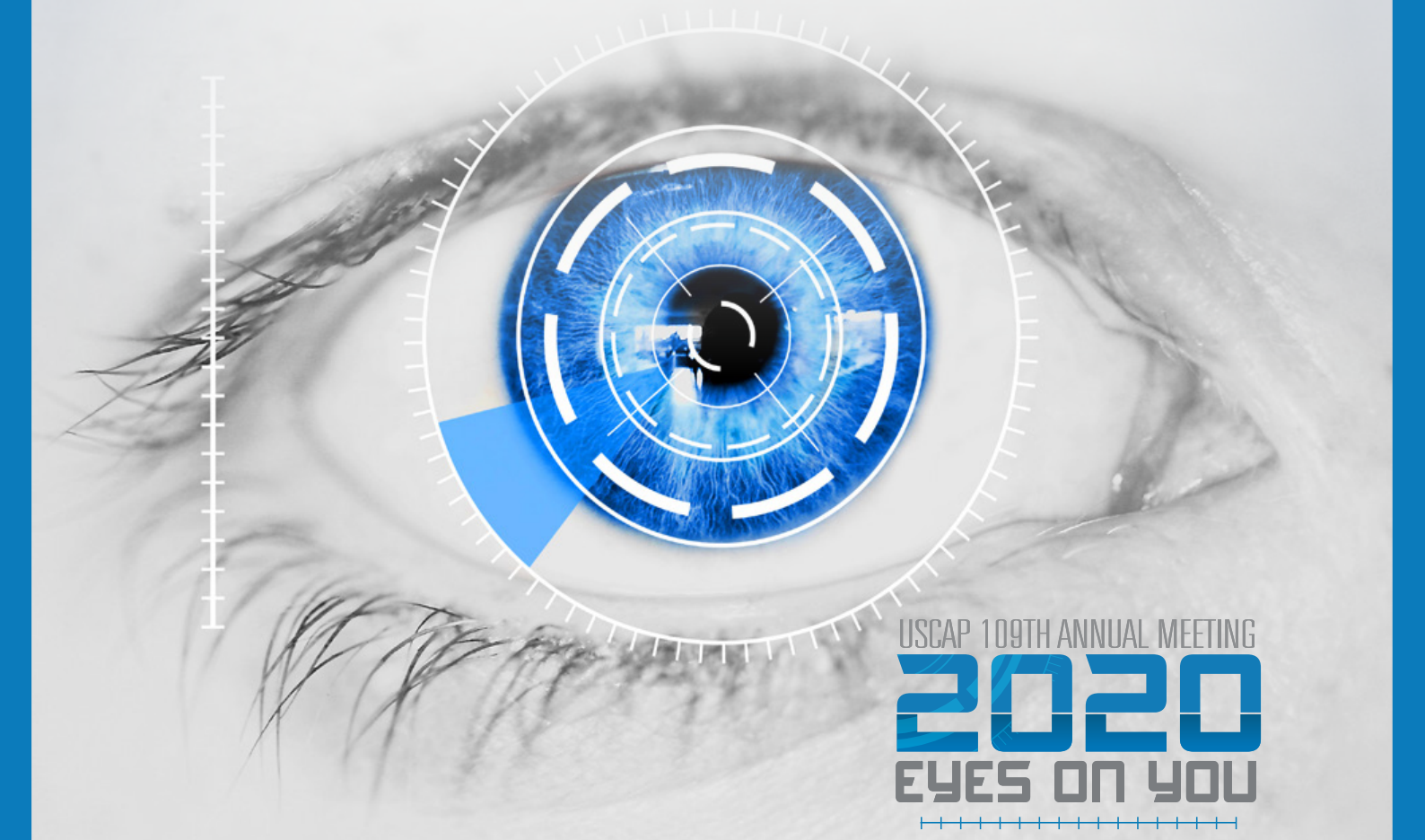

FEBRUARY 29-MARCH 5, 2020

LOS ANGELES CONVENTION CENTER
LOS ANGELES, CALIFORNIA

Published by
SPRINGER NATURE
www.ModernPathology.org

USCAP Creating a Better Pathologist
AN OFFICIAL JOURNAL OF THE UNITED STATES AND CANADIAN ACADEMY OF PATHOLOGY

EDUCATION COMMITTEE

Jason L. Hornick, Chair

Rhonda K. Yantiss, Chair, Abstract Review Board and Assignment Committee

Laura W. Lamps, Chair, CME Subcommittee

Steven D. Billings, Interactive Microscopy Subcommittee

Raja R. Seethala, Short Course Coordinator

Ilan Weinreb, Subcommittee for Unique Live Course Offerings

David B. Kaminsky (Ex-Officio)

Zubair Baloch
Daniel Brat
Ashley M. Cimino-Mathews
James R. Cook
Sarah Dry
William C. Faquin
Yuri Fedoriw
Karen Fritchie
Lakshmi Priya Kunju
Anna Marie Mulligan
Rish K. Pai
David Papke, Pathologist-in-Training
Vinita Parkash
Carlos Parra-Herran
Anil V. Parwani
Rajiv M. Patel
Deepa T. Patil
Lynette M. Sholl
Nicholas A. Zoumberos, Pathologist-in-Training

ABSTRACT REVIEW BOARD

Benjamin Adam
Narasimhan Agaram
Rouba Ali-Fehmi
Ghassan Allo
Isabel Alvarado-Cabrero
Catalina Amador
Roberto Barrios
Rohit Bhargava
Jennifer Boland
Alain Borczuk
Elena Brachtel
Marilyn Bui
Eric Burks
Shelley Caltharp
Barbara Centeno
Joanna Chan
Jennifer Chapman
Hui Chen
Beth Clark
James Conner
Alejandro Contreras
Claudiu Cotta
Jennifer Cotter
Sonika Dahiya
Farbod Darvishian
Jessica Davis
Heather Dawson
Elizabeth Demicco
Katie Dennis
Anand Dighe
Suzanne Dintzis
Michelle Downes
Andrew Evans
Michael Feely
Dennis Firchau
Gregory Fishbein
Andrew Folpe
Larissa Furtado
Billie Fyfe-Kirschner
Giovanna Giannico
Anthony Gill
Paula Ginter
Tamara Giorgadze
Purva Gopal
Anuradha Gopalan
Abha Goyal
Rondell Graham
Alejandro Gru
Nilesh Gupta
Mamta Gupta
Gillian Hale
Suntrea Hammer
Malini Harigopal
Douglas Hartman
John Higgins
Mai Hoang
Mojgan Hosseini
Aaron Huber
Peter Illei
Doina Ivan
Wei Jiang
Vickie Jo
Kirk Jones
Neerja Kambham
Chiah Sui Kao
Dipti Karamchandani
Darcy Kerr
Ashraf Khan
Francesca Khani
Rebecca King
Veronica Klepeis
Gregor Krings
Asangi Kumarapeli
Alvaro Laga
Steven Lagana
Keith Lai
Michael Lee
Cheng-Han Lee
Madelyn Lew
Zaibo Li
Faqian Li
Ying Li
Haiyan Liu
Xiuli Liu
Yen-Chun Liu
Lesley Lomo
Tamara Lotan
Anthony Magliocco
Kruti Maniar
Emily Mason
David McClintock
Bruce McManus
David Meredith
Anne Mills
Neda Moatamed
Sara Monaco
Atis Muehlenbachs
Bita Naini
Dianna Ng
Tony Ng
Michiya Nishino
Scott Owens
Jacqueline Parai
Yan Peng
Manju Prasad
Peter Pytel
Stephen Raab
Joseph Rabban
Stanley Radio
Emad Rakha
Preetha Ramalingam
Priya Rao
Robyn Reed
Michelle Reid
Natasha Rekhtman
Jordan Reynolds
Michael Rivera
Andres Roma
Avi Rosenberg
Esther Rossi
Peter Sadow
Steven Salvatore
Souzan Sanati
Anjali Saqi
Jeanne Shen
Jiaqi Shi
Gabriel Sica
Alexa Siddon
Deepika Sirohi
Kalliopi Siziopikou
Sara Szabo
Julie Teruya-Feldstein
Khin Thway
Rashmi Tondon
Jose Torrealba
Andrew Turk
Evi Vakiani
Christopher VandenBussche
Paul VanderLaan
Olga Weinberg
Sara Wobker
Shaofeng Yan
Anjana Yeldandi
Akihiko Yoshida
Gloria Young
Minghao Zhong
Yaolin Zhou
Hongfa Zhu
Debra Zynger

To cite abstracts in this publication, please use the following format: **Author A, Author B, Author C, et al. Abstract title (abs#). In "File Title."** ***Modern Pathology*** **2020; 33 (suppl 2): page#**

37 A Molecular Reappraisal of Glomus tumors (GT): A Study of 93 Cases with a Focus on NOTCH Gene Fusions

Narasimhan Agaram[1], Lei Zhang[1], Brendan Dickson[2], Cristina Antonescu[1]
[1]Memorial Sloan Kettering Cancer Center, New York, NY, [2]Mount Sinai Health System, Toronto, ON

Disclosures: Narasimhan Agaram: None; Lei Zhang: None; Brendan Dickson: None; Cristina Antonescu: None

Background: GT are neoplams of perivascular smooth muscle differentiation, sharing variable histologic overlap with myofibroma (MF), myopericytoma (MP) and angioleiomyoma (AL). Despite their morphologic similarities, the genetic abnormalities suggest a dichotomy of the perivascular myoid tumor family into 2 categories: *PDGFRB*-mutant MF and MP and *NOTCH*-fusion positive GT. The latter observation was never validated in a larger study, to investigate its prevalence and correlation with clinical features.

Design: 93 GT were selected after pathologic review and with available tissue for molecular studies. The tumors were also assessed for risk of malignancy based on current WHO criteria. All cases were tested by FISH method for *NOTCH 1/2/3* and *MIR143* gene abnormalities and 7 cases were also tested by targeted RNA sequencing. A control group of 41 other pericytic tumors (19 AL, 11 MP and 11 MF) were also investigated for these abnormalities.

Results: FISH analysis revealed *NOTCH* gene rearrangements in 50 (54%) cases. The *NOTCH*-rearranged subset included 34 (68%) benign and 16 (32%) malignant GT. In the benign group, GT were mostly in soft tissue, and showed *NOTCH2* gene rearrangements in 88%, fused to MIR143HG in 76% of cases. Rearrangements of *NOTCH3* in 3 cases (with *ACTB* in 2 and *MIR143HG* in 1) and *NOTCH1* in 1 case was seen. In the malignant group, GT were often located in the viscera (GI and lung, 67%) and showed *NOTCH2* rearrangements in all except 2 cases (88%), with co-existent *MIR143HG* fusions in 69%. The remaining 2 malignant GT showed *NOTCH1* gene fusions.

Among the fusion-negative GT, 88% were benign, 9% of uncertain malignant potential and 2% were malignant. The most common location was the finger/subungual region, occurring in half of the cases.

In the control group, 2 AL (11%) had *NOTCH2* rearrangements, while 2 MP (18%) showed evidence of *MIR143HG-NOTCH* fusions (one involving *NOTCH2* and the other *NOTCH4*).

Conclusions: Rearrangements of *NOTCH* genes are seen in > half of GT, with *MIR143HG-NOTCH2* being the most common fusion (73%). All except one malignant GT were positive for *NOTCH* fusions in contrast to only 47% of benign GT. Fusion-positive benign GT are overwhelmingly seen in males with a predilection for extremities, while the malignant GT occur mostly in visceral sites. Subungual GT lack *NOTCH* fusions, suggesting a different pathogenesis. Additional studies are required to investigate the genetic alterations in the fusion-negative cases. A small subset of AL and MP share the genetics of GT.

38 RANK Ligand (RANKL) Immunoexpression in Extra-Skeletal Osteoclast-Rich Malignant Solid Neoplasms: Analysis of 15 Cases with Clinicopathologic Features

Rana Ajabnoor[1], Qi Yang[2], Brendan Boyce[1]
[1]University of Rochester Medical Center, Rochester, NY, [2]Pittsford, NY

Disclosures: Rana Ajabnoor: None; Qi Yang: None; Brendan Boyce: None

Background: Expression of Receptor activator of NF-kB ligand (RANKL) by osteoblastic cells in bone is essential for osteoclast (OC) formation during skeletal development, and its expression by B and T cells drives OC formation in some pathologic conditions, including rheumatoid arthritis. RANKL also regulates OC formation in extraskeletal OC-rich benign lesions, including pigmented villonodular synovitis, but it is not known if it drives OC formation in extraskeletal malignant tumors. RANKL signaling through its receptor, RANK, also plays essential roles in lymph node and immune cell formation and mammary gland hyperplasia during pregnancy, and it positively regulates breast cancer formation and metastasis to bone. Inhibition of RANKL signaling has significant anti-tumor effects in pre-clinical and clinical studies, but whether anti-RANKL therapy should be administered as a treatment for solid tumors remains controversial. Given the importance of RANKL expression in tumor cell proliferation, there is a need for sensitive and specific tools to detect its expression in tumors. Here, we used IHC to determine if RANKL is expressed in extraskeletal OC-rich malignant solid tumors.

Design: 15 extraskeletal OC-rich malignant solid tumors, including 8 carcinomas and 7 sarcomas were identified from the pathology database in our institution between 2005 and 2018 (Table 1). The percent and intensity of cytoplasmic/membranous expression of RANKL were evaluated in tumor cells using IHC and a RANKL mAb (M366 clone; Amgen).

Results: 11 of 15 cases (73.3%) were RANKL-positive (Table 1); 5 of these had moderate-to-strong positivity in >50% of the tumor cells. 3 of these 5 were high-grade and 2 were intermediate grade. Two cases of high-grade urothelial carcinoma with sarcomatoid differentiation

were RANKL-positive only in the sarcomatoid component. RANKL was expressed by all 7 sarcomas (Figure 1) and by 4/8 carcinomas. 6 of the 11 cases (54.5%) were high-grade and advanced stage (III to IV).

Table-1:

Clinicopathological features of extra-skeletal osteoclast-rich malignant solid tumors:

No.	Location	Diagnosis	Grade	% Positive tumor cells	Intensity	Stage
1	Kidney	Urothelial carcinoma with squamous and sarcomatoid differentiation	High	30% in the sarcomatoid component	Moderate	IV
2	Breast	Invasive ductal carcinoma	Grade 2	90%	Strong	Unknown
3	Buttock	Undifferentiated pleomorphic sarcoma	High	70%	Moderate to strong	IV
4	Parotid gland	Poorly differentiated carcinoma with a squamoid component.	High	Negative	Negative	Unknown
5	Lung	Malignant giant cell-rich neoplasm.	Moderate	90%	Strong	Unknown
6	Uterus	Leiomyosarcoma	High	30%	Strong	IIIA
7	Right thigh	Undifferentiated pleomorphic sarcoma	High	80%	Moderate to strong	IIIA
8	Left kidney	Clear cell renal cell carcinoma	Grade 4	Negative	Negative	I
9	Urinary bladder	Invasive urothelial carcinoma.	High	Negative	Negative	III
10	Urinary bladder	Invasive urothelial carcinoma	High	Negative	Negative	III
11	Urinary bladder	Undifferentiated carcinoma with sarcomatoid features	High	60% in sarcomatoid component	Strong	Unknown
12	Urinary Bladder	Invasive urothelial carcinoma	High grade	20%	Moderate	I
13	Right kidney	Dedifferentiated liposarcoma	High grade	40%	Moderate to strong	IV
14	Skin, left arm	Cutaneous leiomyosarcoma	High grade	35%	Moderate to strong	IV
15	Posterior thigh	Malignant peripheral nerve sheath tumor	Low grade	20%	Strong	I

Figure 1 - 38

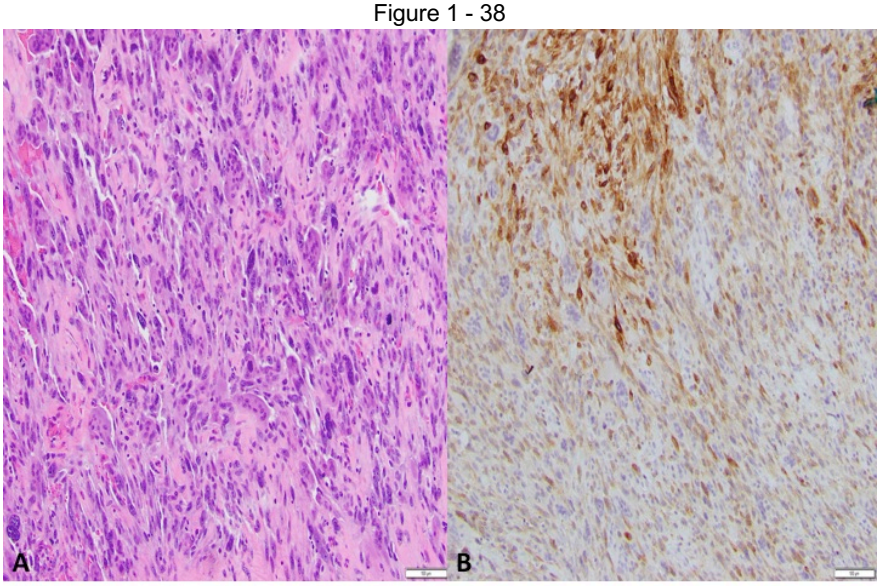

Figure 1: (A) H&E of undifferentiated pleomorphic sarcoma with osteoclasts in the buttock (case# 4). (B) RANKL mAB showing diffuse positive signal in tumor cells with moderate-to-strong intensity. Osteoclasts are negative.

Conclusions: This is the first report that we are aware of showing RANKL expression by tumor cells in OC-rich malignant solid tumors using IHC. We do not know what drives RANKL expression in these tumors or what role, if any, OCs or RANKL might have in the pathogenesis or behavior of these tumors. The RANKL mAB is a useful tool for detection of RANKL expression in a variety of tumors. Further studies are required to determine if RANKL inhibition therapy could affect the behavior of these tumors.

39 NTRK-Rearranged Mesenchymal Tumors of the Gastrointestinal Tract: A Clinicopathological, Immunohistochemical and Molecular Genetic Study of 7 Cases, Emphasizing Their Distinction from Gastrointestinal Stromal Tumor (GIST)

Mazen Atiq[1], Andrew Folpe[2], Jessica Davis[3], Christopher Fletcher[4], Jason Hornick[5], Adrian Marino-Enriquez[4]
[1]Mayo Clinic Rochester, Rochester, MN, [2]Mayo Clinic, Rochester, MN, [3]Oregon Health & Science University, Portland, OR, [4]Brigham and Women's Hospital, Boston, MA, [5]Brigham and Women's Hospital, Harvard Medical School, Boston, MA

Disclosures: Mazen Atiq: None; Andrew Folpe: None; Jessica Davis: *Advisory Board Member*, Bayer Pharmaceuticals/Loxo Oncology; Christopher Fletcher: None; Jason Hornick: *Consultant*, Eli Lilly; *Consultant*, Epizyme; Adrian Marino-Enriquez: None

Background: NTRK is a proto-oncogenic receptor tyrosine kinase (RTK). *NTRK* rearrangements, characteristic of infantile fibrosarcoma (*ETV6-NTRK3*), occur in various mesenchymal and non-mesenchymal tumors, affecting patients with a wide age range and anatomic distribution. *NTRK*-rearranged mesenchymal tumors typically show spindle-cell morphology, TRK expression, and variable expression of CD34 and S100 protein, but not SOX10. They may occur in the GI tract, where the most common RTK-driven mesenchymal tumor is GIST. We comprehensively analyzed 7 *NTRK*-rearranged mesenchymal GI tumors, with the goal of better characterizing these rare lesions and their relationship or lack thereof to GIST.

Design: Slides and blocks from 7 *NTRK*-rearranged GI mesenchymal tumors were retrieved from our archives. Morphologic features were assessed. Immunohistochemistry (IHC) for TRK, KIT (CD117), CD34, DOG1, and S100 was performed using commercially available antibodies and routine laboratory protocols. FISH and targeted NGS were performed.

Results: The tumors occurred in 4F and 3M (ages 2 mo-55 yrs; median 4 yrs), measured 4.5-12.5 cm (mean= 9.0 cm) in size, and involved the small intestine (n=4), stomach (n=2) and rectum (n=1). The tumors consisted of an infiltrative, relatively monomorphic proliferation of spindled cells with variable mitotic activity, absent necrosis and a well-developed vasculature. Unusual features seen in a subset of cases included cytoplasmic vacuoles, regional storiform or fascicular architecture, and focal sarcomatous morphology (pleomorphism and high mitotic activity). Tumor cells expressed diffusely TRK (7/7), S100 protein (3/7) and CD34 (4/7), but not SOX10 or KIT; weak DOG1 staining was detected in 1 case. Molecular genetic testing showed *TPM3-NTRK1* (n=3), *ETV6-NTRK3* (n=2), *TPR-NTRK1* (n=1), and *LMNA-NTRK1* (n=1). Clinical outcomes were variable, ranging from relatively indolent tumors (n=3) to aggressive sarcomas (n=2).

Conclusions: The clinicopathological, immunohistochemical and molecular genetic features of *NTRK*-rearranged GI mesenchymal tumors overlap significantly with those of their somatic soft tissue counterparts and differ from those of GIST. Evaluation of a spindle cell neoplasm of the GI tract without a definitive line of differentiation should include TRK IHC, particularly in pediatric patients. Expression of TRK or demonstration of an *NTRK* rearrangement in the absence of KIT expression supports the diagnosis of NTRK-rearranged mesenchymal tumor.

40 A Novel SS18-SSX Fusion-Specific Antibody for the Diagnosis of Synovial Sarcoma

Esther Baranov[1], Matthew McBride[2], Andrew Bellizzi[3], Christopher Fletcher[1], Cigall Kadoch[4], Jason Hornick[5]
[1]Brigham and Women's Hospital, Boston, MA, [2]Dana Farber Cancer Institute, Boston, MA, [3]University of Iowa Hospitals and Clinics, Iowa City, IA, [4]Dana-Farber Cancer Institute, Boston, MA, [5]Brigham and Women's Hospital, Harvard Medical School, Boston, MA

Disclosures: Esther Baranov: None; Matthew McBride: None; Andrew Bellizzi: None; Christopher Fletcher: None; Cigall Kadoch: *Advisory Board Member*, Foghorn Therapeutics, Inc.; *Speaker*, Cell Signaling Technology, Inc.; Jason Hornick: *Consultant*, Eli Lilly; *Consultant*, Epizyme

Background: Synovial sarcoma (SS) is an aggressive soft tissue sarcoma with a predilection for the extremities of young adults. SS harbors the pathognomonic t(X;18)(p11;q11), resulting in *SS18-SSX* rearrangements. SS includes monophasic, biphasic, and poorly differentiated (PD) variants, which show considerable histologic overlap with a range of other tumor types. Immunohistochemistry (IHC) is routinely used in differential diagnosis; however, presently available markers lack specificity. Cytogenetic or molecular genetic techniques are often employed to confirm the diagnosis. The purpose of this study was to evaluate an SS18-SSX fusion-specific antibody (Ab) as a surrogate for molecular testing.

Design: A rabbit monoclonal Ab (clone E9X9V) was produced by immunization with a synthetic peptide consisting of residues surrounding the SS18-SSX fusion site (identical breakpoints in ~95% of SS cases). Immunoprecipitation (IP), immunoblotting (IB), and chromatin IP followed by next-generation sequencing (ChIP-seq) were performed using SS cell lines. IHC was performed on whole sections from 100 genetically confirmed SS (41 each monophasic and PD; 18 biphasic) and 300 histologic mimics (malignant peripheral nerve sheath tumor; solitary fibrous tumor; dedifferentiated liposarcoma; leiomyosarcoma; fibrosarcomatous dermatofibrosarcoma protuberans; Ewing sarcoma; *CIC* sarcoma; alveolar, embryonal, and spindle cell rhabdomyosarcomas; mesenchymal chondrosarcoma; desmoplastic small round cell tumor; clear cell sarcoma; biphenotypic sinonasal sarcoma; *BCOR*-rearranged sarcoma; and sarcomatoid and biphasic mesotheliomas).

Results: IB of SS and control cell lines revealed that E9X9V detects both SS18-SSX1 and SS18-SSX2 fusion proteins with no cross-reactivity with wild-type SS18. IP captured SS18-SSX as well as core subunits of the mSWI/SNF complex, as expected. ChIP-seq demonstrated that E9X9V captures SS18-SSX on chromatin at established target sites (e.g., *TLE1* and *BCL2*). By IHC, 95 of 100 SS cases showed strong, diffuse nuclear staining with E9X9V (>90% of cells), whereas none of the 300 control tumors showed any staining with the Ab (95% sensitivity; 100% specificity).

Conclusions: A novel SS18-SSX fusion-specific Ab is highly sensitive and specific for SS. IHC using this Ab could replace molecular genetic testing in most cases. In addition, this reagent will provide the research community with a valuable tool for further biochemical and genomic interrogation of the oncogenic activity of the SS18-SSX fusion protein.

41 Prognostic Relevance of Complex Karyotypes in Myxoid Liposarcoma: A Study of 20 Cases

Davsheen Bedi[1], Svetlana Yatsenko[2], Virginia Miller[3], Karen Schoedel[4], Karen Fritchie[5], Ivy John[2]
[1]University of Pittsburgh Medical Center, Pittsburgh, PA, [2]University of Pittsburgh, Pittsburgh, PA, [3]University of Pittsburgh Medical Center Presbyterian Shadyside, Pittsburgh, PA, [4]UPMC-Presbyterian Hospital, Pittsburgh, PA, [5]Mayo Clinic, Rochester, MN

Disclosures: Davsheen Bedi: None; Svetlana Yatsenko: None; Virginia Miller: None; Karen Schoedel: None; Karen Fritchie: None; Ivy John: None

Background: Patients with myxoid liposarcoma (MLS) harboring >5% round cell component are at higher risk of metastasis and tumor related death. The prognostic relevance of complex karyotypes in MLS is yet to be determined.

Design: Cases of MLS with cytogenetic studies were retrieved from our institutional archives. Based on the amount of round cell component present, tumors were classified as high grade (>5%) or low grade (<5%). Karyotypes were classified as simple (isolated t(12;16)(q13;p11)/*FUS-DDIT3* fusion or t(12;22)(q13;q12)/*EWSR1-DDIT3* fusion) or complex (recurrent translocation with additional chromosomal abnormalities). Follow up data was obtained through chart review.

Results: 20 patients (m=13, f=7) were identified with an average age of 49 years (range 30 to 81 years) and median follow up of 60 months (range 9 to 147 months). Nine patients had isolated *FUS/DDIT3* fusions, 10 patients had complex karyotypes including *FUS/DDIT3* fusions and additional chromosomal abnormalities, and a single patient had complex karyotype resulting in *EWSR1/DDIT3* fusion and secondary chromosome rearrangements. Sixty-four percent of tumors with complex karyotypes were

classified as high grade compared to 33% with simple karyotype. Of the 11 patients with complex karyotype, 5 (45%) developed metastatic disease and 4 (36%) died of disease. Of the 9 tumors with simple karyotype, 1 (11%) developed local recurrence, 2 (22%) had metastatic disease and none died of disease. A patient with high grade MLS containing 90% round cell component and simple karyotype had no adverse events at 84 months of follow up. Of patients with low grade MLS, 2 out of 4 patients with a complex karyotype developed metastases and died of disease while only 2 of 6 harboring simple karyotypes experienced adverse events including 1 patient with local recurrence and 1 patient with metastatic disease. The most common additional cytogenetic aberration was trisomy 8, identified in 5 cases, all of which were high grade. Tetraploidization with doubling of an abnormal clone was detected in the patient with shortest survival (9 months).

Conclusions: Complex karyotype may help predict increased risk for adverse events in MLS, including in patients with low grade tumors. Further studies including copy number profiling and whole-genome sequencing may provide new genomic insights into MLS biology, clinical prognosis and metastatic potential.

42 Intimal Sarcomas Have an Active Tumor Immune Microenvironment

Jacqueline Birkness[1], Dwayne Thomas[1], Lysandra Voltaggio[2], Elizabeth D Thompson[3]
[1]Johns Hopkins, Baltimore, MD, [2]Baltimore, MD, [3]Johns Hopkins Hospital, Baltimore, MD

Disclosures: Jacqueline Birkness: None; Dwayne Thomas: None; Lysandra Voltaggio: None; Elizabeth D Thompson: None

Background: Intimal sarcomas (IS) are rare high grade soft tissue tumors that arise from the intima of large blood vessels. These tumors have a poor prognosis and are primarily treated surgically, as chemotherapy and radiation have questionable efficacy. Although PD-L1 expression and response to immunotherapy have been described in other sarcomas, the tumor immune microenvironment (TME) of intimal sarcomas remains to be characterized.

Design: Whole slides from 18 biopsy and resection specimens from 7 patients with pulmonary artery IS were labeled by immunohistochemistry for CD8 and PD-L1. Density of tumor infiltrating immune cells (TIL) was scored as none (0, 0%), rare (1, <5% of tumor area), moderate (2, 5-50%), or brisk (3, >50%). CD8+ T-cell density was quantified with image analysis software (HALO, Indica Labs) and divided into three categories (1 = <100 cells/mm^2, 2 = 100-500 cells/mm^2, 3 = >500 cells/mm^2). Expression of PD-L1 on tumor cells was scored based on membranous staining, with >1% labeling considered positive. PD-L1 expression on TIL was scored as none (0, 0%), focal (1, <5%), moderate (2, 5-50%), or diffuse (3, >50%). These measures were compared with clinical variables, including overall survival.

Results: All cases of IS showed some degree of immune infiltration (39% rare, 56% moderate, 6% brisk). Lymphoid aggregates were observed in 17% of cases. Tumor cell PD-L1 labeling was seen in 35% of cases and immune cell labeling in 76% of cases. Overall immune infiltration was associated with PD-L1 expression on tumor cells (p=0.019). High CD8+ T-cell density score was associated with PD-L1 expression on tumor cells (p=0.009) and immune cells (p=0.013). Although we did not find correlations between these measures and overall survival, one patient with an unusually long survival (9.7 years after diagnosis) had the highest overall immune infiltration, CD8+ T-cell density, and percentage of immune cells expressing PD-L1 in the cohort

Conclusions: IS show an active TME characterized by immune cell infiltration with occasional lymphoid aggregate formation and expression of PD-L1 on both tumor cells and immune cells. The association of overall immune infiltration and CD8+ T cell density with PD-L1 expression in IS suggests the presence of an active immune response and an adaptive pattern of PD-L1 expression. The prolonged survival seen in one patient with many intratumoral lymphocytes and a high level of PD-L1 expression suggests the possibility that this immune response may confer clinical benefit.

43 Stimulator of Interferon Genes (STING) Immunohistochemical Expression in the Spectrum of Perivascular Epithelioid Cell (PEC) Lesions of the Soft Tissue and the Visceral Sites

Anna Calio'[1], Matteo Brunelli[2], Diego Segala[3], Serena Pedron[1], Stefano Gobbo[4], Elena Piazzola[5], Alice Parisi[6], Anna Pesci[7], Giuseppe Zamboni[1], Guido Martignoni[8]
[1]University of Verona, Verona, Italy, [2]Verona, Italy, [3]Peschiera del Garda, Italy, [4]Ospedale Pederzoli, Peschiera del Garda, Italy, [5]AOUI Verona, Verona, Italy, [6]AOUI Verona, Verona, VR, Italy, [7]IRCCS Ospedale Sacro Cuore Don Calabria, Negrar, Verona, Italy, [8]University of Verona, Ospedale Pederzoli, Peschiera del Garda, Italy

Disclosures: Anna Calio': None; Matteo Brunelli: None; Diego Segala: None; Serena Pedron: None; Stefano Gobbo: None; Elena Piazzola: None; Alice Parisi: None; Anna Pesci: None; Giuseppe Zamboni: None; Guido Martignoni: None

Background: Angiomyolipoma is the prototype of the perivascular epithelioid cells (PEC) lesions whose pathogenesis is determined by mutations affecting *TSC* genes, with eventual deregulation of the mTOR pathway. It is well known that mTOR complex protein is involved in autophagy and recently it has been demonstrated the role of STING in this process. Since we have demonstrated the immunolabeling of STING in the PEC lesions of the kidney (abstract ID # 1591), we sought to investigate its immunohistochemical expression in a series of PEC lesions arising at a variety of soft tissue and visceral sites (excluding kidney).

Design: Thirty-six PEComas arose in different sites (17 uteri, 5 lungs, 4 pancreases, 4 retroperitoneum, 3 soft tissues, 2 livers, and 1 bladder) from 32 patients were collected. Immunostaining for STING (anti-TMEM173, clone SP338, dilution 1:150, Abcam) was carried out in all cases.

Results: Strong and diffuse immunolabeling of STING was observed in 91% of PEComas with concordant expression in primary and metastatic samples (4 cases).

Conclusions: We demonstrated the strong and diffuse expression of STING in almost all PEComas from different sites. This finding may be useful for diagnostic purposes and suggests the hypothesis of the alteration of autophagic process in the PEComa.

44 BRAF Immunostaining in Glomus Tumors Correlates with Morphologic Classification and Outcome: Subungual and Deep, with Benign, Atypical, and Malignant Tumors

Carla Caruso[1], Julie Fanburg-Smith[2]
[1]Department of Pathology and Anatomical Sciences, School of Medicine, University of Missouri, Columbia, MO, [2]Penn State Health Milton S. Hershey Medical Center, McLean, VA

Disclosures: Carla Caruso: None; Julie Fanburg-Smith: None

Background: Upon our discovery that protein BRAF V600E, a marker for aggressive behavior in melanoma, correlates with classification and prognosis in glomus tumor (GT), *BRAF* mutation was reported in atypical and malignant GT tumors. GT arise from the modified smooth muscle/pericytic neuromyoarterial glomus body that regulates temperature/pressure. Our concurrent data expands the use of BRAF immunostaining in subungual digital and deep extradigital GT to predict classification and outcome.

Design: Cases coded as "glomus tumor" were classified by three MSK pathologists. We defined reproducible criteria for malignant, atypical and benign GT and independently scored BRAF V600E amplification-enhanced immunostaining performed in our research lab using a 0-2 score, based on intensity and percentage of granular cytoplasmic expression. A mouse monoclonal #790-5095 immunostaining protocol for VENTANA Discovery XT was used. Clinical data and follow-up were obtained.

Results: Fifty-eight cases of benign, atypical and malignant, subungual (n=28) and deep (n=30), GT were included. Extradigital deep included malignant (n=2, median 34 years, median size 4 cm, intramuscular thigh, left arm), atypical (n=9, 6F:3M, median size 0.65 cm, upper arm, popliteal fossa, forearm, hand), and benign (n=18, 2F:16M, median size 0.9 cm, flank, elbow, leg, forearm, buttocks, knee, ear, foot). Subungual only had atypical (n=2; 1F:1M, median 61 years, median size 1.25 cm, fingers) and benign cases (n=26, 21F:5M, median 48 years, median 0.5 cm, fingers and one toe, mainly right side). GT correlated with 2+ (malignant), 0-1+ (atypical), and 0 (benign) immunostaining scores for BRAF, respectively. Additional findings for deep cases include: 2 atypical and 1 malignant with recurrences; benign, with vascular and myxoid features, less distinctive cytoplasmic borders, whereas atypical were solid and more infiltrative; malignant showed bland periphery and atypical center with increased mitotic activity. Subungual GT group presented with pain, while deep reported paresthesia.

Conclusions: This is the first study to find increased BRAF V600E immunostaining in GT that correlates with benign (negative), atypical (weak), and malignant (strong) that predicts recurrence in atypical and malignant tumors. Digital GT commonly presents with pain and female predilection, whereas the equally common extradigital GT presents with paresthesia and male predilection. For challenging atypical and malignant GT, *BRAF* may be a potential therapeutic target.

45 Expression of SWI/SNF Nucleosome Remodeling Complex Proteins in Synovial Sarcoma

Ivan Chebib[1], Ana Larque Daza[2], Santiago Lozano-Calderon[1], Steffen Rickelt[3], Yin Hung[4], Vikram Deshpande[4], G. Pétur Nielsen[5]
[1]Massachusetts General Hospital, Harvard Medical School, Boston, MA, [2]Hospital Clinic of Barcelona, Barcelona, Spain, [3]David H. Koch Institute for Integrative Cancer Research, Cambridge, MA, [4]Massachusetts General Hospital, Boston, MA, [5]Harvard Medical School, Boston, MA

Disclosures: Ivan Chebib: None; Ana Larque Daza: None; Santiago Lozano-Calderon: None; Steffen Rickelt: None; Yin Hung: None; Vikram Deshpande: *Grant or Research Support*, Advanced Cell Diagnostics; *Grant or Research Support*, Viela; *Grant or Research Support*, Agios pharmaceuticals

Background: Synovial sarcoma (SS) is an aggressive soft tissue malignancy characterized by *SS18-SSX* rearrangement. *SS18* is a member of the SWI/SNF nucleosome remodeling complex and studies suggest that *SS18-SSX* fusion product leads to abnormal integration into the SWI/SNF complex and potentially leading to displacement of *SMARCB1* (INI1). Additionally, the fusion interaction with the SWI/SNF complex may lead to abnormal transcription activation. Given this relationship with SWI/SNF complex, we sought to evaluate protein expression of several SWI/SNF complex proteins in a large cohort of uniformly treated SS and determine whether loss of expression is associated with survival.

Design: A cohort of patients with synovial sarcoma who were treated uniformly at one institution were identified between 1990-2015. Tissue microarrays (3-mm cores) were created from formalin-fixed paraffin-embedded tissue blocks from resections of primary sarcoma and metastatic disease. Detailed clinical and pathology data was collected, including survival. Immunohistochemical staining was performed for SWI/SNF complex proteins: ARID1A, SMARCB1, SMARCA4, SMARCA2, SMARCC1, SMARCC2, and SMARCE1. Nuclear expression was semi-quantitatively scored as: 0-no expression; 1-weak expression; 2-strong expression. SWI/SNF complex expression was assessed in relation to survival (log-rank test).

Results: There were 113 patients with synovial sarcoma with absent expression of ARID1A in 39%, SMARCA4 in 46%, SMARCA2 in 2.9%, SMARCC2 in 10%, SMARCE1in 3.5%, and SMARCC1 in 0. Twenty-seven cases showed loss of expression of 2 or more markers: 17 ARID1A/SMARCA4, 4 ARD1A/ SMARCA4/ SMARCE1, 2 SMARCA4/ SMARCC2, and 1 each ARID1A/ SMARCA4/ SMARCC2, ARID1A/ SMARCC2, ARID1A/ SMARCA2, SMARCA2/ SMARCC2. In biphasic synovial sarcoma that retained expression of SWI/SNF proteins, there was strong nuclear positivity in the epithelioid and weak expression in the spindled component. The median overall survival was 19.3 years (range: 4 days-26.4 years). Of the markers evaluated, only absent/decreased (score 0/1) SMARCA4 expression showed a statistically significant improvement in overall survival (p=0.003).

Conclusions: Loss of SWI/SNF nucleosome remodeling complex protein expression is relatively common in synovial sarcoma, with loss of ARID1A and/or SMARCA4 most commonly. Decreased/lost SMARCA4 expression is associated with improved overall survival.

46 Molecular Genetics of Desmoplastic Fibroma of Bone

Soo-Jin Cho[1], Gregory Bean[2], Gregory Charville[2], Richard Jordan[1], Andrew Horvai[1]
[1]University of California San Francisco, San Francisco, CA, [2]Stanford University School of Medicine, Stanford, CA

Disclosures: Soo-Jin Cho: *Stock Ownership*, BHB Therapeutics; Gregory Bean: None; Gregory Charville: None; Richard Jordan: None; Andrew Horvai: None

Background: Desmoplastic fibroma (DF) is a rare tumor of bone, occurring at all ages and in any bone. Histologically, it consists of a hypocellular proliferation of bland spindle cells with associated collagen, similar to desmoid-type fibromatosis of soft tissues. Alterations in the Wnt pathway genes, including *CTNNB1* and *APC*, are characterstic of desmoids, but have rarely been reported in DF. The pathogenesis of DF has not been fully characterized. We profiled DF using capture-based next generation sequencing (NGS) to further characterize these tumors.

Design: Ten cases diagnosed as “desmoplastic fibroma” or “consistent with desmoplastic fibroma” were collected from institutional archives. DNA was extracted from tumor tissue and capture-based NGS was performed targeting exons of approximately 500 cancer genes. Duplicate reads were removed computationally for accurate allele frequency determination and copy number calling. Single nucleotide variants (SNVs), insertions/deletions, and copy number (CN) alterations were evaluated.

Results: The clinical and molecular-genetic results are summarized in the Table. Mean age was 32 years (range 3-87). Locations included mandible (5 cases), maxilla (1), femur (2), radius (1) and calcaneus (1). Mutations in *CTNNB1* (2) and *APC* (1) were identified in a minority. Recurrent amplifications in *COL1A1* (4) and *FGFR2* (4) as well as partial CN gains in chromosomes 19 (7) and 7 (4) were observed. No pathogenic SNV was identified in 4 cases.

Some of the pathogenic SNVs suggested alternative diagnoses. In Case 4, the *PDGFRB* mutation suggested a diagnosis of myofibroma, but it also demonstrated amplifications in *FGFR2* and *COL1A1*. The patient in Case 5 was subsequently found to have neurofibromatosis 2, but the mandibular tumor was negative for S100 and SOX10 by immunohistochemistry, arguing against schwannoma. Case 6 harbored a *H3F3B* mutation seen in chondroblastoma, but no features of chondroblastoma were seen in this case.

Case	Age	Gender	Location	Pathogenic SNVs	Amplifications
1	3	M	Left mandible	CTNNB1 p.S45F	
2	15	M	Right distal radius	CTNNB1 p.S45F	
3	87	F	Right mandible	APC p.E1530fs	FGFR2, TBX3, COL1A1
4	40	F	Left maxilla	PDGFRB p.N666K	FGFR2, TBX3, COL1A1
5	34	F	Left mandible	NF2 p.Q212* with loss of heterozygosity	
6	44	F	Left mandible, ascending ramus	H3F3B p.G35R	COL1A1
7	30	M	Left calcaneus		COL1A1
8	11	M	Right distal femur		FGFR2
9	44	F	Left mandible		TERT, FGFR2, FGFR4
10	17	M	Left proximal femur		

Conclusions: While histologically similar to desmoid-type fibromatosis of soft tissue, only a minority of DF of bone demonstrate Wnt pathway alterations. Cases in which no pathogenic SNVs were seen did show other common changes identified in this study, including amplifications of *FGFR2* and/or *COL1A1*, as well as chromosome 7 and/or 19 gain. This study reveals that desmoplastic fibromas may be a heterogeneous group of tumors with a similar morphologic pattern but different genetic alterations. Further studies may allow for more precise classification.

47 SATB2 Positivity Not Specific for Osteoblastic Differentiation and Caution Needed in Making Diagnoses of Osteosarcoma in the Absence of Histological or Radiological Evidence of Osteoid

Shefali Chopra, University of Southern California, San Marino, CA

Disclosures: Shefali Chopra: None

Background: SATB2 is supposed to be highly sensitive for tumors with osteoblastic differentiation and plays a critical role in osteoblast lineage. It is felt to be helpful in establishing diagnosis of osteosarcoma in absence of osteoid

Design: All sarcomas diagnosed in bone and soft tissue from 2015- present were retrieved by database search and SATB2 was performed/reviewed on representative cases of each sarcoma type. Immunohistochemistry was performed on whole sections using clone EP281 Cell Marque in dilution 1:50 on the Leica Bond autostainer. SATB2 was scored as negative (<50%) and positive (>50%). Only strong nuclear staining was scored<

Results: In the bone sarcomas 20 cases of osteosarcoma were identified on biopsies with biopsy/ followup resection demonstrating osteoid. All were SATB2 positive and 14 were smooth muscle actin(SMA) positive. Additionally there were 4 bone sarcoma cases that were called osteosarcoma based on SATB2 positivity, which had no osteoid seen in biopsy or resection. These cases were SMA positive. There was a single leiomyosarcoma that was SATB2 positive. Tumor had smooth muscle differentiation on histology and was strongly and diffusely positive for desmin and smooth muscle actin. SATB2 was negative on 5 Ewing, and 1 PECOMA and epithelioid hemangio endothelioma of the bone

In the soft tissue sarcomas, there were 4 cases of extraskeletal osteosarcoma, which had osteoid present and were SATB2 positive. Of the sarcomas with myoid differentiation, (SMA +) 20 cases were SATB2 positive and 8 were negative. Out of the 10 leiomyosarcoma cases, none was SATB2 positive. 5 synovial sarcomas were negative. Of the 20 undifferentiated sarcomas, 2 were SATB2 positive while 18 were negative

Conclusions: SATB2 positivity is sensitive but not specific for osteosarcomatous differentiation and caution should be used to make diagnosis of osteosarcoma in the absence of osteoid.

Though sarcomas with SATB2 expression might represent osteoblastic lineage too primitive to synthesize matrix, expression in primary soft tissue sarcomas with myoid differentiation would make this an unlikely scenario.

SATB2 expression is seen more often in tumors which express SMA. Conversely most osteosarcomas are also SMA positive which making accurate classification of especially bone tumors hard in absence of osteoid formation. Long term followup studies would be beneficial in bone tumors without osteoid and SATB2 expression to see if differences exist in tumor behavior from osteosarcoma

48 Tumor-Immune Microenvironment and PD-L1 Expression in SMARCB1/INI1-Deficient Tumors: A Potential Role for Immune-Modulatory Therapy

Jeffrey Cloutier[1], Gregory Charville[2]
[1]Stanford University, Stanford, CA, [2]Stanford University School of Medicine, Stanford, CA

Disclosures: Jeffrey Cloutier: None; Gregory Charville: None

Background: INI1-deficient neoplasms represent a clinically diverse and aggressive group of tumors that share oncogenic defects in *SMARCB1* (i.e. *INI1*), which encodes a component of the SWI/SNF chromatin remodeling complex. Currently, there are limited therapeutic options for patients with advanced-stage INI1-deficient tumors. Given that an inflammatory response is often seen in INI1-deficient tumors, such as epithelioid sarcoma, we hypothesized that they may be candidates for immune-modulatory therapy. To explore this hypothesis, we characterized the tumor-immune microenvironment and tumor PD-L1 expression in a cohort of INI1-deficient neoplasms.

Design: INI1-deficient tumors from 12 patients included 7 primary or metastatic epithelioid sarcomas, 1 sinonasal carcinoma, 1 malignant rhabdoid tumor and 7 cases of unclassified epithelioid malignancies involving pancreas (1), soft tissue (3), lymph node (1), lung (1) and kidney (1). From one patient, there was a primary, recurrent, and metastatic tumor. The density of tumor-associated lymphocytes was

estimated using a semi-quantitative scale: none, rare (<5% of stromal area), mild (5-10%), moderate (11-49%), and brisk (>50%). By immunohistochemistry, we determined the relative density of cells expressing CD3, CD8, FOXP3, and CD68. Finally, we quantified the percentage of viable tumor cells with positive membranous staining for PD-L1 (SP263) (Tumor Proportion Score; TPS).

Results: In our cohort of INI1-deficient tumors, 6 of 11 patients with follow-up data were dead of disease within one year of diagnosis. The majority of cases (7/12) had a mild to moderate density of tumor-associated lymphocytes; one case had a brisk infiltrate (Figure 1, left panel). Five cases (40%) had a TPS of >10%, and in two cases the TPS was 80% or greater (Figure 1, right panel). A high density of tumor-associated CD8-positive lymphocytes, reflected as a CD8:CD3 ratio of >50%, was associated with a positive TPS (defined as >1%; p=0.01). In one patient, the TPS increased between primary tumor (1%), local recurrence (20%), and distant metastasis (40%), suggesting evolution of PD-L1 expression with therapeutic intervention and disease progression.

Figure 1 - 48

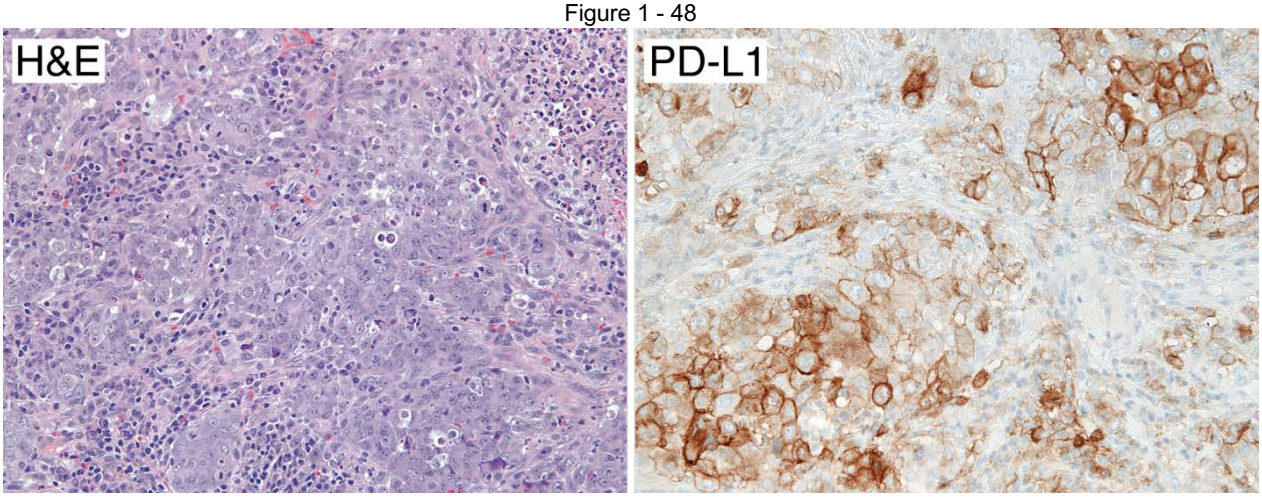

Conclusions: Our study demonstrates that a subset of INI1-deficient neoplasms express PD-L1, and that PD-L1 expression correlates with features of the tumor-immune microenvironment. Future work is needed to determine if PD-L1 expression is predictive of favorable responses to immunotherapies in these lethal tumors.

49 Clinically Advanced Chordoma of Bone: A Comparative Comprehensive Genomic Profiling Study

James Corines[1], Julia Elvin[2], Jo-Anne Vergilio[2], Keith Killian[2], Douglas Lin[2], Erik Williams[3], Natalie Danziger[4], James Haberberger[5], Julie Tse[3], Shakti Ramkissoon[5], Eric Severson[5], Amanda Hemmerich[5], Naomi Lynn Ferguson[5], Claire Edgerly[5], Daniel Duncan[5], Richard Huang[6], Russell Madison[2], Jon Chung[2], Venkataprasanth Reddy[2], Kimberly McGregor[2], Jeffrey Ross[1]
[1]Upstate Medical University, Syracuse, NY, [2]Foundation Medicine, Inc., Cambridge, MA, [3]Boston, MA, [4]Foundation Medicine, Inc., Somerville, MA, [5]Foundation Medicine, Inc., Morrisville, NC, [6]Foundation Medicine, Inc., Cary, NC

Disclosures: James Corines: None; Julia Elvin: *Employee*, Foundation Medicine, Inc.; *Stock Ownership*, Hoffman La Roche; Jo-Anne Vergilio: *Employee*, Foundation Medicine, Inc; *Employee*, Foundation Medicine, Inc; Keith Killian: *Employee*, FMI; Douglas Lin: *Employee*, Foundation Medicine; Erik Williams: *Stock Ownership*, F. Hoffman La-Roche, Ltd.; *Employee*, Foundation Medicine, Inc.; Natalie Danziger: *Employee*, Foundation Medicine Incorporated; James Haberberger: *Employee*, Foundation Medicine Inc.; Julie Tse: *Employee*, Foundation Medicine, Inc.; *Consultant*, Pathology Watch, LLC.; Shakti Ramkissoon: *Employee*, Foundation Medicine/Roche; Eric Severson: *Employee*, Foundation Medicine; Amanda Hemmerich: *Employee*, Foundation Medicine, Inc; Naomi Lynn Ferguson: *Employee*, Foundation Medicine; Claire Edgerly: *Employee*, Foundation Medicine, Inc.; Daniel Duncan: *Employee*, Foundation Medicine; Richard Huang: *Employee*, Roche/Foundation Medicine; Russell Madison: *Employee*, Foundation Medicine Inc.; *Stock Ownership*, Roche; Jon Chung: *Employee*, Foundation Medicine; *Stock Ownership*, Roche; Venkataprasanth Reddy: *Employee*, Foundation Medicine; Kimberly McGregor: *Employee*, Foundation Medicine; Jeffrey Ross: *Employee*, Foundation Medicine

Background: Chordomas and chondrosarcomas are aggressive malignancies that can arise from the skull base and sacrum with similar clinical and neuroradiological features. We used comprehensive genomic profiling (CGP) to compare the genomic alterations (GA) between these 2 tumor types.

Design: Comprehensive genomic profiling was performed on FFPE samples from 226 cases of clinically advanced bone chordomas and 221 bone chondrosarcomas. Tumor mutational burden (TMB) was determined on 0.8-1.1 Mbp of sequenced DNA and microsatellite instability (MSI) was determined on 114 loci. PD-L1 expression in tumor cells (Dako 22C3) was measured by IHC.

Results: The 226 bone chordomas (BCHOR) had similar age and gender status as the comparison group of 221 bone chondrosarcomas (BCHON). The frequency of genomic alterations per tumor was significantly higher in BCHON than BCHOR. MSI high status was not seen in BCHOR and extremely rare in BCHON (see Table). Relatively low TMB levels were observed in both groups. PD-L1 high (>50%) expression was not identified in BCHOR and was extremely uncommon in BCHON. Among the untargetable GA, the *TP53* mutation frequency in BCHON (36%) was significantly higher than seen in BCHOR (7%). *CDKN2A/B* mutation frequencies were similar in both groups. BCHOR featured very rare potentially targetable GA almost exclusively limited to the MTOR pathway (*PTEN*, *PIK3CA* and *TSC1*). BCHON featured fewer MTOR pathway targets compared to BCHOR. BCHON, in contrast, did feature relatively high GA frequencies in the *IDH1/2* genes which have been successfully targeted with approved drugs in AML and are in development for other solid tumors.

	Chordoma (BCHOR)		Chondrosarcoma (BCHON)	
Cases	226		221	
Gender	Female 37%; Male 63%		Female 47%; Male 53%	
Median Age/Range (years)	58 (1-89)		54 (15-87)	
GA/tumor	2.2		3.5	
Most Frequently Altered Currently Untargetable GA	*CDKN2A* *CDKN2B* *PBRM1* *TP53* *SMARCB1*	36% 30% 11% 7% 4%	*TP53* *CDKN2A* *CDKN2B* *RB1*	36% 30% 23% 6%
Potential Targeted Therapy Impacting GA	*PTEN* *PIK3CA* *TSC1* *PTCH1* *MET*	9% 5% 2% 1% 1%	*IDH1* *IDH2* *CDK4* *PTEN*	27% 12% 5% 5%
MSI High Status	0%		1%	
TMB Median (mut/Mb)	1.6		1.6	
TMB > 10 mut/Mb	1%		3%	
TMB > 20 mut/Mb	0%		1%	
PD-L1 IHC Low	16%		7%	
PD-L1 IHC High	0%		4%	

Conclusions: The BCHOR and BCHON patients have a similar median age (54-58 years) and male preponderance (Table). BCHON features a higher distribution of both non-CR and CR GA. BCHOR features GA in targetable genes of the MTOR pathway indicating potential for immunotherapy benefit. In addition, BCHON features GA in genes which have been successfully targeted with approved drugs for other malignancies. Based on these findings, CGP shows promise for personalizing therapies for chordoma and chondrosarcoma patients and improving their clinical outcomes.

50 Clinical, Radiographic, and Pathologic Analysis of Total Hip Arthroplasty in Patients with Legg-Calvé-Perthes Disease

Christian Curcio[1], Robert Schneider[1], Roman Savelyev[1], Thomas Bauer[1], Yaxia Zhang[1]
[1]*Hospital for Special Surgery, New York, NY*

Disclosures: Christian Curcio: None; Robert Schneider: None; Roman Savelyev: None; Yaxia Zhang: None

Background: Legg-Calvé-Perthes disease (LCPD) is a disorder characterized by idiopathic avascular necrosis of the femoral head in children. The underlying etiology remains unclear. Total hip arthroplasty may be necessary in some patients. The specific histopathologic findings seen in femoral heads from these patients have not been thoroughly described. The purpose of this study is to further understand the underlying pathophysiology of this disease by evaluating the radiographic and pathologic features of hip joints of LCPD patients.

Design: A retrospective pathology database search was performed to identify all cases of LCPD diagnosed at our high-volume tertiary orthopedic treatment center from 2016 to 2019. Patients' demographics, clinical history, imaging studies, and gross and microscopic findings were documented and compared.

Results: Ten patients with LCPD were identified, nine male (90%) and one female (10%), with present ages ranging from 13 to 54 years and ages of LCPD diagnosis ranging from five to 13 years. Two (20%) had bilateral hip involvement. Clinically, all complained of pain of the affected joints. Eight (80%) underwent unilateral total hip arthroplasty with time from diagnosis to surgery ranging from four to 39 years in a bimodal distribution. Presurgical diagnoses of secondary osteoarthritis were provided based on radiographic studies. Grossly, all femoral heads were enlarged and deformed with lengthened lateral-medial and anterior-posterior dimensions and a shortened superior-inferior dimension. Two femoral heads (25%) demonstrated subchondral osteonecrosis; the patients were aged 13 and 29 at time of surgery with times from initial diagnosis to surgery of <1 and 23 years, respectively. The femoral head of the 13-year-old demonstrated unhealed primary osteonecrosis, while that of the 29-year-old had developed osteonecrosis secondarily after the primary necrosis had healed. Six femoral heads (75%) had relatively normal hyaline cartilage, while the remaining two (25%), from patients with longstanding diagnoses of LCPD aged 38 and 53 at time of surgery, had developed features of osteoarthritis.

Conclusions: Patients with LCPD who undergo total hip arthroplasty frequently exhibit secondary hip dysplasia characterized by an enlarged, ovoid femoral head typically overriding a shallow acetabulum. Secondary hip dysplasia and secondary osteoarthritis are the leading etiology for total hip replacement in these patients.

51 Mono-Articular Multifocal Localized Tenosynovial Giant Cell Tumors

Christian Curcio[1], Thomas Bauer[1], Yaxia Zhang[1]
[1]Hospital for Special Surgery, New York, NY

Disclosures: Christian Curcio: None; Yaxia Zhang: None

Background: Tenosynovial giant cell tumor (TGCT) is a rare and benign but potentially destructive neoplasm arising from synovium, tendon sheath, or bursae that can assume either a localized or diffuse form. Localized TGCT is often treated with marginal resection with 8% recurrence, while treatment for diffuse TGCT is more challenging with recurrence rates reported up to 46% even with wide resection. Recently, pexidartinib, a systemic CSF1R antagonist, was approved in the United States as a new therapy limited to patients with severely morbid TGCTs. In the wake of this release, the question as to the existence of multifocal localized TGCT, and whether such an entity may cause significant complications, has been raised. To assess for such an entity, we systemically analyzed the TGCT cases collected at our high-volume tertiary orthopedic treatment center.

Design: A retrospective pathology database search was performed to identify all TGCTs diagnosed at our institution from 2016 to 2019. Patients' demographics, clinical history, imaging studies, gross and microscopic findings, and patient outcome were documented and reviewed.

Results: Identified were 118 cases, 50 male (42%) and 68 female (58%) aged nine to 92 (mean: 49.7), including 52 knees (44%), 37 digits (31%), 11 ankles (9%), five hips (4%), four wrists (3%), three hands (3%), two shoulders (2%), two elbows (2%), and two feet (2%) with 59 intra-articular localized (50%), 40 extra-articular localized (34%), 16 intra-articular diffuse (14%), and three extra-articular diffuse (2%). Fifteen, all intra-articular localized, were incidental (13%) with 13 from knee arthroplasties (25% of involved knees) and two from hip arthroplasties (40% of involved hips). Two cases of intra-articular TGCTs exhibited multiple discrete localized foci within a single joint space (3% of intra-articular localized TGCTs and 2% of all TGCTs). These were identified in the knee of a 52-year-old man and the ankle of a 14-year-old woman. The latter was multiply recurrent, prompting four surgeries over five years; arthroscopic images showed distinct, well-circumscribed nodules in the anterior and posterior compartments without involvement of intervening synovium.

Conclusions: Multifocal intra-articular localized TGCT is extremely rare but does exist. Further study is warranted to understand the clinical course and proper treatment. The high rate of incidental TGCT diagnosis in arthroplasty samples should warrant submission of such specimens for microscopic examination.

52 Retroperitoneal Dedifferentiated Liposarcoma: Dedifferentiated Component at the Margin Is Associated with Prognosis

Carina Dehner[1], Ian Hagemann[1], John Chrisinger[1]
[1]Washington University School of Medicine, St. Louis, MO

Disclosures: Carina Dehner: None; Ian Hagemann: None; John Chrisinger: None

Background: Dedifferentiated liposarcoma (DDLS) is a sarcomatous (typically non-lipogenic) component of a well-differentiated liposarcoma (WD) and frequently involves the retroperitoneum. Its development in WD heralds progression from a low to at least intermediate grade tumor with increased risk of local recurrence and metastasis. There is very limited data on the prognostic significance of margin involvement by DD tumor compared to margin involvement by only the well-differentiated (WD) component in retroperitoneal DDLS.

Design: The pathology department archive was retrospectively searched for resections of retroperitoneal DDLS performed at our institution (1990-2017). Available slides of were reviewed for diagnosis, and the presence of WD or DD tumor at the resection margin. Patient age, gender, tumor size, local recurrence, recurrence free survival, overall survival and follow-up duration were noted.

Results: Seventeen men and thirteen women with DDLS of the retroperitoneum were identified. The mean age was 61 years (range 42-85). Median follow-up time was 36 months (range 3-120). All tumors showed areas of well-differentiated liposarcoma (WDLS) and/or amplification of MDM2 by fluorescence in-situ hybridization testing. All cases showed WDLS at the margin or the presence of WD tumor at the margin could not be excluded. Resection margins were positive for the DD component in 17 cases (56.7%), while negative in 13 cases (43.3%). Thirteen of 17 (76%) cases with DD tumor at the margin locally recurred, compared to 4 of 13 (31%) cases without DD tumor at the margin. Survival curve analysis showed that recurrence-free survival was significantly longer if the margin was negative for the DD component (p=0.011) (Figure 1), while overall survival was not significantly different (p=0.67) (Figure 2). Patient age, tumor size and follow-up duration were not significantly different between the margin positive and margin negative groups (p=0.93, p=0.36 and p=0.66, respectively).

Figure 1 - 52

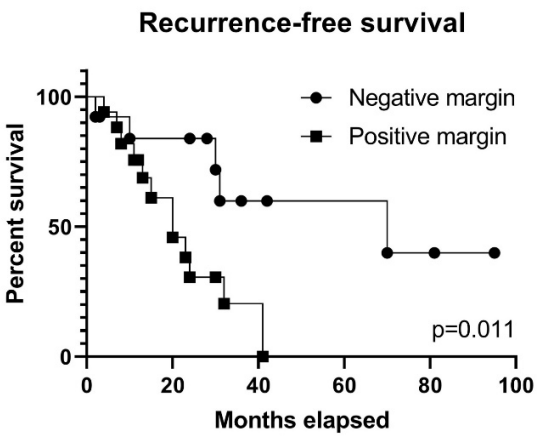

Figure 2 - 52

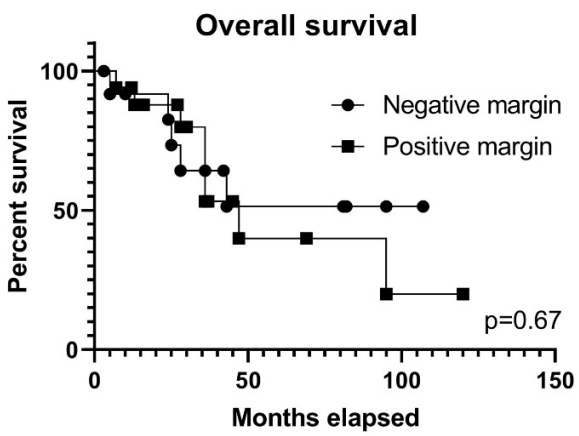

Conclusions: DD tumor at the resection margin in retroperitoneal DDLS was associated with shorter recurrence free survival. Therefore, reporting of DD at the resection margin is recommended as patients with positive margins may benefit from at least closer surveillance or additional local therapy. No difference was seen in overall survival, suggesting other factors are involved in these tumors besides complete surgical resection of the DD component.

53 TRPV4 Expression Cartilaginous Neoplasms

Carina Dehner[1], Christopher O'Conor[2], John Chrisinger[1]
[1]Washington University School of Medicine, St. Louis, MO, [2]Barnes Jewish Hospital/Washington University, St. Louis, MO

Disclosures: Carina Dehner: None; Christopher O'Conor: None; John Chrisinger: None

Background: TRPV4 is a calcium-permeable membrane ion channel known to play a key role in skeletogenesis and is highly expressed in chondrocytes and pre-chondrogenic cells. TRP channels are currently being investigated as targets for therapy. We set out to study if TRPV4 is expressed in cartilaginous tumors.

Design: Cases of conventional, dedifferentiated, mesenchymal and clear cell chondrosarcoma, as well as chondroblastic osteosarcoma and extraskeletal myxoid chondrosarcoma (EMC) were retrieved from the archive. A single whole slide was selected from each case and stained with an immunohistochemical study for TRPV4. Staining was scored based on proportion of positive cells (0: 0%, 1: 1-33%, 2: 34-66%, 3: 67-100%) and area of the most intense staining (0: no staining, 1: weak, 2: moderate, 3: strong). Positive staining was defined as a combined proportion and intensity score greater than 2.

Results: Five conventional (grade 1-3, including 1 arising in osteochondroma), 5 dedifferentiated, 1 clear cell and 4 mesenchymal chondrosarcomas as well as 1 chondroblastic osteosarcoma and 4 EMC were selected. Diffuse moderate to intense positive staining for TRPV4 was present in all conventional chondrosarcomas. The cartilage forming component of dedifferentiated chondrosarcomas also showed consistent positive staining with TRPV4 with all cases showing moderate to intense staining in greater than 34% of cartilage forming cells. The dedifferentiated component showed negative staining in 4 cases, while one case showed diffuse moderate staining in the dedifferentiated cells. A similar pattern was observed in mesenchymal chondrosarcoma. The cartilage forming areas of mesenchymal chondrosarcoma showed positive staining with all cases, while the round cell component showed negative staining in 2 cases, and positive

staining in 2 cases (proportion score 2, intensity score 1, and proportion score 1, intensity score 3). Clear cell chondrosarcoma was diffusely and strongly positive for TRPV4. TRPV4 was negative in 2 cases of EMC, while 2 cases were positive. Chondroblastic osteosarcoma showed positive staining in both cartilage and bone forming areas.

Conclusions: Our pilot study suggests that TRPV4 may be highly expressed in cartilaginous neoplasms making it a potential drug-targetable antigen. However, its expression appears diminished in components without recognizable cartilaginous differentiation. Further, the role of TRPV4 in the oncogenesis of these tumors is unclear and deserves further investigation.

54 Accurate Diagnosis of Avascular Necrosis of the Femoral Head from Total Hip Arthroplasty Specimens Requires Pathologic Examination

Josephine Dermawan[1], Andrew Goldblum[2], John Reith[3], Scott Kilpatrick[1]
[1]Cleveland Clinic, Cleveland, OH, [2]Cleveland Clinic Akron General, Stow, OH, [3]Cleveland Clinic Foundation, Cleveland, OH

Disclosures: Josephine Dermawan: None; Andrew Goldblum: None; John Reith: None; Scott Kilpatrick: None

Background: Pathologic examination of femoral heads from total hip arthroplasties is decreasing due to the perception of limited cost effectiveness relative to clinical information gained. Data from more recent studies, at institutions where pathologic examination remains routinely and meticulously performed, have challenged this notion. Due to an increased risk of avascular necrosis (AVN) developing contralaterally (and elsewhere) and an increased risk of arthroplasty failure, accurate diagnosis of AVN is important. A timely diagnosis of AVN may lead to behavioral changes in affected patients that reduce the risk of subsequent lesions.

Design: We retrospectively reviewed all total hip arthroplasty cases confirmed pathologically (n=2005), consecutively between 1/1/17 and 10/10/18, interpreted by the authors, comparing clinical diagnoses and the final histologic diagnoses, focusing on AVN. To ensure accurate clinical preoperative diagnoses, the operative report also was compared to the surgical pathology requisition. AVN was defined as a geographic area of subchondral bone necrosis, visible both microscopically and grossly, with or without detached overlying articular cartilage, not associated with fracture. Clinicopathologic information including patient age (age = years) and gender were correlated with the above data.

Results: Among 201 patients with a pathologically confirmed diagnosis of AVN, 81 (40%) had a preoperative clinical diagnosis of degenerative joint disease (DJD). Patients with AVN but clinically diagnosed as DJD were significantly older (mean age 63) than patients with AVN correctly suspected clinically (mean age 51, $P < 0.00001$). For the 147 patients with a preoperative clinical diagnosis of AVN, 27 (18%) were diagnosed as DJD. The latter patients also were significantly older (mean age 61) than patients with AVN correctly diagnosed clinically ($P = 0.0008$). There were no significant differences in gender ratios among any of these patient groups, nor a significant association among specific surgeons or treatment hospitals.

Hip Arthroplasty		Clinical Diagnosis	Histologic Diagnosis	
			DJD	AVN
DJD	Total	1560	1479 (95%)	81 (5%)
	Male:Female	1:1.2	1:1.2	1:0.8
	Age range (Mean)	25-93 (65)	25-93 (65)	30-87 (63)
AVN	Total	147	27 (18%)	120 (82%)
	Male:Female	1:0.6	1:0.8	1:0.6
	Age range (Mean)	17-83 (52)	28-79 (61)	17-83 (51)

Figure 1 - 54

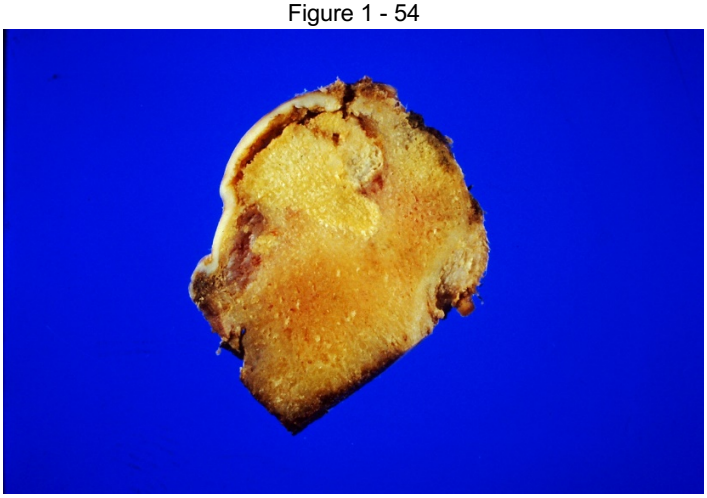

Figure 2 - 54

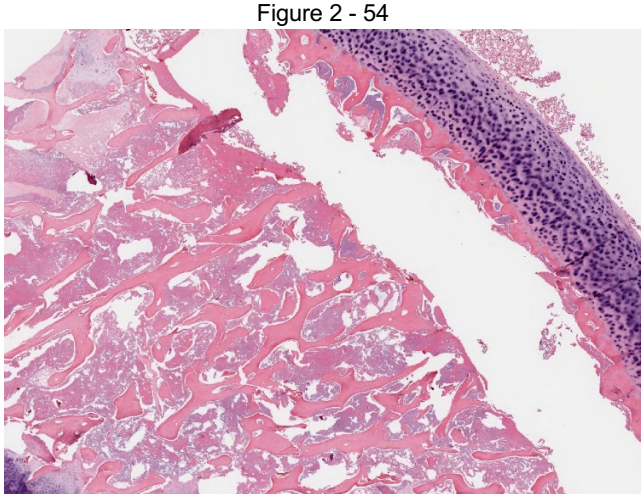

Conclusions: Accurate and reliable diagnosis of AVN requires pathologic examination, especially among older patients where the diagnosis of AVN may be less often suspected clinically. Prompt diagnosis may lead to cost avoidance, if patients make the needed lifestyle changes to reduce their risks of developing AVN elsewhere. Public health tracking and research studies relying only on clinical data for establishing a diagnosis of AVN are probably unreliable.

55 The Incidence and Significance of Calcium Pyrophosphate Dihydrate Deposits in Histologic Examinations of Total Hip, Knee, and Shoulder Joint Arthroplasties

Josephine Dermawan[1], Andrew Goldblum[2], John Reith[3], Scott Kilpatrick[1]
[1]Cleveland Clinic, Cleveland, OH, [2]Cleveland Clinic Akron General, Stow, OH, [3]Cleveland Clinic Foundation, Cleveland, OH

Disclosures: Josephine Dermawan: None; Andrew Goldblum: None; Andrew Goldblum: None; John Reith: None; Scott Kilpatrick: None

Background: Calcium pyrophosphate deposition disease (CPPD) is a metabolic arthritis which may complicate (or even cause) degenerative joint disease. The incidence and significance of these deposits among total joint resections has not been extensively studied.

Design: We retrospectively reviewed consecutive total hip, knee, and shoulder arthroplasties (n=3172), between 1/1/17 and 10/10/18, evaluated by the authors, focusing on the presence of CPPD pathologically. Clinicopathologic information including patient age (years), gender, site, underlying disease, and distribution of CPPD were correlated.

Results: For 1984 hip arthroplasties (902 males, 1082 females; ages 17-102), 54 (3%) had incidental CPPD. Specifically, the majority [46, 85% of total; 3% of DJD cases] had a clinical diagnosis of degenerative joint disease (DJD), followed by fracture (FX) [6, 11%; 2% of FX], and avascular necrosis (AVN) [2, 4%; 1% of AVN]. The mean age of patients with hip CPPD was significantly older than those without CPPD (73 vs. 66, $P < 0.0001$). Among 1106 knee arthroplasty cases (403 males, 703 females; ages 38-93), 98 (9%) had CPPD. All but 2 had a clinical diagnosis of DJD. The mean age of patients with knee CPPD also was significantly older than those without CPPD (72 vs. 68, $P < 0.0001$). For 82 shoulder joint cases (40 males, 42 females; ages 38-85), 11 (13%) had CPPD on pathologic examination, 5 (45%) with a clinical diagnosis of DJD, 4 (36%) rotator cuff injury, 1 FX, and 1 neoplasm, but there was no significant difference in age among those with and those without CPPD (67 vs. 64, $P = 0.3075$). The frequencies of CPPD in knee (9%) and shoulder (13%) were significantly higher than that in hip (3%) ($P < 0.00001$). There were no significant differences in gender ratios among any of these patient groups. Histologically, regardless of anatomic site, calcium deposits always involved the separately submitted joint capsules/synovium when sampled, but only rarely involved the adjacent articular cartilage (6.4%).

Figure 1 - 55

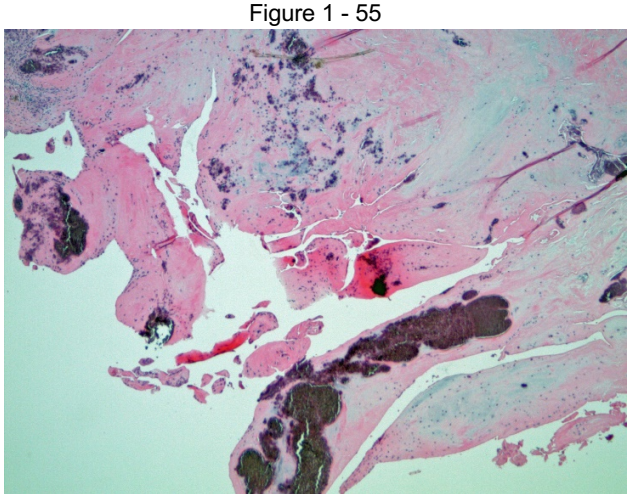

Figure 2 - 55

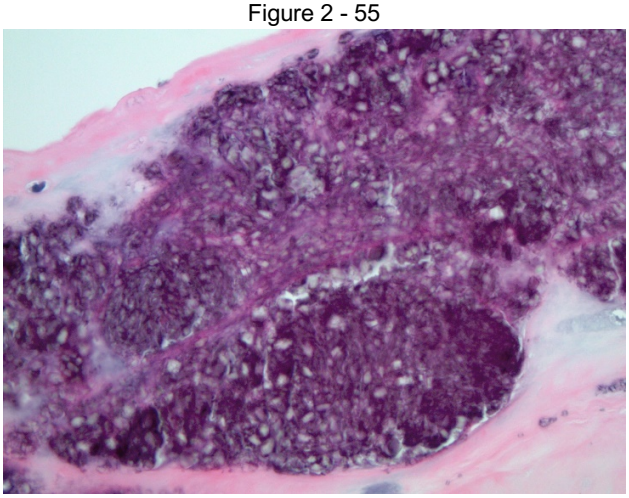

Conclusions: In total joint arthroplasties, CPPD is at least three times as likely to occur in the knees and shoulders, when compared to the hips. Patients with CPPD in the knees and hips constitute a significantly older population than those without CPPD. Among hip arthroplasties, CPPD may be found in patients presenting with DJD, AVN, or FX. To reliably establish the diagnosis of CPPD requires pathologic examination of the adjacent joint capsule/synovium, as it is only rarely seen in the articular cartilage.

56 Clinicopathological Features of Sarcoma in Patients with HIV Controlled by Combined Antiretroviral Therapy

Julio Diaz-Perez[1], Jaylou Velez Torres[1], Yin Hung[2], Smiljana Spasic[3], Jonathan Trent[4], G. Pétur Nielsen[5], Andrew Rosenberg[1]
[1]University of Miami Miller School of Medicine, Miami, FL, [2]Massachusetts General Hospital, Boston, MA, [3]University of Miami/Jackson Memorial Hospital, Miami, FL, [4]University of Miami Sylvester Comprehensive Cancer Center, Miami, FL, [5]Harvard Medical School, Boston, MA

Disclosures: Julio Diaz-Perez: None; Jaylou Velez Torres: None; Yin Hung: None; Smiljana Spasic: None; Jonathan Trent: None; Andrew Rosenberg: None

Background: Human immunodeficiency virus (HIV) infection is associated with immunodeficiency-associated malignancies including Kaposi sarcoma, lymphoma, squamous cell carcinoma, and less frequently leiomyosarcoma. The introduction of combined antiretroviral therapy has significantly reduced the incidence of these malignancies. However, patients with controlled HIV have a longer life-span and the potential to develop neoplasms. There is very little information on the clinicopathological features of sarcoma developing in patients living with controlled HIV.

Design: We analyzed the clinical and pathologic features of sarcoma arising in HIV positive patients well-controlled by antiretroviral therapy.

Results: The cohort consists of 9 patients (8 males, 1 female) with sarcoma in the setting of well-controlled HIV infection with combined antiretroviral therapy. The median age at sarcoma diagnosis was 61 years, range 27-66. The CD4 T lymphocyte count at diagnosis of sarcoma was 498/mm3, and the HIV viral load was undetectable (5 cases) or low (<400) (2 cases). 2 patients had chronic hepatitis B co-infection, 1 with hepatitis C. The diagnosis of sarcoma occurred 0.5 - 29 years, average 14 years, of living with HIV. The types of sarcoma involved included chondrosarcoma (2 cases, 1 dedifferentiated and 1 conventional), epithelioid hemangioendothelioma, dedifferentiated liposarcoma, malignant ossifying fibromyxoid tumor, histiocytic sarcoma, low grade fibromyxoid sarcoma / sclerosing epithelioid fibrosarcoma, adult-type fibrosarcoma, and leiomyosarcoma. Most cases (6) were grade 2 or 3 and tumor size range 1.8 – 21 cm, mean 10. Immunohistochemistry for HHV-8 (0/7) and in-situ hybridization for EBV (0/8) were negative in all tested cases. All sarcomas were treated with surgery and adjuvant radiation (3 cases) and chemotherapy (4 cases). Metastases were documented in 5 patients; the most common site was lung (4 cases), followed by bone (2 cases) and brain (1 case). Two patients died secondary to sarcoma, and 3 are living with disease after a median follow-up of 10.5 months.

Conclusions: Patients with HIV well-controlled by combined antiviral therapy have the potential to develop aggressive sarcomas. HHV8 and EBV oncogenic viral infection are not associated with these neoplasms. The type of sarcomas that develop in these patients differ from those in patients with poorly-controlled HIV infection. Diagnosis of HIV should not preclude optimal sarcoma management including chemotherapy, radiation therapy and surgery.

57 Xanthogranulomatous Epithelial Tumor of Soft Tissues: Report of 3 Cases of a Novel, Potentially Deceptive Lesion with a Predilection for Young Women

Karen Fritchie[1], Jorge Torres-Mora[1], Carrie Inwards[1], Rory Jackson[1], Kay Minn[1], Kevin Halling[2], Carola Arndt[1], Matthew Houdek[1], Jaime Davila[1], Andrew Folpe[1]
[1]Mayo Clinic, Rochester, MN

Disclosures: Karen Fritchie: None; Jorge Torres-Mora: None; Carrie Inwards: None; Rory Jackson: None; Kay Minn: None; Kevin Halling: None; Carola Arndt: None; Matthew Houdek: None; Jaime Davila: None; Andrew Folpe: None

Background: Epithelial marker expression and/or epithelial differentiation are features of some soft tissue neoplasms (e.g., epithelioid sarcoma, synovial sarcoma). Others (in particular endothelial and myoid tumors) show "aberrant" expression of keratins. Recently, we have encountered 3 unusual soft tissue tumors composed of bland, keratin-positive epithelial cells, which were almost entirely obscured by xanthogranulomatous inflammation, closely mimicking solitary (juvenile) xanthogranuloma (SXG). We studied these unique tumors.

Design: The morphologic features of the 3 tumors were assessed. Immunohistochemistry (IHC) for broad spectrum keratins (OSCAR, AE1/AE3), high molecular weight keratins (34betaE12), histiocytic markers (CD68, CD163, CD11c), S100 protein, endothelial markers (CD31, CD34, ERG, FLI1), myoid markers (SMA, desmin, myogenin, MyoD1), BRAFV600E, Langerin and SMARCB1 was performed. RNA-seq was performed on 2 cases. Clinical data was catalogued.

Results: Cases occurred in young females (16, 20, 22 years old) and arose in the subcutis of the posterior calf, thigh and back without dermal and/or adnexal involvement. The tumors measured 3, 3.7 and 6.5 cm. The tumors were circumscribed with a fibrous capsule containing lymphoid aggregates, and initially resembled SXG, with a sheet-like proliferation of foamy histiocytes, Touton-type giant cells, osteoclasts and inflammatory cells. Closer inspection disclosed a distinct population of uniform, cytologically bland mononuclear cells with brightly eosinophilic cytoplasm, round to reniform nuclei and pinpoint nucleoli, arranged singly and in small nests and cords. Overt squamous and/or glandular differentiation was absent. Punctate necrosis was present in one case; mitotic activity was absent. By IHC, these cells were diffusely positive with OSCAR and AE1/AE3, and focally positive for high-molecular weight keratins; endothelial and myoid markers were negative and SMARCB1 was retained. The histiocytic component expressed only CD68, CD11c and CD163. RNA-seq identified a *PLEKHM1* variant of undetermined significance in one case. Two patients with follow-up (5, 10 months) remain free of disease after excision.

Conclusions: We have identified a novel tumor of the subcutis in young females, provisionally termed "xanthogranuloma-like epithelial tumor of soft tissues". These do not appear to arise from adnexa, or represent known keratin-positive soft tissue tumors. Based on limited follow-up, they appear to behave in an indolent fashion.

58 Lipoblastomas Presenting in Older Children and Adults: Analysis of 28 Cases with Identification of a New Fibroblastic Variant

Karen Fritchie[1], Lu Wang[2], Andrew Horvai[3], Jorge Torres-Mora[1], Faizan Malik[4], Andrew Folpe[1], Armita Bahrami[5]
[1]Mayo Clinic, Rochester, MN, [2]St Jude Children's Research Hospital, Memphis, TN, [3]University of California San Francisco, San Francisco, CA, [4]University of Tennessee Health Science Center, Memphis, TN, [5]St. Jude Children's Research Hospital, Memphis, TN

Disclosures: Karen Fritchie: None; Lu Wang: None; Andrew Horvai: None; Jorge Torres-Mora: None; Faizan Malik: None; Andrew Folpe: None; Armita Bahrami: None

Background: Lipoblastomas are benign lipomatous neoplasms that typically present in the first 3 years of life and show a lobular arrangement of maturing adipocytes with variable amounts of myxoid change. We recently encountered an unusual CD34 and desmin-positive, lipomatous neoplasm showing some morphological features of lipoblastoma, but occurring in a 10-year-old male. Prompted by this case, we systematically studied the clinicopathologic and genetic features of lipoblastomas arising in older children and adults.

Design: Cases with a diagnosis of lipoblastoma or maturing lipoblastoma in patients >3 years of age were retrieved from our archives. Histologic features were assessed and catalogued as: conventional, maturing, or fibroblastic. A representative section from each tumor was immunostained for CD34 and desmin, and molecular studies (FISH, RNA sequencing) were performed on tumors with fibroblastic features. Clinical data was collected.

Results: 28 cases (12F; 16M) were identified in patients ranging from 4 to 44 years of age (median 10 years). Sites included extremity (n=19), head and neck (n=5), and trunk (n=4) with tumor sizes varying from 1.6 to 17.5 cm (median 5). The majority of tumors (n=20) were composed of variable sized lobules of mature adipose tissue partitioned by thin fibrous septa ("maturing"), while a smaller subset (n=4) had features of conventional lipoblastoma. The remaining 4 cases consisted predominantly of bland spindled to plump ovoid cells embedded in a fibrous stroma, with a vaguely plexiform arrangement of small myxoid and adipocytic nodules ("fibroblastic"). CD34 was positive in all cases tested (22/22; diffuse=21, focal=1), while desmin immunoreactivity was identified in 12 of 22 cases (diffuse=6, focal=6). The fibroblastic tumors all carried a *PLAG1* fusion, identified in 2 tumors by FISH and in 2 tumors by RNA sequencing showing *CTDSP2*-

PLAG1 and *PPP2R2A-PLAG1* fusions. 15 cases had follow-up (1 to 107 months; median 25 months), and no recurrences were reported. Molecular studies on the remaining cases are ongoing.

Conclusions: Lipoblastomas may occur in older children and adults, and may be difficult to recognize due to their predominantly adipocytic or fibrous appearance. Awareness that lipoblastomas may occur in older patients, careful evaluation for foci showing more typical morphologic features, ancillary immunohistochemistry for CD34 and desmin, and molecular genetic studies to identify *PLAG1* rearrangements are the keys to recognizing these unusual tumors.

59 Does "Low-Grade" Dedifferentiated Liposarcoma Exist? A Single Institution 25-Year Retroperitoneal Liposarcoma Experience

Danielle Graham[1], Amir Qorbani[2], Mark Eckardt[3], Lucia Chen[1], Shefali Chopra[4], Fritz Eilber[1], Sarah Dry[1]
[1]University of California Los Angeles, Los Angeles, CA, [2]University of California San Francisco Medical Center, San Francisco, CA, [3]Yale New Haven Hospital, New Haven, CT, [4]University of Southern California, San Marino, CA

Disclosures: Danielle Graham: None; Amir Qorbani: None; Mark Eckardt: None; Lucia Chen: None; Shefali Chopra: None; Fritz Eilber: *Advisory Board Member*, Certis Oncology; Sarah Dry: None

Background: Treatment options differ for dedifferentiated (DD) and well-differentiated (WD) liposarcoma (LPS). Controversy in pathologically defining the differentiation of LPS include the use of "low-grade DDLPS," as not all DDLPS are clinically aggressive. We aim to determine the association between mitotic rate in primary retroperitoneal (RP) LPS and overall survival (OS) in patients treated at a single institution with 25-year follow-up.

Design: 97 patients with primary presentation and surgical resection of RP WD/DD LPS at our institution from 1/1/1989–12/31/2013 were included. Pathology slides were evaluated for non-lipogenic areas (NLA), mitotic rate (MR)/10 HPFs and other histologic features. NLA were at least a 10x-field wide and 50% of a single slide. Cases were defined as WD (no NLA), LS0-4 (NLA, MR 0-4) or LS5+ (NLA, MR 5+). Kaplan-Meier (KM; log-rank test) and multivariate Cox analyses were performed. To study whether further grading was prognostic, a subgroup analysis of LS5+ patients was performed where these were further divided into MR 5-9 (LS5-9), MR 10-19 (LS10-19), and MR 20+ (LS20+), and the analysis was repeated.

Results: Follow-up data was available for 92/97 (95%) of patients. Median follow-up of survivors was 80 months (range 1-251 months). Distant metastases occurred in 2/97 (2%) and local recurrences in 32/97 (33%). KM showed a statistically significant difference in OS between WD, LS0-4, LS5+ (p=0.002, Figure 1). Multivariate Cox model showed no difference in OS between WD and LS0-4 groups (HR 0.50; 95% CI 0.14-1.86, p=0.301), and decreased OS between LS0-4 and LS5+ groups (HR 2.13; 95% CI 0.99-4.58, p=0.053) (Table 1). In the subgroup analysis, KM showed a statistically significant difference in OS between LS5-9, LS10-19 and LS20+ (p=0.034, Figure 2), but multivariate Cox model revealed no difference in OS between LS5-9 and LS10-19 (HR 0.57; 95% CI 0.17-1.86, p=0.352) or LS 5-9 and LS20+ groups (HR 1.76; 95% CI 0.49-6.28, p=0.382) (data not shown).

Table 1: Multivariate Cox model demonstrating the association between the comparison groups (WD, LS0-4, LS5+) and OS in patients treated for RP LPS from 1/1/1989-12/31/2013 (n=97).

Characteristic	HR (95% CI)	p
WD (ref=LS0-4)	0.50 (0.14-1.86)	0.301
LS5+ (ref=LS0-4)	2.13 (0.99-4.58)	0.053
M (ref=F)	1.04 (0.53-2.05)	0.903
Age at diagnosis (yrs)	1.03 (1.00-1.06)	0.050
Tumor size (cm)	1.00 (0.97-1.03)	0.785

Figure 1 - 59

Figure 1: Kaplan-Meier survival estimates comparing WD, LS0-4, and LS5+ in patients treated for RP LPS from 1/1/1989-12/31/2013 (n=97, p=0.002).

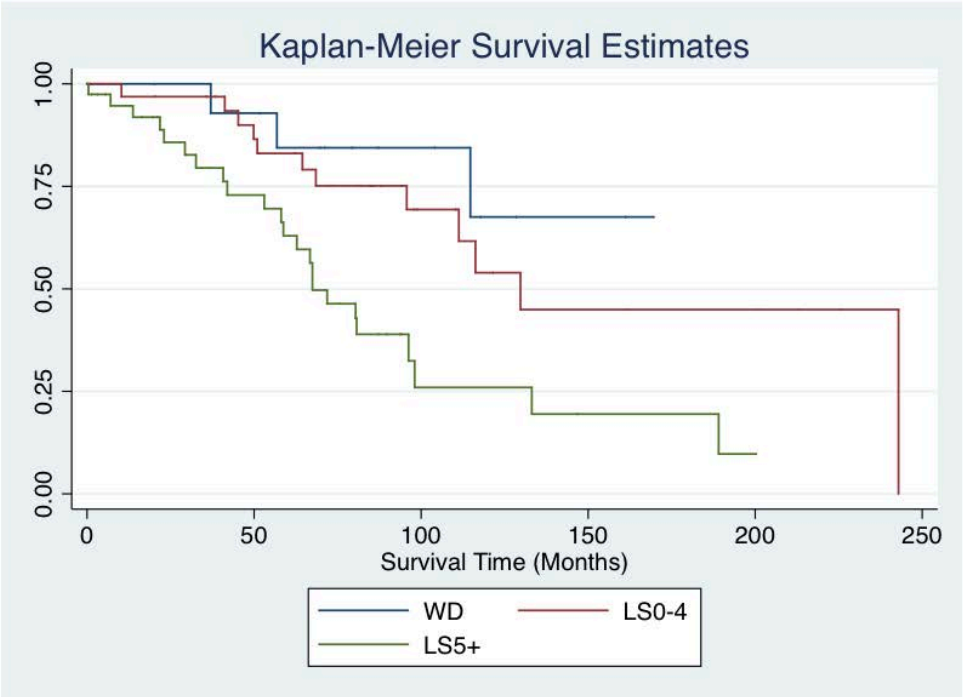

Figure 2 - 59

Figure 2: Kaplan-Meier survival estimates comparing LS5-9, LS10-19, and LS20+ in patients treated for RP LPS from 1/1/1989-12/31/2013 (n=40, p=0.034).

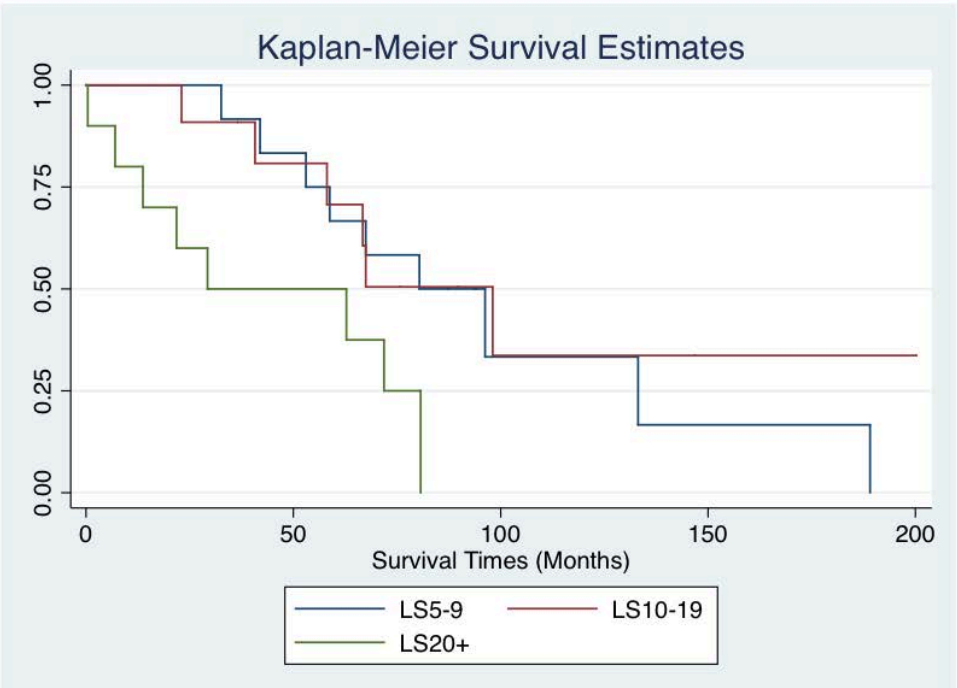

Conclusions: LS5+ RP LPS at primary presentation had decreased OS compared to WD and LS0-4 with no difference in OS between WD and LS0-4. This suggests "DD" should be used only for MR 5+, while patients with MR 0-4 can be called WD or "cellular WD" LPS. Further subdivision of LS5+ showed a significant trend in OS, yet multivariate Cox analysis did not show significance, suggesting that grading in this group is of uncertain prognostic significance.

60 Molecular and Immunohistochemical Reappraisal of Desmoplastic Fibromas Reveals a Subset of Misclassified Low-Grade Central Osteosarcomas

Omar Habeeb[1], Justin Cates[2], Scott Kilpatrick[1], Jacquelyn Knapik[3], John Reith[4]
[1]Cleveland Clinic, Cleveland, OH, [2]Vanderbilt University Medical Center, Nashville, TN, [3]University of Florida College of Medicine, Gainesville, FL, [4]Cleveland Clinic Foundation, Cleveland, OH

Disclosures: Omar Habeeb: None; Justin Cates: None; Scott Kilpatrick: None; Jacquelyn Knapik: None; John Reith: None

Background: Desmoplastic fibroma is a locally aggressive neoplasm of bone composed of fascicles of bland spindle cells lacking bone production, closely resembling fibromatosis. Low-grade central osteosarcoma (LGCOS), on the other hand, is a malignant bone-forming neoplasm containing bland fibrous stroma with foci of bone formation, characterized by amplification of the *MDM2* locus on chromosome 12q15. Occasionally, LGCOS will contain large areas of fibroblastic stroma devoid of bone, resembling benign fibroblastic neoplasms, particularly when sampling is limited. We reviewed seven cases of desmoplastic fibroma to determine whether any harbored *MDM2* amplification by fluorescence *in situ* hybridization (FISH) or nuclear reactivity for MDM2 by immunohistochemistry (IHC), thus redefining these as LGCOS.

Design: Seven cases of desmoplastic fibroma were collected from the archives of three academic medical centers or the consultation files of the authors from 1996-2019. Immunohistochemical staining for MDM2 and FISH for *MDM2* gene amplification was performed. FISH for DDIT3 was also performed for a single case.

Results: Seven cases initially diagnosed as desmoplastic fibroma were evaluated. All were characterized histologically by fascicles of bland spindle cells lacking cytologic atypia and mitotic activity. Bone formation, when present, was limited to very small foci. The patients included 5 females and 2 males ranging in age from 19-74 years. Lesions arose in the vertebrae (2 cases), 8th rib, scapula, ulna, femur, and ilium. Two of 7 (29%) cases demonstrated *MDM2* amplification by FISH, one of which was also immunoreactive for MDM2 by IHC. One of the cases with *MDM2* amplification also showed amplification of *DDIT3*. Of the cases with *MDM2* amplification, one was initially diagnosed as a desmoplastic fibroma, the other initially as an aneurysmal bone cyst, then as a non-ossifying fibroma, and finally as a desmoplastic fibroma following multiple biopsies. The remaining 5 cases were negative by both IHC and FISH, thereby supporting their diagnoses as desmoplastic fibroma (Table 1).

Case	Age	Gender	Site	Primary Dx	MDM2 by IHC	MDM2 by FISH
1	36	Female	Scapula	Desmoplastic fibroma	Negative	Amplified
2	19	Female	Femur	Aneurysmal bone cyst, non-ossifying fibroma vs. desmoplastic fibroma	Positive	Amplified (also DDIT3 amplified)
3	19	Female	Ulna	Desmoplastic fibroma	Negative	Unamplified
4	20	Female	L4 spine	Desmoplastic fibroma	Negative	Unamplified
5	74	Female	8th rib	Desmoplastic fibroma	Negative	Unamplified
6	60	Male	C6 vertebra	Desmoplastic fibroma	Negative	Unamplified
7	42	Male	Left ilium	Desmoplastic fibroma	Negative	Unamplified

Conclusions: These findings suggest that a subset of lesions diagnosed as desmoplastic fibroma will harbor amplification of the *MDM2* gene, thereby establishing that they are better classified as LGCOS. Not all *MDM2*-amplified lesions are immunoreactive for MDM2 by IHC. We recommend that any lesion suspected to be desmoplastic fibroma be routinely evaluated by both immunohistochemistry and FISH for MDM2 expression and amplification.

61 Clinicopathologic and Molecular Characteristics of Dedifferentiated Chordoma

Yin Hung[1], G. Pétur Nielsen[2], Andrew Rosenberg[3], Julio Diaz-Perez[3]
[1]Massachusetts General Hospital, Boston, MA, [2]Harvard Medical School, Boston, MA, [3]University of Miami Miller School of Medicine, Miami, FL

Disclosures: Yin Hung: None; G. Pétur Nielsen: None; Andrew Rosenberg: None; Julio Diaz-Perez: None

Background: Chordoma is a rare malignant bone tumor exhibiting notochordal differentiation. Dedifferentiated chordoma is an unusual subtype with a biphasic appearance, comprising a high-grade sarcoma juxtaposed to conventional chordoma. Clinicopathologic and molecular features of dedifferentiated chordoma remain poorly understood.

Design: Surgical pathology files from 1990-2019 of 2 institutions and 1 author were searched for cases of dedifferentiated chordoma. Clinicopathological features were reviewed. Targeted next-generation DNA sequencing was performed in select cases.

Results: Of >1000 chordoma patients, dedifferentiated chordomas were identified in 9 (<1.0%; 7 men, 2 women; age 25-80 [median 62] years), involving sacrum (including 3 as local recurrence at 75-114 months after initial diagnosis) in 5, and 1 each in lumbar region, splenoid, clivus, and lung as metastasis (at 28 months after initial diagnosis). The tumor size ranged from 0.9-22.0 (median 5.5) cm. The sarcomatous components comprised 3-99% (median 60%) of the tumor and showed predominantly pleomorphic or fibrosarcomatous, rarely osteosarcomatous morphology; whereas the chordoma component is of conventional type in 7 tumors and chondroid type in 2 tumors. By immunohistochemistry, expression of brachyury and cytokeratins was strong/diffuse in the chordoma component but entirely lost/diminished in the sarcomatous component in 8 cases tested. p53 was of wild-type pattern in the chordoma component but aberrantly over-expressed in the sarcomatous component in 2 cases tested. Targeted next-generation sequencing in 3 cases identified pathogenic mutations in tumor suppressors/epigenetic regulators: *TP53* and *PTEN* each in 2 tumors; *CDKN2A*, *RB1*, *KMT2C*, and *FBXW7* each in 1 tumor. Of the 7 patients with available follow-up, 5 developed multiple metastases in visceral organs, and 4 died of disease at 15-99 (median 24) months after diagnosis of dedifferentiated chordoma.

Conclusions: Dedifferentiated chordomas usually arise in the sacrum, present *de novo* or as recurrence/metastasis months-to-years after the initial chordoma diagnosis, and exhibit an aggressive clinical course. The aberrant p53 over-expression and loss of brachyury in the sarcomatous components, along with recurrent mutations in *TP53* and *PTEN*, implicate dysregulation of tumor suppressors in chordoma dedifferentiation and potential therapeutic targets.

62 Gastrointestinal Stromal Tumor KIT Mutation Rates Vary by Patient and Tumor Characteristics

Yin Hung[1], J. Bryan Iorgulescu[2]
[1]Massachusetts General Hospital, Boston, MA, [2]Boston, MA

Disclosures: Yin Hung: None; J. Bryan Iorgulescu: None

Background: Gastrointestinal Stromal Tumors (GISTs) are often driven by activating mutations in the tyrosine receptor kinase *KIT* oncogene, Herein we evaluate the clinical and tumor characteristics associated with *KIT* mutations nationwide.

Design: Patients newly-diagnosed with a GIST were identified from the National Cancer Database (comprising >70% of newly-diagnosed cancers in the US) between 2010-2016 were identified and evaluated for patient, GIST, and molecular characteristics using multivariable logistic regression.

Results: 14,324 pathologically-diagnosed GISTs were identified, 7,725 with complete KIT testing data. In these cases, KIT IHC was only conducted in 62%, in which 93% were KIT positive; whereas KIT molecular testing was conducted in 64%, in which 89% were positive for KIT mutations.

In multivariable logistic regression, *KIT* mutations (by molecular testing) were more common in patients 60+ year-old and black or Asian/pacific islander race/ethnicity, and in tumors ≤2cm or located in the rectum and small intestines (Table 1); and less common in young patients and esophageal GISTs. *KIT* mutation rates were not associated with sex or mitotic rate. The rate of *KIT* mutation ranged from 78% of esophageal GISTs to 96% of rectal GISTs (p=0.001). Exon 11 was the predominant mutated *KIT* locus across all tumor locations. The stomach was the predominant site for GISTs with exon 11 (55%) mutations; whereas the small intestines predominated for GISTs with exon 9 (59%) and exon 13 (47%) mutations (p<0.001).

In GISTs with negative KIT IHC, KIT mutations were detected in 14% of cases – the majority involving exon 11. Conversely, 4% of KIT IHC positive cases were negative by KIT molecular testing.

		Multivar logistic regression for having KIT mutations		
		OR	**95%CI**	**p-val**
Age at Diagnosis (yr)				
	<40	0.39	(0.28-0.55)	<0.001
	40-59	0.77	(0.62-0.95)	0.01
	60-79		Reference	
	80+	1.56	(1.01-2.41)	0.04
Sex				
	Male		Reference	
	Female	1.04	(0.86-1.26)	0.71
Race/Ethnicity				
	White		Reference	
	Black	1.54	(1.16-2.04)	0.003
	Asian/Pacific islander	1.81	(1.07-3.06)	0.03
	Hispanic	1.00	(0.69-1.45)	0.98
	Other/Unknown	0.81	(0.43-1.52)	0.52
GIST Mitotic Rate				
	≤5 mit/50HPF		Reference	
	>5 mit/50HPF	1.19	(0.93-1.52)	0.16
GIST Size (cm)				
	≤2		Reference	
	2 to ≤5	0.63	(0.44-0.91)	0.02
	5 to ≤10	0.68	(0.47-1)	0.05
	>10	0.58	(0.39-0.86)	0.007
GIST Location				
	Stomach		Reference	
	Small intestines	1.34	(1.07-1.67)	0.01
	Rectum	3.22	(1.17-8.83)	0.02
	Peritoneum	0.58	(0.31-1.08)	0.08
	Colon	0.72	(0.36-1.44)	0.36
	Esophagus	0.35	(0.14-0.88)	0.03

Conclusions: *KIT* mutations are more common in older patients and patients with black or Asian/pacific islander race/ethnicity; as well as in smaller tumors or rectal/small intestinal GISTs. GISTs with exon 9 or exon 13 mutations are more likely to involve the small intestines than stomach. Because approximately 13% of GISTs with negative KIT IHC demonstrate *KIT* mutations, molecular testing should be considered in cases with characteristic histology of GIST but negative KIT IHC. Additionally, in order to serve as a reliable and sensitive marker of GISTs, KIT IHC protocols must be properly titrated – 4% of positive KIT IHC cases nationwide were in fact negative by molecular testing.

63 RNA-seq Analysis of Gastrointestinal Stromal Tumors

Soumya Jaladi[1], Jaime Davila[2], Jesse Voss[2], Rory Jackson[2], Mounika Angirekula[2], Mazen Atiq[2], Benjamin Kipp[2], Rohini Mopuri[2], Cristiane Ida[3], Kay Minn[4], Kevin Halling[2]
[1]University of Louisville, Louisville, KY, [2]Mayo Clinic Rochester, Rochester, MN, [3]Rochester, MN, [4]Mayo Clinic, Rochester, MN

Disclosures: Soumya Jaladi: None; Jaime Davila: None; Jesse Voss: None; Rory Jackson: None; Mounika Angirekula: None; Mazen Atiq: None; Benjamin Kipp: None; Rohini Mopuri: None; Cristiane Ida: None; Kay Minn: None; Kevin Halling: None

Background: KIT and PDGFRA mutations are found in approximately 85% and 10% of gastrointestinal stromal tumors (GIST's), respectively. DNA next generation sequencing (NGS) or Sanger sequencing is routinely performed on these tumors to identify mutations in

the KIT and PDGFRA to predict response to imatinib and second and third generation KIT and PDGFRA inhibitors. Few if any studies have assessed the ability of RNA-seq to detect KIT and PDGFRA mutations in GIST's.

Design: Twenty-six GIST's that had previously been assessed for KIT and PDGFRA mutations by DNA NGS in the Mayo Clinic Genomics laboratory were identified. Nineteen had a KIT mutation, 3 had a PDGFRA mutation and 4 were wild type. Of the 26, only 23 had a successful RNA-seq analysis, 20 tumors with a mutation and 3 wildtype. Of the 20 tumors with a mutation, 9 had a deletion, 5 had an insertion, and 6 had a single nucleotide variant. All of the indel mutations were in-frame and ranged from 3-45 base pairs (bp) in length. Whole transcriptome RNA-seq analysis was performed using the Agilent SureSelectXT RNA direct library preparation kit with v7 baits. Bioinformatic analysis utilized our in house developed MAPRSeq v3 pipeline.

Results: RNA-seq analysis using the STAR aligner detected 16/17 KIT mutations and all 3 PDGFRA mutations. The only mutation that RNA-seq did not detect was a 45bp indel (50bp deletion with a 5bp insertion) and on further inspection we found evidence of the indel as low frequency event(<10% of the reads) in the original sequencing files and evidence of soft-clipped reads supporting the indel on the alignment file. An additional advantage of RNA-seq over DNA NGS is that it can measure the level of expression of the mutant gene. All cases with a mutation identified by DNA NGS exhibited a high level of mRNA expression by RNA-seq which is consistent with the activating nature of these mutations. One tumor with a 1648-2 to 1674 deletion by DNA NGS was proven to lead to a new acceptor splice site by RNA-seq.

Conclusions: These findings demonstrate the ability of RNA-seq to accurately detect mutations that are detected by DNA NGS with the extra benefit of being able to determine the level of expression of the mutated gene. RNA-seq is also able to confirm the effect of putative splice site mutations identified by DNA NGS. Further bioinformatic analyses are ongoing to determine if RNA-seq identifies mutations in other genes that are infrequently mutated in GIST's such as BRAF and the SDH genes.

64 The Genomic Landscape of Low-Grade Cartilage Tumors Distinguishes Enchondroma from Chondrosarcoma

Nancy Joseph[1], Kevin McGill[1], Andrew Horvai[1]
[1]*University of California San Francisco, San Francisco, CA*

Disclosures: Nancy Joseph: None; Kevin McGill: None; Andrew Horvai: None

Background: Low-grade cartilage tumors of bone include enchondroma (EC) and low-grade chondrosarcoma (CS). Despite careful clinical-pathologic-radiographic correlation, overlapping diagnostic features and small sample size preclude definitive classification of a subset of cartilage tumors resulting in an intermediate "atypical cartilage tumor" (ACT) category. Whether ACT represents a true intermediate biologic potential between EC or CS or a heterogeneous group that can be classified as either EC or US is unknown. The genomic landscape of these tumors is poorly understood but may inform an improved classification. Here we studied a group of well-characterized EC, low-grade CS and ACT using next-generation sequencing to identify abnormalities that provide diagnostic information.

Design: Twenty-five low-grade cartilage tumors were classified as EC (n=10), grade 1 CS (n=6) and ACT (n=9) based on a clinical, radiographic and pathologic findings. Capture-based next-generation sequencing targeting the coding regions of 479 cancer genes and select introns was performed on extracted genomic DNA from all 25 cases. Single nucleotide variants, insertions/deletions, copy number alterations (CNAs), and selected rearrangements were evaluated.

Results: Seventy percent of ECs demonstrated *IDH1* or *IDH2* hotspot activating mutations and 40% had either duplication or deletion of *COL2A1* (Figure 1). Eighty % of EC had no CNAs with the remaining 20% showing only 1-3 copy number losses. Similarly, 89% and 67% of ACT had hotspot mutations in *IDH1*/*IDH2* or *COL2A1* alterations, respectively and 78% of cases showed no CNAs. One (11%) ACT showed rare CNAs and one (11%) had multiple copy number losses and *COL2A1* deletion. In contrast, 17% of CS had *IDH1* or *IDH2* alterations, 100% demonstrated alteration of *COL2A1*, and 67% had genomes with numerous CNAs. 80% of CS demonstrated truncating mutations or deep deletions in an additional tumor suppressor gene including *CDKN2A, SETD2*, *PALB2*, and *MRE11.* (Figure 1)

Figure 1 - 64

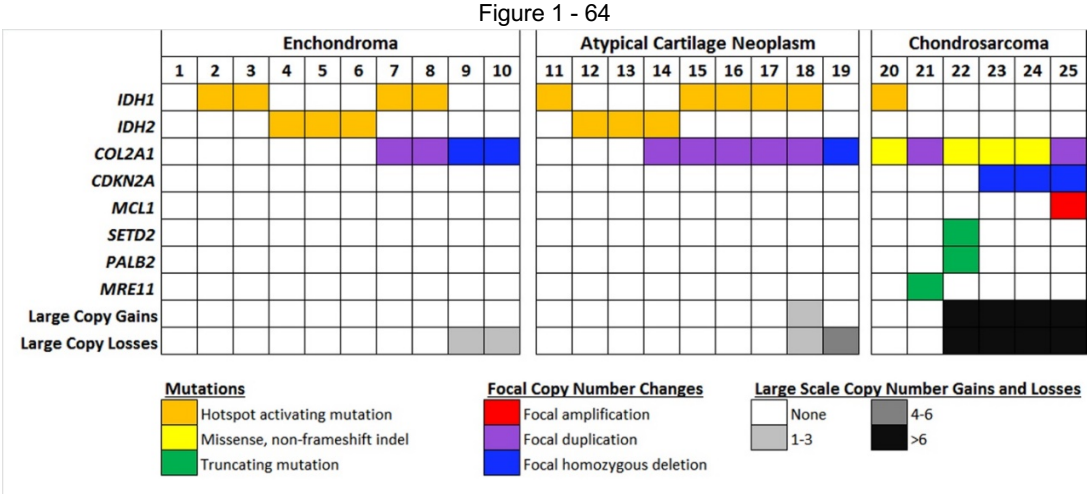

Conclusions: Our data demonstrate that mutations in *IDH1*, *IDH2*, and *COL2A1* do not discriminate among low-grade cartilage tumors. However, truncating mutations or homozygous deletion of tumor suppressor genes including *CDKN2A, SETD2, PALB2*, and *MRE11* and numerous CNAs are specific to low-grade chondrosarcoma. Eight of nine ACT in our study were genomically indistinguishable from enchondroma. One ACT demonstrated *COL2A1* alteration and multiple copy number losses, raising concern for chondrosarcoma.

65 PHF1-TFE3-rearranged Ossifying Fibromyxoid Tumors (OFMT): Are They Overrepresented Among Malignant OFMT?

Antonina Kalmykova[1], Jiří Lenz[2], Marian Svajdler[3], Michal Michal[3], Michael Michal[4]
[1]Kyiv, Ukraine, [2]Department of Pathology, Znojmo Hospital, Czech Republic, Znojmo, Czech Republic, [3]Biopticka laborator s.r.o., Plzen, Czech Republic, [4]Biopticka Laborator Ltd., Plzen, Czech Republic

Disclosures: Antonina Kalmykova: None; Jiří Lenz: None; Marian Svajdler: None; Michal Michal: None; Michael Michal: None

Background: OFMT is a tumor of intermediate malignant potential. Criteria identifying the relatively minor subset of cases with a higher risk of malignant behavior have been established (Folpe 2003). About 80% of OFMT cases harbor rearrangements of the *PHF1* gene, most commonly fused with the *EP400 gene*. A recent study reported a novel *PHF1-TFE3* fusion in 5 OFMT cases, 3 of which were classified as malignant. In our practice, we have encountered 2 OFMT with an identical fusion. The aim of this study was to present these 2 cases as well as to analyze all cases of malignant OFMT from our archive in order to establish, whether this novel fusion is overrepresented among the aggressive subset.

Design: The 2 cases with *PHF1-TFE3* fusion were recently detected by RNA-seq (Archer FusionPlex) and confirmed by RT-PCR. Using the criteria for malignancy described previously, we identified 7 cases of malignant OFMT with appropriate material for analysis with the *TFE3* FISH probe.

Results: The clinicopathological features of the PHF1-TFE3-rearranged OFMT are listed in the Table. Case 1 was a well-circumscribed multinodular tumor growing in moderately cellular cords and trabeculae. The tumor cells had moderate to high nuclear grade and showed 6 mitoses/50 HPF. The background stroma was mostly sclerotic, occasioning a close resemblance of the tumor to sclerosing epithelioid fibrosarcoma (Fig. 1). No ossification was present. The patient had a metastatic disease at presentation showing similar features but higher mitotic activity (10/50 HPF). Case 2 had an uncharacteristic lace-like growth pattern consisting of moderately cellular proliferation of relative bland cells in predominantly myxoid stroma, ossified areas were absent as well (Fig. 2). Two mitoses/50 HPF were detected. This case was classified as atypical OFMT. The patient had no metastases at presentation. Among the 7 malignant OFMTs, no case showed *TFE3* gene break by FISH.

	Case 1 – Fig. 1	**Case 2** – Fig. 2
Age/Sex	56/M	60/M
Location	Subcutis of the shin	Back of the thigh
Size (cm)	4 nodules altogether 3x2.5x2.5	4.5x2x2
Outcome	Inguinal LN mets at presentation	NA (no mets at presentation)
Original diagnosis	Sclerosing Ep. Fibrosarcoma	Myxofibrosarcoma grade 1
Tumor border	Sharp	Sharp
Capsule	No	No
Growth pattern	Cords and trabeculae	Uncharacteristic, lace-like
Cellularity	Moderate/high	Moderate
Nuclear grade	Medium	Low
Mitoses/50 HPF	6 (10 in the metastasis)	2
Necrosis	No	No
Stroma	Hyalinized, focally fibromyxoid	Myxoid
Overall histology	Malignant	Atypical
S100	Diffuse positivity (Fig. 1)	Neg.
TFE3	Diffuse nuclear positivity	Diffuse nuclear positivity (Fig. 2)
CD10	Diffuse positivity	Diffuse positivity
Ki-67	30%	<1%
Negative IHC	AE1/3, Desmin, SMA, MUC4, EMA, Claudin-1, CD34, Sox-10, HMB-45	AE1/3, Desmin, SMA, MUC4, EMA, BCOR, ERG, Beta-catenin
Fusion breakpoints	*PHF1*(Ex 13) - *TFE3*(Ex 7)	*PHF1*(Ex12) - *TFE3*(Ex7)

Figure 1 - 65

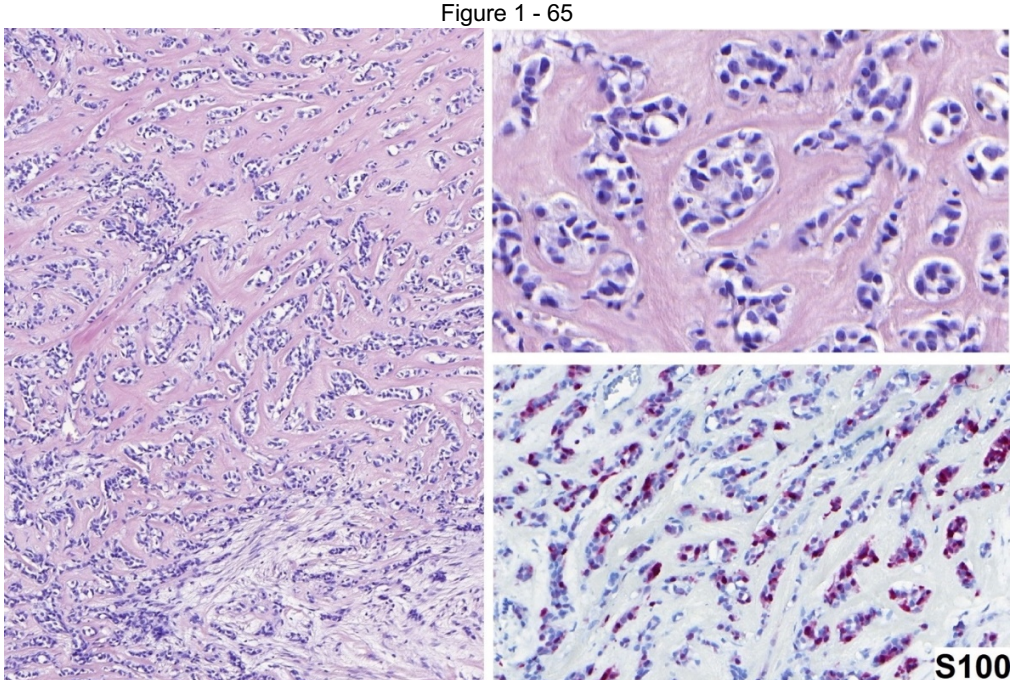

Figure 2 - 65

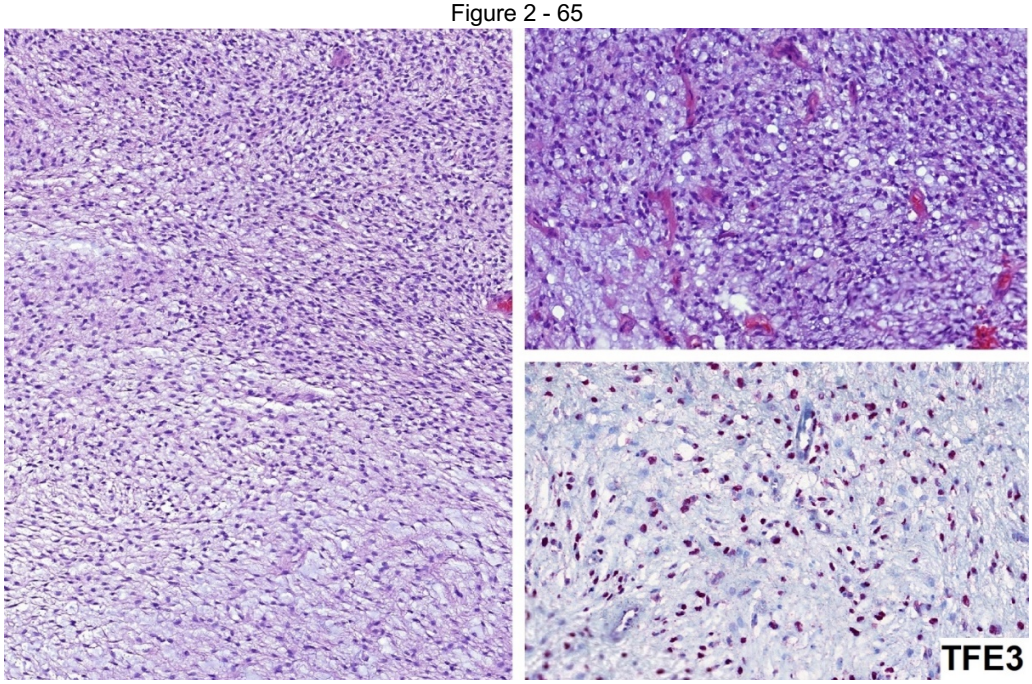

Conclusions: We report 2 novel cases of *PHF1-TFE3*-rearranged OFMT, one with both malignant histology and behavior. Although in the second case the behavior is yet unknown, histologically the tumor was classified as atypical. Based on the available data, the *PHF1-TFE3* fusion seems to be associated with a higher chance of atypical/malignant histology and aggressive behavior. However, probably due to the rarity of this molecular aberration, *PHF1-TFE3* fusion is not overrepresented among the malignant subset of OFMT.

66 Giant Cell Tumor of Extracraniofacial Bone - Clinicopathological Analysis of 263 Cases

Eiichi Konishi[1], Yasuaki Nakashima[2], Masayuki Mano[3], Shigenori Nagata[4], Yuko Kuwae[5], Yumiko Hori[6], Takeshi Inoue[7], Hironori Haga[8], Yukiko Morinaga[1], Hidetatsu Outani[6], Toshiharu Shirai[1], Shigeki Kakunaga[9], Norifumi Naka[4], Masanari Aono[7], Manabu Hoshi[10], Jyunya Toguchida[11]

[1]Kyoto Prefectural University of Medicine, Kyoto, Japan, [2]Kyoto University, Kyoto, Kyoto, Japan, [3]National Hospital Organization Osaka National Hospital, Osaka, Japan, [4]Osaka International Cancer Institute, Osaka, Japan, [5]Osaka City University Graduate School of Medicine, Osaka City, Japan, [6]Osaka University Hospital, Suita, Osaka, Japan, [7]Osaka City General Hospital, Osaka, Japan, [8]Kyoto, Japan, [9]Osaka National Hospital, Osaka, Japan, [10]Osaka City University Hospital, Osaka, Japan, [11]Kyoto University, Kyoto, Japan

Disclosures: Eiichi Konishi: None; Yasuaki Nakashima: None; Yuko Kuwae: None; Takeshi Inoue: None; Hironori Haga: None; Norifumi Naka: None; Manabu Hoshi: None

Background: Giant cell tumor of bone (GCTB) is categorized as an intermediate grade tumor, which can recur locally and metastasize mainly in lung. In the previous literatures, no reliable histological predictors for local recurrence have been found. In this study, we analyze clinicopathological characteristics of GCTB of extracraniofacial bones statistically, to elucidate predictive features for the local recurrence.

Design: Clinicopathological profiles of 263 cases of histologically proven GCTB of extracraniofacial bones were retrieved. All cases had first surgery in the Kansai Musculoskeletal Oncology Group, Japan. Pathological slides obtained at the surgery were reviewed. For each case, thirteen pathological features, such as mitotic count, ischemic necrosis, etc. were evaluated by numerical scoring. These numerical scores and clinical profiles, such as age, gender, were analyzed statistically in terms of prognostic significance. Statistical analyses were performed with SPSS Statistics 26 (IBM, Armonk, NY, USA).

Results: Of 263 Japanese patients, 137 were females and 126 were males (Female: Male=1.09:1). Age ranged 9-80 years (Average 38.3 years). Long bones were most frequently affected (223 cases, 84.8%), especially around knee (163 cases, 62.0%). Histologically, mitotic figures (78.6%, average 3.75/10HPF), stromal hemorrhage (96.6%), secondary aneurysmal bone cyst (76.4%) and area of spindle cells (98.9%) were quite common. Bone/osteoid formation (53.4%), foamy cell infiltrate (52.3%) and storiform pattern (62.2%) were also noted. Permeative growth pattern, such as entrapment, was uncommon (4.7%). Within a follow-up period [1–316 months (average 88.9 months)], the local recurrence rate was 27.0% [1-131 months (average 27.2 months)]. Cox regression analysis on age, sex, type of bone, type of surgical procedure, mitotic count, vascular invasion, stromal hemorrhage, ischemic necrosis, ossification, and denosumab administration

showed that age, type of surgical procedure, denosumab administration and mitotic count were each statistically significant factor (P<0.05) for local recurrence.

Figure 1 - 66

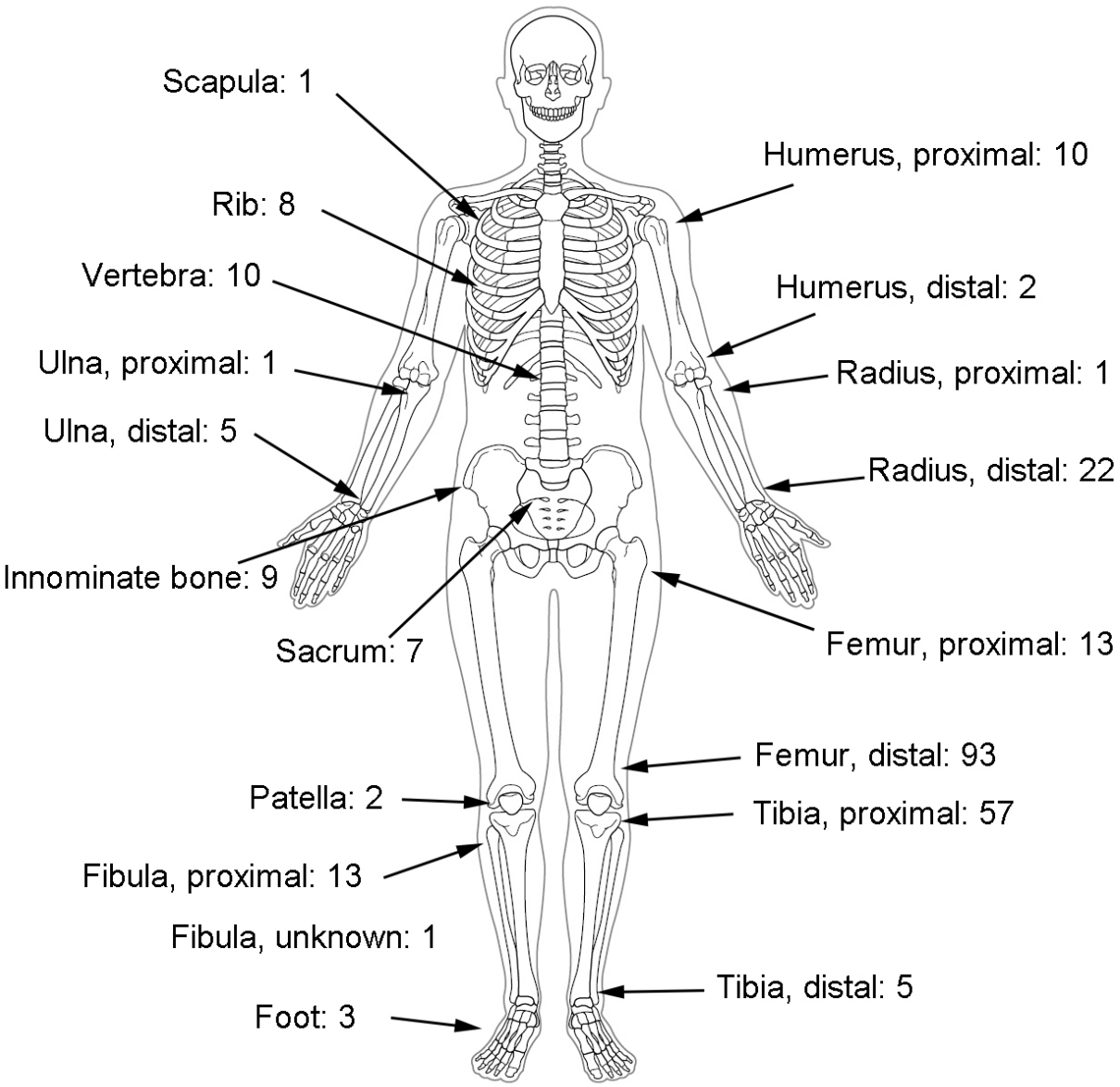

Conclusions: Features predicting local recurrence of GCTB of extracraniofacial bones were more mitotes, younger age, non-curettage surgical procedure and denosumab administration. Only mitotic count was significant among pathological findings, which has not been reported previously. We have done neither radiological analysis nor analysis of metastatic disease, yet. Further investigation is mandatory.

67 Sclerosing Epithelioid Fibrosarcoma of Bone: Morphological, Immunophenotypical and Molecular Findings of 8 Cases

Kemal Kosemehmetoglu[1], Michael Michal[2], Fisun Ardic[3], VP Sumathi[4]
[1]Hacettepe University, Ankara, Turkey, [2]Biopticka Laborator Ltd., Plzen, Czech Republic, [3]Ankara, Turkey, [4]Royal Orthopaedic Hospital, Birmingham, West Midlands, United Kingdom

Disclosures: Kemal Kosemehmetoglu: None; Michael Michal: None; Fisun Ardic: None; VP Sumathi: None

Background: Sclerosing epithelioid fibrosarcoma (SEF) is known to occur primarily in bone, but due to its rarity, very few cases have been reported so far. Here, we present clinicopathological, immunohistochemical and molecular features of 8 cases of primary SEF of bone.

Design: Clinicopathological findings were recorded. MUC4 (Invitrogen, 8G-7, 1:200, Leica Autostainer) and SATB2 (Santa Cruz, sc-81376, 1:50, manual) immunostains were performed.

Results: M:F was 5:3 with a mean age of 39 (range; 14-71). The majority of tumors were located in flat bones, whereas only one case involved a long bone (tibia). One case also had metachronous soft tissue mass in the upper arm. Radiological presentation was mixed sclerotic and lytic, infiltrative or expansile mass with ill-defined borders. Median tumor size was 6 cm (range; 2.5-9 cm). Macroscopically, tumors had a solid, homogeneous, cream-white colored cut surface devoid of hemorrhage or necrosis. Previous diagnoses were SEF in 3 cases, low-grade osteosarcoma in 2 cases, chondrosarcoma and chondromyxoid fibroma in 1 case each.

Histopathologic examination revealed classical morphology of SEF of soft tissue: small-medium sized, monotonous epithelioid with round nuclei and narrow, pale, eosinophilic cytoplasm. Neither significant mitotic activity nor obvious necrosis was detected. Prominent vasculature was noted in 3 cases. Osteoid-like material was encountered in two cases, while parallel bone trabeculae were seen in one case each. Two cases had features of hybrid SEF/low-grade fibromyxoid sarcoma.

Immunohistochemically, all cases showed diffuse and strong MUC4 expression. In addition, focal EMA (1/4) and focal SATB2 (2/4) positivity were detected. EWSR1 rearrangement was detected in 3 cases by FISH. EWSR1-CREB3L1 and ESWR1-CREB3L2 fusion genes were identified in 2 cases by next-generation sequencing.

Recurrence was observed in one case and metastasis in 3 cases. Metastases were to the ribs, pelvic bones, and lungs. All but one patient were alive with disease for a mean survival of 30 months. One case showed a very good response to neoadjuvant radio/chemotherapy.

Case	Age	Sex	Site	Size (cm)	Morphology	MUC4	SATB2	Other IHC	Molecular Findings	Outcome
#1	34	M	L scapula	7	Classical	+	-	EMA-	Break-apart FISH: EWSR1 NGS: EWSR1-CREB3L2	AWD, 26 mos, met to pelvic bones
#2	23	M	L mandible	5.3	Classical	+	focal	Cam5.2-	Breakapart FISH: EWSR1	AWD, 72 mos, met to ileum and lung
#3	14	M	L maxilla	6	Classical	+	focal	EMA-, AE1/3--, desmin-, myogenin-, myoD1-, S100-, Ki67 20%	Break apart FISH: EWSR1	AWD, 60 mos, recurrence
#4	36	M	L 3rd costa	7	Hybrid	+	NA	EMA focal, SMA-, S100-, Ki67 10%	NA	AWD, 12 mos
#5	59	F	R tibia	9	Classical	+	NA	AE1/3-, LCA-, desmin-, Ki67 10%	NA	AWD, 3 mos
#6	71	M	R clavicle	NA	Classical	+	-	AE1/3-, S100-, desmin-, SMA-	NA	DOD, 24 mos, met to lung, rib, pelvis
#7	22	F	C6-T1	2.5	Classical	+	NA	EMA-, AE1/3-, CD31-, CD34-, ERG-, Brachyury-	NGS: EWSR1(Ex10)-CREB3L1(Ex6) with EWSR1 deletion Ex8 and 9	AWD, recent
#8	51	F	L3-S1	2.5	Hybrid	+	NA	EMA-, AE1/3-, CD34-, desmin-, SMA-, S100-, Ki67 5-10%	NA	AWD, 12 mos

Conclusions: This is the first series of primary skeletal SEF with molecular findings. SEF of the bone is a very rare, relatively indolent sarcoma of young adults with slight male predominance, essentially located in the flat bones and is often misdiagnosed due to overlapping histological features with osteosarcoma and chondroid tumors. There is a conspicuous tendency for bone metastasis.

68 Detection of Fusion Genes in Inflammatory Myofibroblastic Tumor/Inflammatory Pseudotumor by Nanostring-Based Screening System

Taisei Kurihara[1], Yoshiyuki Suehara[1], Keisuke Akaike[2], Takuo Hayashi[3], Shinji Kohsaka[4], Nobuhiko Hasegawa[4], Tatsuya Takagi[1], Taketo Okubo[1], Youngji Kim[1], Takashi Yao[5], Kazuo Kaneko[1], Tsuyoshi Saito[1]

[1]Juntendo University, School of Medicine, Tokyo, Japan, [2]Juntendo University, Bunkyo-ku, Tokyo, Japan, [3]Juntendo University Graduate School of Medicine, Tokyo, Japan, [4]Division of Cellular Signaling, National Cancer Center Research Institute, Tokyo, Japan, [5]Juntendo University, Tokyo, Japan

Disclosures: Taisei Kurihara: None; Yoshiyuki Suehara: None; Keisuke Akaike: None; Takuo Hayashi: None; Shinji Kohsaka: None; Nobuhiko Hasegawa: None; Tatsuya Takagi: None; Taketo Okubo: None; Youngji Kim: None; Takashi Yao: None; Kazuo Kaneko: None; Tsuyoshi Saito: None

Background: Inflammatory myofibroblastic tumor (IMT)/inflammatory pseudotumor (IPT) is an intermediate malignancy and histologically characterized by admixed proliferation of myofibroblasts and inflammatory cells such as, lymphocytes, plasma cells and eosinophils. Approximately half of IMTs are considered to have *ALK* fusion and recently other fusions such as *ROS1, PDGFRB* and *NTRK3* have also been reported in addition to *ALK*. In this study, we conducted comprehensive TK fusion screening to identify novel fusions in these tumors.

Design: We enrolled 8 cases of IMT and 16 cases of IPT. RNA was extracted from formalin-fixed paraffin embedded (FFPE) tissue, and the imbalances of 5'-side/3'-side of the gene expressions were comprehensively measured for 90 TK (Tyrosine Kinase) genes by Nanostring. Cases with imbalanced expressions were further analyzed by either immunohistochemistry (IHC), FISH（Fluorescence in-situ hybridization）, RT-PCR（Reverse transcription-polymerase chain reaction） and RNA sequencing. In addition, to confirm the specificity and sensitivity of this screening strategy, all cases were retrospectively stained by pan-trk and ALK IHC.

Results: Among 24 cases, 9 cases (4 for IMT, 5 for IPT) were emerged as imbalanced cases (2 for *NTRK3*, 6 for *ALK* and 1 for *ROS1*). Further analysis confirmed *ETV6-NTRK3* fusion by RT-PCR in 2 IPT cases, *ALK* rearrangement by FISH in 5 cases (4 IMTs and 1 IPT). *FN1-ROS1* fusion gene was detected by RNA sequencing (1 IPT). One IMT with imbalanced ALK expression was negative for ALK IHC and FISH. Interestingly, 2 cases with *ETV6-NTRK3* fusion were not positively stained by pan-trk IHC. All *ALK* rearranged cases were positive for ALK IHC and all cases other than *ALK* rearranged/*NTRK3* fusion-positive cases were negative for pan-trk and ALK IHC. Thus, specificity and sensitivity in this Nanostring based screening system were 88.9% and 100%, respectively.

Conclusions: We could identify 8 cases (33.3%) with TK fusions from among 24 cases of IMT/IPT. We found new ROS-1 fusion in IMT/IPT;*FN1-ROS1*. Pan-trk IHC in IMT/IPT was less sensitive than previously reported for *NTRK3* fusions. This Nanostring-based screening system would be useful for detection of TK fusions, especially for NTRK3 fusions.

Acknowledgements: We thank Dr. Toshihide Ueno and Dr. Hiroyuki Mano at Division of Cellular Signaling, National Cancer Center Research Institute, Tokyo, Japan for their excellent technical assistance and advice.

69 Epstein-Barr Virus-Related Smooth Muscle Tumors Show Distinct Copy Number Profiles from Extra-Uterine Leiomyosarcomas

Victor Lee[1], Yingting Mok[2], Timothy Tay[3], Lai Ng[1]
[1]National University of Singapore, Singapore, Singapore, [2]National University Hospital, Singapore, Singapore, [3]Singapore General Hospital, Singapore, Singapore

Disclosures: Victor Lee: None; Yingting Mok: None; Timothy Tay: None; Lai Ng: None

Background: EBV-related smooth muscle tumors (EBV-SMT) are very rare viral-driven smooth muscle neoplasms that arise in immunodeficient patients (e.g. post-transplant, post-chemotherapy or AIDS). When first characterized, these were initially diagnosed as a subtype of leiomyosarcoma, an aggressive malignant soft tissue tumor with poor survival and metastases. This characterization is due to their often multifocal presentation, which is interpreted as metastases. However, it was later found that the clinical behavior of EBV-SMT was much better compared with leiomyosarcomas even in those cases with multiple site involvement. The deaths of most of these patients are often due to events unrelated to the tumor (e.g. infections or morbidities associated with immunodeficiency). Morphological studies have shown that EBV-SMT and leiomyosarcomas are histologically distinct. Furthermore, studies on clonality have demonstrated that multiple sites involvement is a reflection of different infective events rather than true metastasis. Although the cytogenetic properties of LMS have been well studied, very little (if any) genomic studies have been done on EBV-SMTs. A genomically distinct profile in EBV-SMT would further confirm that EBV-SMT and LMS are indeed different; and these tumours should not be classified as a subtype of LMS as in the current WHO classification.

Design: This study aims to analyze and compare genomic-wide copy number changes of extra-uterine EBV-SMT, leiomyomas, and leiomyosarcomas. Our study group included EBV-SMT (n=7), leiomyomas (n=5) and leiomyosarcomas (n=5), occurring in extra-uterine locations in adults. Copy number analysis was performed on paraffin tissue extracted from these cases using the OncoScan® FFPE assay (Affymetrix) according to manufacturer's instructions. Data analysis was performed using the OncoScan® Console (v1.3) software.

Results: 1) EBV-SMT: No conclusive copy number variation changes were identified. 2) Leiomyomas: Few copy number changes were identified. 3) Leiomyosarcoma: Complex copy number profiles were identified.

Figure 1 - 69

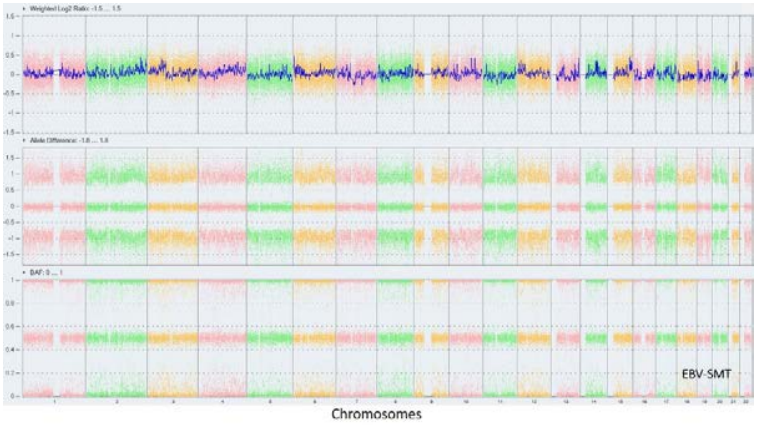

Figure 2 - 69

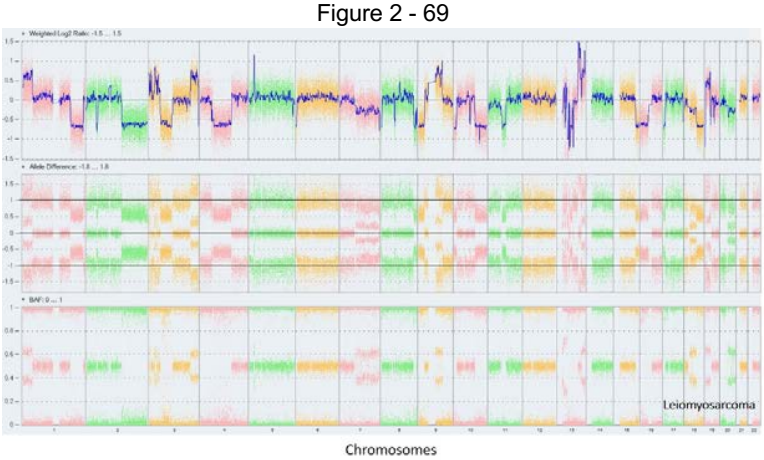

Conclusions: The genomic profile of EBV-SMT differs significantly from extra-uterine LMS based on Oncoscan, in keeping with their distinctive histological characteristics and clinical behaviour. Unlike leiomyosarcomas, EBV-SMT demonstrate no complex profile or aberrations. Therefore, they should be classified differently from leiomyosarcoma. This finding would have significant implication on how to approach and manage these rare tumors.

70 Analysis of Chromosomal Abnormalities and of Cell Cycle Genes Alterations in a Series of 32 Chordomas

Leslie Lemnos[1], Henri Salle[2], Anne Guyot[3], Sylvie Bourthoumieu[1], Karine Durand[1], Homa Adle-Biassette[4], Francois Labrousse[5]
[1]Limoges Dupuytren University Hospital, Limoges, Haute-Vienne, France, [2]Dupuytren University Hospital, Limoges, Haute-Vienne, France, [3]Limoges, Nouvelle Aquitaine, France, [4]Lariboisière University Hospital, Paris, Ile de France, France, [5]Limoges, France

Disclosures: Leslie Lemnos: None; Henri Salle: None; Anne Guyot: None; Sylvie Bourthoumieu: None; Karine Durand: None; Homa Adle-Biassette: None; Francois Labrousse: None

Background: Chordoma is a rare tumor mainly located in the clivus and the sacrum. After surgery, these tumors have a high rate of recurrence. The elevation of mitotic and Ki67 indices, reflecting cell cycle deregulation, are factors of poor prognosis. Analysis of chromosomal abnormalities and genomic alterations of genes involved in cell cycle regulation, could improve the histomolecular classification of chordomas.

Design: Thirty-two chordomas, were classified according to their histological type i.e. classical, chondroid, myxoid and dedifferentiated. Myxoid subtype was defined on the presence of a myxoid component in at least 50% of the tumor. Chromosomal deletions and duplications were analyzed using array comparative genomic hybridization (aCGH). Coding sequences of 84 genes involved in cell cycle regulation were investigated by next-generation-sequencing (NGS) and Sanger sequencing. Results were compared with clinical and histopathological data: gender, age, location, histological type, nuclear atypia, necrosis and, mitotic and Ki67 indices.

Results: There were 21 men and 11 women. Mean age at diagnosis was 51,75 ± 14,57 years. Twenty-eight tumors were localized in the clivus and four in the sacrum. Histologically, 24 tumors were of classical type whereas myxoid and chondroid types were observed in five and three cases, respectively. aCGH detected loss of chromosomes 1p, 3, 4, 9, 10, 13q, 14q, 15q, 18, 19 and 22q. Gains were less frequent and involved chromosomes 1q, 5, 7, 8, 12, 13, 17, 19, 20 and 21q. Statistically significant associations were found with: location in the clivus and 7q31duplication *(p=0.031)*; myxoid histological type and 1q23 duplication*(p=0.036)*; presence of nuclear atypia and 9p21 deletion *(p=0.039)*; Ki67 labeling index > 5%and 1q41duplication *(p=0.037).*The NGS analysis revealed *CDKN1A* c.*20C>T,*PPP2R3B*c.457G>A and *PPP2R3B*n.-84G>A variants that were significantly associated with classical and chondroid histological types *(p=0.01).*These mutations, confirmed by Sanger sequencing, have not been previously reported in chordomas.

Conclusions: Our study suggests that chordomas located in the clivus could have different chromosomal abnormalities than those located in the sacrum. In addition, our results could indicate that myxoid chordomas have a chromosomal and genomic profile distinct from that of the classical and chondroid types. The prognostic value of our findings remains to be assessed.

71 Comparing New and Old: The Impact on Survival Between 7th and 8th Editions of the American Joint Committee on Cancer (AJCC) in the Staging of Soft Tissue Sarcomas

Chiu-Hsiang Liao[1], Monica Rodriguez[2], Randi Woodbeck[3], Mitra Afsharpad[4], Tilley Derek[5], Brittany Popowich[5], Lloyd Mack[2], Shannon Puloski[6], Michael Monument[1], Antoine Bouchard-Fortier[2], Elizabeth Kurien[2], Alex Balogh[2], Jan-Willem Henning[2], Don Morris[2], Doha Itani[7]

[1]University of Calgary, Cumming School of Medicine, Calgary, AB, [2]Cumming School of Medicine, University of Calgary, Calgary, AB, [3]University of Calgary, Calgary, AB, [4]Cumming School of Medicine, University of Calgary and Division of Hematopathology, Alberta Public Laboratories, Calgary, AB, [5]Cancer Control Alberta, Alberta Health Services, Calgary, AB, [6]University of Calgary, Cumming School of Medicine, Calgary, AB, [7]Calgary Laboratory Services/University of Calgary, Calgary, AB

Disclosures: Chiu-Hsiang Liao: None; Monica Rodriguez: None; Randi Woodbeck: None; Tilley Derek: None; Brittany Popowich: None; Alex Balogh: None; Jan-Willem Henning: None; Don Morris: None; Doha Itani: None

Background: The staging of soft tissue sarcomas (STS) up to AJCC7 followed a simple scheme with the exception of gastrointestinal stromal sarcoma and uterine sarcomas. The 8th Edition of AJCC made drastic changes to the staging of STS by dividing them into 4 anatomical sites: trunk and extremities (TE), retroperitoneum (RP), abdomen and thoracic visceral organs (ATVO) and head and neck (H&N). Each site was assigned a tumor specific size cut-off and recommendations for prognostic staging was issued for TE and RP. We aim to compare the AJCC 7 and 8 schemes as related to survival in the province in Alberta.

Design: STS cases listed in the Alberta Cancer Registry (ACR) between 2009 and 2016 were included. We collected patient demographics, clinical staging, treatment, survival, pathologic diagnosis, tumor site, tumour size, grade, mitosis, necrosis, metastasis to lymph nodes and distant sites. Pathologic tumor (T) and overall clinical stage were established using both AJCC 7 and 8 classifications. Sarcomas from TE, RP and ATVO were selected for statistical analysis including Cox regression and Holm-Sidak method calculations.

Results: Our study sample included 558 patients with a mean age of 61 years. The majority of STS (73.7%) originated in TE. The three most common diagnoses were leiomyosarcomas (31.9%), undifferentiated sarcomas (19.5%) and liposarcomas (18.3%). Well-differentiated liposarcomas were not captured in our cohort. Of the cases classified as stage II based on AJCC7 (195/558), 46.4% were upstaged to stage III using AJCC8. Subgroup analysis showed a similar trend in TE cases with 37.8% of AJCC7 stage II cases upstaged to stage III using AJCC8. AJCC7 showed better separation between prognostic stages using stage I as reference: Stage IV HR= 15.193 (AJCC7) versus 12.375 (AJCC8); Stage III HR = 3.685 (AJCC7) versus 3.007 (AJCC8).

Conclusions: AJCC 7 shows better separation of prognostic stages than AJCC 8 in TE sarcomas. Our study sample did not include enough cases to allow for evaluation of RP and ATVO sarcomas.

72 Human Sarcoma Nude Mice Xenografts: A Collection of 438 Cases in Twenty-Five Years' Experience

Antonio Llombart-Bosch[1], Carmen Carda[2], Amparo Mayordomo[2], Francisco Giner[3], Rosa Noguera[2], Samuel Navarro[2], Isidro Machado[4]

[1]Universidad de Valencia, Valencia, Spain, [2]Department of Pathology, University of Valencia, Valencia, Spain, [3]University of Valencia, Valencia, Spain, [4]Instituto Valenciano de Oncología, Valencia, Spain

Disclosures: Antonio Llombart-Bosch: None; Francisco Giner: None; Isidro Machado: None

Background: Biological and molecular studies of human sarcomas require fresh tumor tissue, cell lines or frozen tissue in order to provide access to adequate material. However, such material is not always available and a shortage of tissue is frequent. Nude mice xenografts of human sarcomas offer an alternative method to obtain large amounts of tissue, over an indefinite period, in so far as the tumor can be transferred, in vivo, throughout generations, maintaining the histological and genetic characteristics. Since 1990 we have produced a xenograft tissue bank of sarcomas on nude mice (Balb-c, nu nu) storing available tissue in vivo for several passages and frozen in tissue banks. A total of 438 human tumors have been maintained throughout several generations (up to 40).

Design: Tumor tissue is transferred into the animal (two for each experience) within two hours of surgery, under sterile conditions (1–2 mm^3 of tumor tissue), inoculated subcutaneously in the back of the animal. Nude mice are kept in germ-free conditions (complying with all required ethical regulations). The tumor is followed until it reaches a size of 1–2 cm in diameter, and transferred to new nude mice for several generations. Material obtained from each transplant is kept for histology, cell culture, EM, and frozen.

Results: Figure 1 indicates the number of tumors transferred into nude mice and the number of positive grafts (Average 40%, Range 27-60%). Special emphasis is given to Osteosarcoma, Chondrosarcoma, Es/PNET and Soft tissue tumors. Several cell lines in vitro have been established. Frozen tissue and PFETB are available in almost all cases.

Figure 1 - 72

Histological type	Nº T	+	%
Osteogenic sarcoma/ Chondrosarcomas	100	44	44.0
Small round cell sarcomas	80	30	37.5
Malignant fibrous histiocytoma	48	18	37.5
Muscle cell sarcomas (Rhabdo- Leiomyosarcomas)	41	18	43.9
Synovial sarcomas	28	17	60.7
Liposarcomas	39	12	30.7
Fibrosarcomas	11	4	36.3
Vascular sarcomas	8	5	62.5
GIST	22	6	27.2
Miscellanous: Retinoblastoma, melanoma, rhabdoid tumor, MPSNT, epitheliod sarcoma, carcinosarcoma, lymphomas, chordoma, germinal tumors	61	22	36.0
Total:	**438**	**176**	**40.18**

Conclusions: Sarcoma xenografts in nude mice provide a suitable model, useful for the study of tumor morphology, biology and molecular genetics. Numerous papers have been produced by the authors. Samples of tumors are available to interested researchers.

This study was partially funded by grants PI040822 from the Instituto Carlos III de Madrid, Spain Contract nº: 018814 (EuroBoNet) from the 6th FP of the EC and Instituto Valenciano de Oncología Valencia Spain

73 Next Generation Sequencing Identifies TERT Promoter Mutations as Early Events and TP53 Mutations as Late Events in Chondrosarcoma Dedifferentiation

Calixto-Hope Lucas[1], James Grenert[1], Andrew Horvai[1]
[1]*University of California San Francisco, San Francisco, CA*

Disclosures: Calixto-Hope Lucas: None; James Grenert: None; Andrew Horvai: None

Background: Progression of conventional low-grade chondrosarcoma (CS) to high-grade non-chondrogenic “dedifferentiated” chondrosarcoma (DDCS) is well described. Whereas low-grade CS often shows a protracted course, DDCS frequently metastasizes with high mortality despite aggressive multimodal therapy. The genetic and molecular events that drive progression to DDCS are poorly understood. A clearer picture of the genomic landscape of DDCS may reveal specific therapeutic targets and improve our understanding of sarcoma progression. Using next generation sequencing, we analyzed the molecular and genetic changes in DDCS with matched low-grade CS components.

Design: The clinical, radiographic and pathologic features of DDCS from departmental archives were reviewed. Capture-based next gen sequencing targeting the coding regions of 479 cancer genes, select introns, and the *TERT* promoter was performed on extracted DNA from DDCS (paired low-grade chondrosarcoma (CS) and dedifferentiated (DD) components). Single nucleotide variants, insertions/deletions, copy number alterations (CNAs), and selected rearrangements were evaluated.

Results: 11 DDCS were included in this study (7 males, 4 females). Mean age at diagnosis was 58 years (range 36-70 years). Tumors were located in the femur (4), scapula (3), pelvis (3), and humerus (1). DNA was adequate for sequencing from all 11 DD components and 9 matched low-grade CS components. Sequencing results are summarized in Figure 1. All DD components harbored either *IDH1* p.R132 (9) or *IDH2* p.R172 (2) hotspot mutation, and 8 of 9 (89%) matched low-grade CS components had the same mutation.
Identical *TERT* promoter mutations were present in 4 of 9 CS-DD pairs (44%) and three additional DD components. 7 (64%) DD components harbored at least one *COL2A1* alteration, 6 of which (86%) had the same alteration(s) in the matched low-grade CS. Pathogenic missense or truncating mutations in *TP53* were identified in 8 DD components (73%), but only 1 of 6 (17%) showing the same mutation in matched low-grade CS component. Large scale CNAs were more common in DD components (Figure 1).

Figure 1 - 73

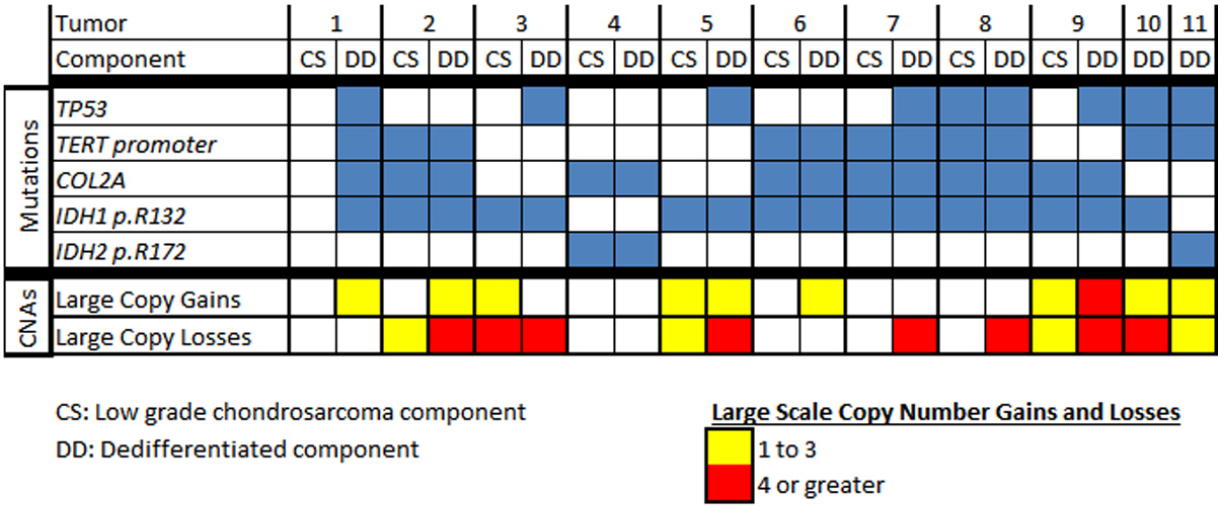

Figure 1. Genomic landscape of dedifferentiated chondrosarcoma.

Conclusions: *TERT* promoter mutation in both components of DDCS suggests an early event in the pathogenesis of these tumors with possible prognostic utility. Conversely, inactivating mutations of *TP53* and high level CNAs are late events in progression to the DD phenotype. The latter may include therapeutic targets for DDCS.

74 Benign Infiltrating Myofibroblastic Neoplasms of Childhood with USP6 Rearrangement

Faizan Malik[1], Dale Hedges[2], Seung Lee[2], Rachel Brennan[3], Zhongxin Yu[4], Lili Miles[5], Michael Clay[2], Lu Wang[6], Morris Edelman[7], Beth McCarville[2], Scott Newman[3], Kim Nichols[2], Armita Bahrami[3]
[1]University of Tennessee Health Science Center, Memphis, TN, [2]St. Jude Children's Research Hospital, Memphis, TN, [3]St. Jude Children's Research Hospital, Memphis, TN, [4]Oklahoma University Health Sciences Center, Oklahoma City, OK, [5]Nemours Children's Hospital, Orlando, FL, [6]St Jude Children's Research Hospital, Memphis, TN, [7]Donald and Barbara Zucker School of Medicine at Hofstra/Northwell, New Hyde Park, NY

Disclosures: Faizan Malik: None; Dale Hedges: None; Seung Lee: None; Rachel Brennan: None; Zhongxin Yu: None; Lili Miles: None; Michael Clay: None; Lu Wang: None; Morris Edelman: None; Beth McCarville: None; Scott Newman: None; Kim Nichols: None; Armita Bahrami: None

Background: Several morphologically-overlapping benign myofibroblastic neoplasms are known to harbor *USP6* fusion, including aneurysmal bone cyst (conventional and solid-variant), nodular fasciitis, myositis ossificans, fibro-osseous pseudotumor of digits, and cellular fibroma of tendon sheath. These tumors are typically well defined from the surrounding healthy tissue.

Design: Three deep-seated, radiographically-aggressive and rapidly-growing childhood myofibroblastic neoplasms were morphologically and molecularly characterized by histologic and radiographic imaging, *USP6* rearrangement fluorescence *in situ* hybridization (FISH) and whole-genome or transcriptome next-generation sequencing (NGS).

Results: Each tumor occurred in the deep soft tissue of the lower extremity of a child presenting with pain, limping, or a palpable mass. Imaging studies in all 3 patients showed a solid mass that infiltrated into the surrounding skeletal muscle or involved/eroded the underlying bone (Table 1). Biopsy specimens showed a variably cellular myofibroblastic tumor with bland cytologic features that extended into skeletal muscle and surrounding soft tissue. Tumor mitotic activity ranged from low to high. FISH showed *USP6* rearrangements in all tumors. All 3 patients were treated by conservative excision of the mass with positive margins. Tumor morphological features on excisions included foci resembling nodular fasciitis, sarcomatous proliferation, and fibromatosis (Figure 1). Two tumors had inflammatory and multinucleated giant cells and 1 had central osteocartilaginous metaplasia. NGS revealed *COL1A1-USP6* fusions in 2 tumors, a novel *COL3A1-USP6* fusion in the third tumor, and a subclonal somatic *APC* in-frame deletion in 1 tumor. The *APC*-mutant tumor did not have nuclear beta-catenin by immunohistochemistry. No recurrence was observed in short-term follow-up.

TABLE 1. Clinicopatholgic characteristics of patients

Case No.	Age	Gender	Site	Size (cm) on imaging	Radiographic findings	Histologic findings	IHC findings	Genetic abnormality	Follow-up
Case 1	10 months	Male	Deep-seated soft tissue / muscle of right proximal anterior tibia	4.5 x 2.3 x 1.7	Infiltrative mass in the anterior compartment musculature, extending through interosseous membrane, encasing patellar tendon, and invading proximal tibial diaphysis	"Nodular fasciitis-like" myofibroblastic proliferation; brisk mitotic activity; foci of myxoid and hyalinized stroma; extension into skeletal muscle; scattered inflammatory and multinucleated giant cells	SMA (+)	*COL3A1-USP6*	No evidence of disease at 2-month follow-up
Case 2	2.5 years	Female	Subperiosteal space on right distal femur metaphysis	1.6 x 1.2 x 1.1	Subperiosteal mass growing inward, associated with a lytic right femur metaphyseal lesion; extensive edema in the surrounding musculature	Highly proliferative myofibroblastic proliferation; brisk mitotic activity; areas with high cellularity, monotonous fascicular arrangement; scattered inflammatory and multinucleated giant cells	SMA (+)	*COL1A1-USP6*	No evidence of disease at 8-month follow-up
Case 3	7 years	Male	Deep-seated soft tissue and muscle of left posterior tibia	5.1 x 2.9 x 1.8	Ill-defined, infiltrative mass in the posterior muscle compartment; extension into surrounding muscle groups	Multinodular, infiltrative and fibromatosis-like spindle-cell proliferation; low mitotic activity; central osteocartilaginous metaplasia	SMA (+); beta-catenin (-)	*COL1A1-USP6* and *APC* mutation (allele frequency: 3% WGS)	No evidence of disease at 36-month follow-up

Figure 1 - 74

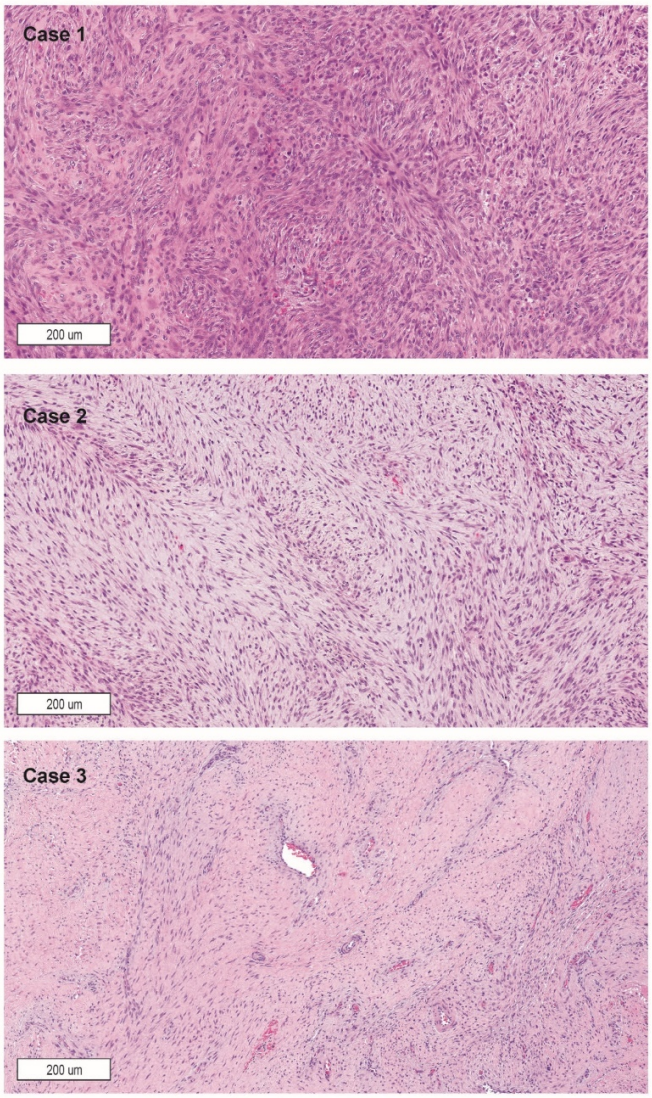

Conclusions: We present a series of benign, yet radiologically aggressive-appearing, *USP6*-rearranged myofibroblastic tumors. These deep-seated tumors had atypical clinical, radiographic, and histologic presentations and did not fit into one specific histologic category. Our results expand the scope of *USP6*-induced tumors and highlight the importance of their accurate identification to avoid over-treatment, especially in small biopsy specimens. These tumors can be accurately identified by appropriate molecular and cytogenetic studies.

75 Methylation Profiling of Soft Tissue Neoplasms with EWSR1-Translocation Reveals Epigenetic Disparity in Myoepithelial Tumors

Faizan Malik[1], Nasir Ud Din[2], Cynthia Cline[3], Quynh Tran[3], Brent Orr[3], Michael Clay[3]
[1]University of Tennessee Health Science Center, Memphis, TN, [2]The Aga Khan University Hospital, Karachi, Sindh, Pakistan, [3]St. Jude Children's Research Hospital, Memphis, TN

Disclosures: Faizan Malik: None; Nasir Ud Din: None; Cynthia Cline: None; Quynh Tran: None; Michael Clay: None

Background: Soft tissue myoepithelial tumors (MET) are a morphologically heterogeneous group of tumors that require extensive histologic and immunohistochemical characterization for accurate diagnosis. Up to 45% of METs show recurrent *EWSR1* gene rearrangements with a diverse set of fusion partners including *POU5F1, PBX1, PBX3, ZNF444,* and *ATF1*. These fusion partners are not typically seen in other well-characterized tumor classes with *EWSR1* translocations, such as clear cell sarcoma of soft tissue (CCS; *CREB1* and *ATF1*), angiomatoid fibrous histiocytoma (AFH; *CREB1* and *ATF1*), desmoplastic small round cell tumor (DSRCT; *WT1*), and Ewing sarcoma (ES; *FLI1, ERG, ETV1, ETV4,* and *FEV*). Emerging technologies such as methylation profiling of MET

and other EWSR1-rearranged tumors could reveal insights into tumor biology, refine diagnostic criteria, and eventually aid in accurate classification.

Design: A total of 17 METs, 12 CCSs, 5 AFHs, 19 DSRCTs, and 16 ESs were selected. FISH testing was performed for *EWSR1* rearrangement in all cases. Tumors classified as MET underwent additional immunohistochemical staining for P63, SMA, cytokeratin AE1/AE3, GFAP, and S100-protein. All tumors underwent DNA-methylation profiling utilizing the Illumina Infinium MethylationEPIC BeadChip array and were compared via unsupervised analysis utilizing a cohort of previously methylated pediatric sarcoma and solid tumors (23 entities, overall n=755 cases).

Results: *EWSR1* rearrangement by FISH was positive in 7 (41%) cases of MET, 11 (91%) cases of CCS, 4 (80%) cases of AFH, and all cases of ES and DSRCT (16 and 19, 100%). Unsupervised analysis using the methylation sites with the highest variability showed distinct grouping of the CCS, AFH, ES, and DSRCT cases. METs failed to cluster into a cohesive group, instead distributing amongst other well-established entities or individually.

Conclusions: In contrast to most EWSR1-driven entities (CCS, AFH, DSRCT, ES), our findings suggest that METs may represent a heterogeneous group of neoplasms with disparate epigenetic profiles.

76 Targetable Alterations and Rare Fusions in Sarcomas Identified by Custom RNA Sequencing

Douglas Mata[1], Ryma Benayed[1], Kerry Mullaney[1], Kelly Rios[2], Narasimhan Agaram[1], Maria Arcila[1], Marc Ladanyi[1], Meera Hameed[1]
[1]Memorial Sloan Kettering Cancer Center, New York, NY, [2]Memorial Sloan Kettering Cancer Center, Fairfield, CT

Disclosures: Douglas Mata: None; Ryma Benayed: None; Kerry Mullaney: None; Kelly Rios: None; Narasimhan Agaram: None; Maria Arcila: *Speaker*, Biocartis; *Speaker*, invivoscribe; Marc Ladanyi: None; Meera Hameed: None

Background: Many soft tissue sarcomas harbor gene fusions that drive tumorigenesis and inform diagnosis. While FISH and RT-PCR are widely used for detecting known rearrangements, identifying novel fusions requires ancillary testing. A custom clinical gene-fusion detection assay for solid tumors that utilizes ArcherDx Anchored Multiplex PCR (AMP™) technology for targeted RNA sequencing was previously validated at our institution. In this study, we report on its utility for identifying targetable alterations and novel fusions in diagnostically challenging soft tissue sarcomas.

Design: A retrospective analysis of all sarcoma cases submitted for targeted RNA sequencing at this institution from March 2018 to March 2019 was performed.

Results: In all, 294 soft tissue tumors (all FFPE) were submitted for targeted RNA sequencing. Among these, 7.1% (21/294) demonstrated novel and/or targetable fusions and are summarized below. The median age at diagnosis was 34.5 years (range, 0.1 to 71.6). The specimens included 13 primary, 3 locally recurrent, and 5 metastatic tumors. The most commonly rendered diagnoses prior to molecular testing were sarcoma, NOS (57.1% [12/21]), rhabdomyosarcoma (19.0% [4/21]), and angiosarcoma (14.3% [3/21]) (Table). Targeted RNA sequencing revealed 19 unique fusions or intragenic deletion events (Figure). The most common 5' partners were *EWSR1* (19.0% [4/21]) and *MEIS1* (9.5% [2/21]), while the most common 3' partners were *BRAF* (3/21), *MET* (9.5% [2/21]), *NCOA2* (9.5% [2/21]), and *NUTM1* (9.5% [2/21]). In all, 76.2% (16/21) of cases underwent orthogonal testing with a hybridization capture-based DNA NGS assay for targeted sequencing of 468 key cancer genes and select introns. This assay detected the same alteration in 37.5% (6/16) of cases, identified an alteration in one but not both fusion partners in 12.5% (2/16) of cases, and failed to detect the alteration in 50% (8/16) of cases. Of the alterations identified in this study, *BRAF*, *MET*, *NRG1*, *NTRK3*, *NUTM1*, *PDGFB*, and *RET* are potentially targetable.

Diagnosis at Submission	Targeted RNA Sequencing Result
Embryonal Rhabdomyosarcoma	*ST7* exon 1 - *MET* exon 6 fusion
Epithelioid and Spindle-Cell Neoplasm	*BRAF* exons 4-8 deletion
Epithelioid and Spindle-Cell Sarcoma	*YAP1* exon 5 - *KMT2A* exon 4 fusion
Ewing Sarcoma-Like Round-Cell Sarcoma	*EWSR1* exon 8 - *VEZF1* exon 2 fusion
HG Epithelioid and Spindle-Cell Sarcoma	*EGFRvIII* (exons 2-7 deletion)
HG Epithelioid Angiosarcoma	*DOCK4* None - *BRAF* exon 9 fusion
HG Epithelioid Angiosarcoma	*PTBP1* exon 10 - *MAML2* exon 2 fusion
HG Spindle and Pleomorphic Sarcoma	*TFG* exon 5 - *NTRK3* exon 14 fusion
HG Spindle-Cell Sarcoma	*COL1A1* exon 25 - *PDGFB* exon 2 fusion
HG Spindle-Cell Sarcoma	*EWSR1* exon 5 - *TFCP2* exon 2 fusion
HG Spindle-Cell Sarcoma	*HMBOX1* exon 1 - *NRG1* exon 2 fusion
HG Spindle-Cell Sarcoma	*MGA* exon 22 - *NUTM1* exon 2 fusion
HG Spindle-Cell Sarcoma	*MXD4* exon 5 - *NUTM1* exon 2 fusion
HG Spindle-Cell Sarcoma	*SPECC1L* exon 9 - *RET* exon 12 fusion
Infantile Fibrosarcoma	*RBPMS* exon 5 - *MET* exon 15 fusion
Myxoid Spindle-Cell Neoplasm	*MKRN1* exon 4 - *BRAF* exon 11 fusion
Radiation-Associated Angiosarcoma of the Breast	*PEAR1* exon 15 - *NTRK1* exon 10 fusion
Rhabdomyosarcoma	*EWSR1* exon 5 - *TFCP2* exon 2 fusion
Rhabdomyosarcoma	*MEIS1* exon 6 - *NCOA2* exon 12 fusion
Sclerosing Epithelioid Fibrosarcoma	*EWSR1* exon 11 - *CREB3L1* exon 6 fusion
Spindle-Cell Rhabdomyosarcoma	*MEIS1* exon 7 - *NCOA2* exon 13 fusion

Figure 1 - 76

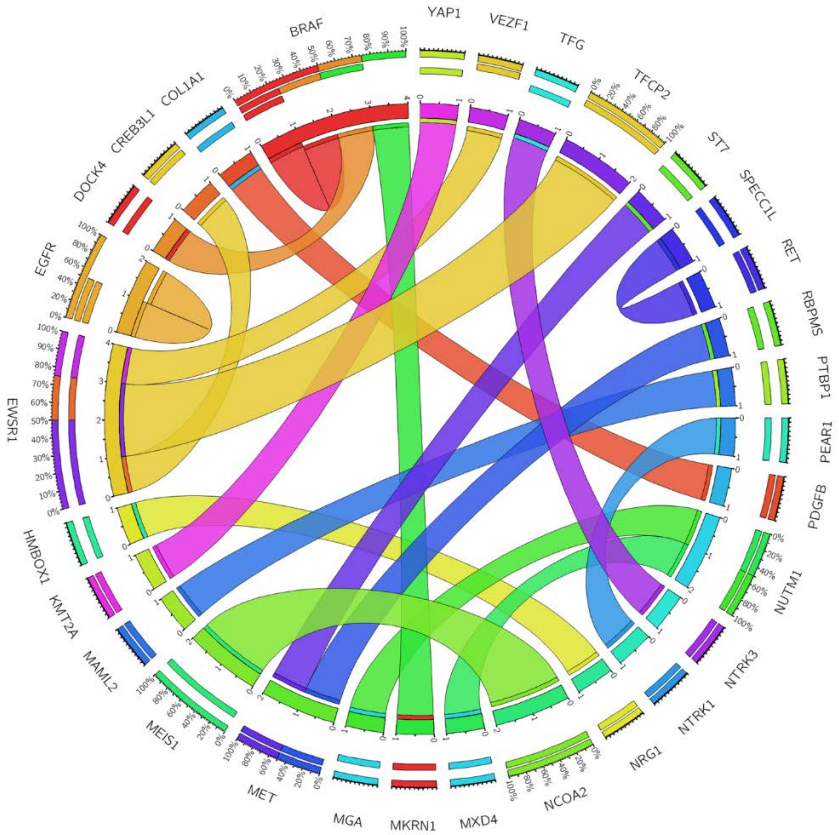

Conclusions: In diagnostically challenging sarcoma cases, novel fusions can be discovered by targeted RNA sequencing, a sensitive method for detecting gene fusions that may be otherwise difficult to detect with traditional DNA-based NGS sequencing or single-gene assays like FISH or conventional RT-PCR. This testing can reveal potential targets which may guide diagnosis and clinical management.

77 Evaluation of INSM1 and NR4A3 Expression in Extraskeletal Myxoid Chondrosarcoma and Histologic Mimics

David Meredith[1], Christopher Fletcher[2], Jason Hornick[3]
[1]Boston, MA, [2]Brigham and Women's Hospital, Boston, MA, [3]Brigham and Women's Hospital, Harvard Medical School, Boston, MA

Disclosures: David Meredith: None; Christopher Fletcher: None; Jason Hornick: *Consultant*, Eli Lilly; *Consultant*, Epizyme

Background: Extraskeletal myxoid chondrosarcoma (EMC) is a rare soft tissue sarcoma composed of lobules of uniform spindle cells arranged in a reticular pattern within a myxoid matrix; however, high-grade variants containing solid regions of epithelioid cells may be encountered. EMC possesses recurrent fusions in *NR4A3*, most commonly *EWSR1-NR4A3*, which currently require FISH or other molecular techniques for confirmation. Although EMC exhibits no distinctive immunophenotype, expression of the neuroendocrine marker INSM1 was recently reported. In this study, we examine the utility of immunohistochemistry (IHC) for INSM1 and NR4A3 in EMC and histologic mimics, both individually and in combination.

Design: IHC for INSM1 (clone A-8) and NR4A3 (clone H-7) was performed on whole sections of 57 EMC, 20 soft tissue myoepitheliomas/myoepithelial carcinomas, and 10 each myxoid malignant peripheral nerve sheath tumor (MPNST), myxoid liposarcoma, myxoid leiomyosarcoma, ossifying fibromyxoid tumor (OFMT), skeletal myxoid chondrosarcoma, myxofibrosarcoma, and proximal-type epithelioid sarcoma. The EMC cohort included both low-grade (n=39) and high-grade (n=18) tumors; all were verified by FISH using break-apart probes against either *EWSR1* or *NR4A3*.

Results: By IHC, INSM1 was positive in 35/57 (61%) EMC, including 19/39 (49%) low-grade and 14/18 (78%) high-grade tumors. NR4A3 immunopositivity was observed in 37/57 (65%) EMC, including 20/39 (51%) low-grade and 17/18 (94%) high-grade tumors. Of histologic mimics, INSM1 positivity was observed in 2/10 (20%) OFMT, while no expression was detected in other tumor types. NR4A3 expression, however, was observed in 5/8 (63%) myoepitheliomas, 2/12 (17%) myoepithelial carcinomas, 1/10 (10%) OFMT, 7/10 (70%) myxoid MPNST, and 5/10 (50%) proximal-type epithelioid sarcomas. Overall, 46/57 (81%) EMC showed expression of at least one marker, including 28/39 (72%) low-grade tumors and all 18 high-grade tumors.

Conclusions: Given the broad differential diagnosis for EMC, there is need for specific biomarkers to ensure accurate and timely diagnosis. Herein, we confirm that INSM1, in context, is a specific marker for EMC, though sensitivity is considerably lower than previously reported. IHC for NR4A3 is more sensitive in the detection of EMC; however, it is also less specific. Intriguingly, both markers show higher rates of detection in high-grade EMC and when used together.

78 Dysplastic Lipomas (DL) are Highly Overrepresented among Lipomatous Tumors in Retinoblastoma (RB) Survivors

Michael Michal[1], Alejandro Luina Contreras[2], Maria Tretiakova[3], Tatjana Antic[4], Kvetoslava Michalova[1], Michal Michal[5], John Fetsch[6]
[1]Biopticka Laborator Ltd., Plzen, Czech Republic, [2]Arlignton, VA, [3]University of Washington, Seattle, WA, [4]The University of Chicago, Chicago, IL, [5]Biopticka laborator s.r.o., Plzen, Czech Republic, [6]The Joint Pathology Center, Silver Spring, MD

Disclosures: Michael Michal: None; Alejandro Luina Contreras: None; Maria Tretiakova: None; Tatjana Antic: None; Kvetoslava Michalova: None; Michal Michal: None; John Fetsch: None

Background: DL is a recently described well-differentiated fatty neoplasm that has distinct clinicopathological features and commonly shows *RB1* gene abnormalities. Besides the characteristic histology, it is clinically distinguished by a strong predilection for subcutaneous areas of the upper back, posterior neck and shoulders of middle-aged men. It also has a high tendency for multifocality (~20% of cases) and mildly increased risk for local recurrence (~10%) as compared to ordinary lipoma. Interestingly, 2 out of 67 reported patients with clinical information had a history of childhood RB, and these patients also showed the highest number of synchronous or metachronous DL (≥5), some of them occurring at unusual sites (i.e. groin). Previous studies noted increased susceptibility of both bilateral and unilateral RB survivors for the developments of (often multiple) lipomas[1-3] with the identical anatomical and gender distribution as is seen in DL[1,2]. Unfortunately, the publications lacked any microscopic illustrations. In light of these facts, we hypothesized that the reported “lipomas” might, in fact, represent DL.

Design: A multi-institutional (n=11) search for lipomatous tumors in RB patients was undertaken, followed by a morphological review and IHC analysis.

Results: Altogether 4 lipomatous tumors from 4 RB patients were identified. On review, all 4 showed classic immunomorphologic features of DL. Their clinicopathological characteristics are shown in the Table.

Case	Age at DL presentation/sex	Location	Size	p53 IHC	RB1 IHC	RB	Other tumors
1	25/M	L Axilla	Ø 7.5 cm	+	-	Bilateral	Multiple cutaneous lesions of which scalp and shoulder lesion showed leiomyosarcoma, metastasis to lungs, liver, retroperitoneum
2	26/M	Scrotum	9x12x6 cm	+	-	Bilateral	Age 18 - L vestibular schwannoma; Age 29 - LG bladder leiomyosarcoma metastasizing to the liver, small bowel at age 33-34; Age 34 – recurrent brain meningioma and dedifferentiated chondrosarcoma of the humerus; Age 36 - died
3	37/M	Suprapubic - recurrent	15.5x6.7 x4 cm	+	-	Unilateral	Age 30 - excision of a neck lipoma; Age 52 - alive and well, lumps of left and right neck (new lipomas, watchful waiting)
4	37/F	Neck	2.5x1.3x0.7 cm	+	-	Unilateral	Not available

References:1) Li, FP, J Natl Cancer Inst., 1997; 2) Rieder H, J Natl Cancer Inst., 1998; 3) Woo, KI, Arch Ophtalmol, 2010; 4) Genuardi M, Eur J Hum Genet., 2001

The views expressed in this abstract are those of the author and do not reflect the official policy of the Department of Army/Navy/Air Force, Department of Defense, or U.S. Government.

Conclusions: Although the assembly of a representative study cohort is hampered by the rare co-occurrence of both diseases, our study supports the notion that most, if not all, lipomatous tumors in patients with childhood RB represent DL. Previous studies have shown that RB survivors presenting with lipomas have a higher risk of subsequent secondary cancer (30%) as compared to those lacking lipomas (12%)[1]. Thus, the detection of DL in an RB patient could have follow-up implications. In a previous analysis of a large extended family pedigree with a splice site mutation in the *RB1* gene, almost all adult carriers had multiple lipomas, but the penetrance for RB was low[4]. Given this finding, it is tempting to speculate that patients with multiple DL but not history of RB might have low penetrance *RB1* mutations. The overrepresentation of DL in RB survivors further supports the view that DL is a distinct lipomatous tumor entity.

79 Next-Generation Sequencing of Myxoinflammatory Fibroblastic Sarcomas (MIFS) Reveals 3 Different Molecular Aberrations with the Potential to Upregulate the TEAD1 Gene

Michael Michal[1], Dmitry Kazakov[2], Kvetoslava Michalova[1], Petr Martinek[3], Veronika Hajkova[1], Nikola Ptakova[4], Petr Steiner[2], Petr Grossmann[3], Michal Michal[3]

[1]Biopticka Laborator Ltd., Plzen, Czech Republic, [2]Biopticka laborator s.r.o., Pilsen, Czech Republic, [3]Biopticka laborator s.r.o., Plzen, Czech Republic, [4]Molecular and Genetic Laboratory, Biopticka Lab, Ltd, Plzen, Czech Republic

Disclosures: Michael Michal: None; Dmitry Kazakov: None; Kvetoslava Michalova: None; Petr Martinek: None; Veronika Hajkova: None; Nikola Ptakova: None; Petr Steiner: None; Petr Grossmann: None; Michal Michal: None

Background: MIFS has been shown to harbor various recurrent molecular aberrations, most of which, however, seem to be present in only a minority of cases. They mainly include *TGFBR3-MGEA5* fusions, *BRAF* gene amplifications or rearrangements as well as amplifications and subsequent upregulation of the *VGLL3* gene. The latter finding is present in over a half of cases and seems to be the most common molecular abnormality detected in MIFS. VGLL3 protein acts as a co-factor of the *TEAD* transcription factors and is thus integrated into the wider Hippo signal transduction network. Previous studies have shown VGLL3 to be involved in oncogenesis by stimulating the proliferation and migration of tumors cells.

Design: In order to better characterize the molecular underpinning of MIFS, 29 tumors with a typical, low-grade morphology were analyzed by NGS using the customized version of Archer FusionPlex Sarcoma Kit. It detects fusion transcripts and point mutations in 57 and 7 genes, respectively. Among others, it detects *BRAF*, *MGEA5* and *VGLL3* gene fusions, *BRAF* V600 mutations and can measure the relative expression of VGLL3 mRNA. The results were further validated by RT-PCR or by FISH using V*GLL3* enumeration probe, *BRAF* break-apart (BA) probe and BRAF enumeration probe.

Results: NGS analysis was informative in 10/29 cases and only those were included for a further study. Their clinicopathological features are listed in the Table. No *TGFBR3-MGEA5* fusions or *BRAF* fusions/amplifications were found. Four cases showed increased mRNA expression of VGLL3 by NGS and corresponding *VGLL3* gene amplification by FISH. All 6 remaining cases were negative for this abnormality. Interestingly, 2 of the 6 negative cases harbored either a *SEC23IP-VGLL3* (Figure 1) or *TEAD1-MKL2* (Figure 2) rearrangement, both confirmed by RT-PCR. The latter fusion was also detected in the re-excision specimen.

Case	Age/sex	Location	Outcome/length (years)	Fusion	RT-PCR	VGLL3 mRNA Overexp.	VGLL3 FISH amp.	BRAF FISH amp./ break
1	39/M	Palm	NED/3	TEAD1-MKL2	+	-	-	-/-
2	48/M	Palm	Recent	SEC23IP-VGLL3	+	-	-	-/-
3	58/F	Lower leg	NED/2	-	ND	+	+	-/-
4	33/M	Wrist	NED/3	-	ND	+	+	-/-
5	45/F	Thigh	NA	-	ND	+	+	-/-
6	28/F	Knee	NA	-	ND	+	+	-/-
7	79/F	Cheek	Recurred after 6 years, NED/1	-	ND	-	-	-/-
8	69/M	NA	NA	-	ND	-	-	-/-
9	71/F	Clavicular area	NA	-	ND	-	-	-/-
10	58/F	Arm	NA	-	ND	-	-	-/-
ND – Not done; NED – no evidence of disease								

Figure 1 - 79

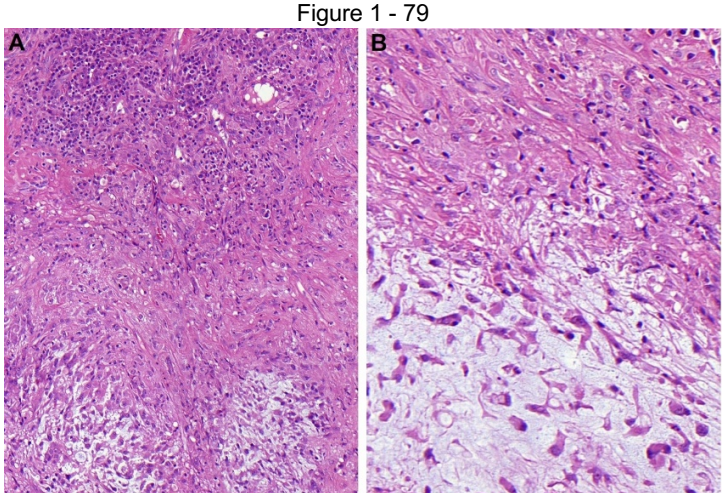

Figure 2 - 79

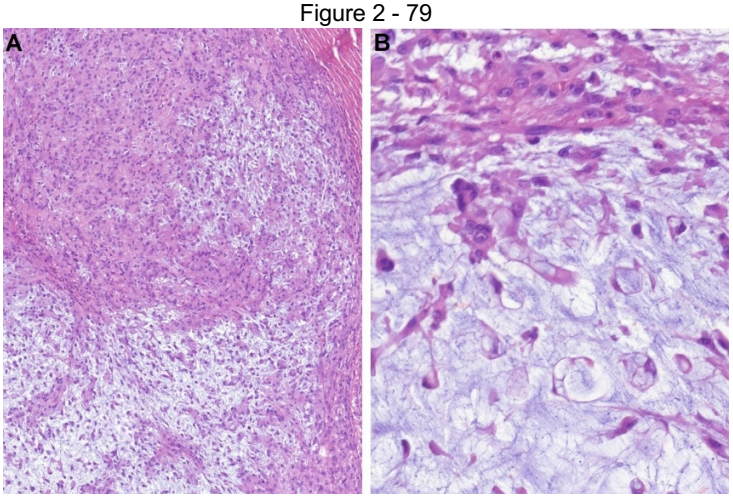

Conclusions: Aberrations with the potential to upregulate the *TEAD1* gene were detected in 60% of cases in MIFS. The major contribution of this study is the demonstration of 2 novel mechanisms likely exerting the same effect as *VGLL3* gene amplification, namely the *SEC23IP-VGLL3* and *TEAD1-MKL2* fusions. This finding might point towards a more important role of the Hippo signal transduction network in MIFS pathogenesis than previously thought. Future studies may uncover more aberrations within this network undetected by our NGS platform which might account for the negative cases.

80 HMGA1/HMGA2 Gene Rearrangements and HMGA1/HMGA2 Protein Overexpression in Spindle Cell/Pleomorphic Lipomas (SPL)

Kvetoslava Michalova[1], Petr Steiner[2], Petr Grossmann[3], Saul Suster[4], Abbas Agaimy[5], Dmitry Kazakov[2], Michal Michal[3], Michael Michal[1]

[1]Biopticka Laborator Ltd., Plzen, Czech Republic, [2]Biopticka laborator s.r.o., Pilsen, Czech Republic, [3]Biopticka laborator s.r.o., Plzen, Czech Republic, [4]Medical College of Wisconsin, Milwaukee, WI, [5]Universitätsklinikum Erlangen, Germany, Erlangen, Germany

Disclosures: Kvetoslava Michalova: None; Petr Steiner: None; Petr Grossmann: None; Abbas Agaimy: None; Dmitry Kazakov: None; Michal Michal: None; Michael Michal: None

Background: Although SPL represent fairly common mesenchymal neoplasms, the knowledge of their cytogenetic features is relatively limited. They are known to harbor an unbalanced, mostly hypodiploid karyotype with loss of either entire chromosome 13 or 13q, often in combination with loss of 16q. *HMGA2* and *HMGA1* are structurally homologous genes commonly rearranged in ordinary lipomas. A recent study has uncovered more complex cytogenetic abnormalities in a subset of SPL, including *HMGA2* gene rearrangements as well as structural aberrations involving 6p21 (targeting the *HMGA1* gene) (1).

Design: Fifteen cases of SPL were examined by FISH for *HMGA1* and *HMGA2* gene rearrangements; the same assay was used to exclude *MDM2* amplifications. The neoplasms were further analyzed by IHC using HMGA1, HMGA2, RB1 and CD34 antibodies.

Results: The clinicopathological features are summarized in the Table. A mean age of the patients (9M/6F) was 53.5 years. Tumors were of mean size 5.5 cm, subcutaneous, predominantly located in the upper back, posterior neck and shoulders. Follow-up was available for 8 patients with an average of 5.5 years and revealed no recurrences. Typical SPL immunomorphology (CD34+, loss of RB1) was seen in all cases. *MDM2* FISH was negative in all 9 tested cases. Most importantly, FISH showed a mutually exclusive *HMGA1* and *HMGA2* gene break in 6/15 and 3/10 cases, respectively. It further showed either monosomy of the entire chromosome 13 or deletion of 13q (*RB1* gene) in 10/13 analyzable cases, in 6 of them occurring together with either *HMGA1* or *HMGA2* rearrangement. IHC expression of HMGA1 was observed in both *HMGA1* rearranged tumors (n=4/4 tested; 70-100% positive tumor cells) as well as in some non-rearranged cases (n=4; 10-80% positive tumor cells); 4 non-rearranged cases were completely negative. All 3 *HMGA2*-rearranged cases showed strong nuclear positivity of HMGA2 in 100% neoplastic cells, while all FISH negative cases were negative by IHC as well.

Case Nr.	Age/Sex	Location	HMGA1 IHC *	HMGA2 IHC *	*HMGA1* FISH	*HMGA2* FISH	Monosomy 13/*RB1* deletion FISH	*MDM2* FISH
1	46/M	Upper back	100%	0%	Pos	NP	Monosomy 13	NP
2	40/F	Upper back	100%	0%	Pos	Neg	Monosomy 13	NP
3	U/M	Neck	NP	NP	Pos	NP	Monosomy 13	Neg
4	40/F	Shoulder	100%	0%	Pos	NP	NP	NP
5	73/F	Popliteal area	70%	0%	Pos	Neg	Neg	Neg
6	U/M	Neck	NP	NP	Pos	Neg	Neg	Neg
7	42/M	Posterior neck	70%	100%	Neg	Pos	Deletion *RB1*	Neg
8	U/M	Shoulder	0%	100%	Neg	Pos	Monosomy 13	Neg
9	U/M	Neck	0%	100%	Neg	Pos	Monosomy 13	Neg
10	53/F	Upper back	10%	0%	Neg	NP	NP	NP
11	55/M	Posterior neck	10%	0%	Neg	NP	Monosomy 13	NP
12	U/F	Unknown	NP	NP	Neg	Neg	Monosomy13	Neg
13	66/M	Nuchal area	0%	0%	Neg	Neg	Monosomy 13	NP
14	58/M	Posterior neck	80%	0%	Neg	Neg	Deletion *RB1*	Neg
15	62/F	Shoulder	0%	0%	Neg	Neg	Neg	Neg

Legens to Table: U unknown; NP not performed; * indicates number of positive tumor cells; Pos positive; Neg negative

Reference: (1) Cytogenetics of Spindle Cell/Pleomorphic Lipomas: Karyotyping and FISH Analysis of 31 Tumors

IOANNIS PANAGOPOULOS, LUDMILA GORUNOVA, MARIUS LUND-IVERSEN, KRISTIN ANDERSEN, HEGE KILEN ANDERSEN, INGVILD LOBMAIER, BODIL BJERKEHAGEN, SVERRE HEIM

Cancer Genomics Proteomics. 2018 May-Jun; 15(3): 193–200. Published online 2018 May 3. doi: 10.21873/cgp.20077

Conclusions: This study shows that almost 2/3 of SPL harbor mutually exclusive rearrangements of either *HMGA1* or *HMGA2* genes, further highlighting the complex molecular underpinnings of SPL. Moreover, along with the lack of either chromosome 13 or *RB1* gene rearrangements in 3/13 tested cases, it also questions the role of *RB1* gene aberrations as the main tumorigenic event. Although limited by the small sample size, it seems that HMGA1 and HMGA2 IHC antibodies could serve as relatively useful ancillary tools in detecting both rearrangements.

81 USP6 Rearrangement Negative Nodular Fasciitis: An Entity for Further Investigation

Jeremy Molligan[1], Paul Zhang[2]
[1]University of Pennsylvania, Philadelphia, PA, [2]Hospital of the University of Pennsylvania, Media, PA

Disclosures: Jeremy Molligan: None; Paul Zhang: None

Background: Nodular fasciitis (NF) is one of the most common soft tissue lesions and is a diagnostic challenge due to its morphologic similarities to other sarcomas. Although originally thought of a reactive process, identification of the recurrent MYH9-USP6 fusion gene confirmed the clonal neoplastic nature of NF. Molecular cytogenetic studies have identified genomic rearrangements of the USP6 locus in more than 90% of NF cases. FISH for USP6 breakapart signals has been used in diagnosis of NF. The aim of this study was to evaluate the diagnostic efficacy of USP6 break apart FISH in the setting of spindle cell lesions at a single institution.

Design: From 2012 and 2019, USP6 FISH was tested in 48 spindle cell lesions where NF was considered in the differential diagnosis. Of these, 35 were diagnosed as NF. Dual colored DNA probes each with different fluorochrome, were hybridized to the region flanking the breakpoint of USP6 gene (17p13.2) in interphase nuclei on paraffin sections using a commercially available Dual Color DNA Probe kit (EMPIRE GENOMICS). The case reports were reviewed for immunoprofiles and histomorphology and correlated with the FISH results.

Results: Of the 48 cases which USP6 FISH was conducted, 35 cases were morphologically consistent with nodular fasciitis and 13 cases were NF mimics. Of the nodular fasciitis cases (n=35), 19 were USP6 FISH positive (54.3%), 16 were FISH negative for USP6 rearrangements (45.7%). Of the other spindle cell lesions (n=13), FISH was negative for USP6 in all 13 NF mimics. Immunoprofiles were reviewed (available in 30/35 cases) and showed that of the USP6 positive FISH cases 17/19 (89.5%) showed immunoreactivity for SMA, 0/35 (0%) for S100, 1/19 (0.5%) for CD34, and 0/19 (0%) for nuclear beta-catenin, 0/10 (0%) for MUC4.

Conclusions: This study found an overall concordance rate between histomorphologic diagnosis of nodular fasciitis and FISH for USP6 rearrangements of 54.3%. There is high incidence of UPS6 negative NF. The significance of the USP6 negative NF is unclear and it might reflect 1. low frequency of tumor cells with translocation and the difficulty in detecting low frequency translocations by FISH, 2. possibly another novel form of oncogenesis in these USP6 negative NF or 3. a form of true reactive process. Until then, NF should still be remained as the histologic diagnosis to report this group of potential diverse fibro/myofibroblastic lesions in soft tissue regardless of positive or negative USP6 FISH result.

82 Novel Wild-Type Rodent Animal Model Induces Neuroarthropathic Change

Ben Murie[1], Julie Fanburg-Smith[2], Christopher Stauch[3], Jesse King[4], Michael Aynardi[4]
[1]Penn State Health Milton S. Hershey Medical Center, Palmyra, PA, [2]Penn State Health Milton S. Hershey Medical Center, McLean, VA, [3]Penn State College of Medicine, Hershey, PA, [4]Penn State Health Milton S. Hershey Medical Center, Hershey, PA

Disclosures: Ben Murie: None; Julie Fanburg-Smith: None; Christopher Stauch: None; Jesse King: None; Michael Aynardi: *Consultant*, Stryker Corporation; *Consultant*, Arthrex; *Grant or Research Support*, Arthrex

Background: Destructive (Charcot-like) neuroarthropathy leads to bone/joint loss, limb deformity and often amputation. We hypothesize that obese mice with vasculopathic sensory neuropathy, combined with repetitive micro-trauma by treadmill exercise, may stimulate pre-Charcot neuroarthropathic change and wanted to create the first animal model for Charcot arthropathy.

Design: Following IAUCUC approval, 14 wild-type C57BL/6J mice were fed a high-fat diet ad libitum (60% fat by kcal) to facilitate diet-induced obesity (DIO, n= 8) or low-fat control diet (LFCM, n= 6). At 14 weeks, all mice underwent seven-weeks of high-intensity treadmill running on uphill ten-degree grade, four times per week at 30-minute intervals, with constants speed, distance, and time. Von Frey filament and hotplate testing performed bi-weekly assessed hind-paw sensory-neuropathic changes. Hind-paw X-rays were obtained prior to and following the treadmill protocol, with analysis of talar-first metatarsal (T1MT) and calcaneal-fifth metatarsal (C5MT) angles. H&E sections of sacrificed bilateral hind limbs were used to assess musculoskeletal parameters.

Results: While initial hotplate testing revealed no difference in thermal sensory function (p=0.53), following the seven-week running protocol DIO mice showed increased thermal response latency compared to controls (p=0.006). Von Frey testing revealed significantly reduced withdrawal reflexes in DIO mice compared to LFCM at all timepoints (p<0.001). DIO mice increased T1MT and C5MT angle by 7.7 degrees (p=0.001) and 3.1 degrees (p=0.007), respectively. Histopathology revealed significant abnormal bone remodeling in DIO mice. Although no fragmentation of bone or cartilage into soft tissue, the DIO cases had distinctive intraneural arteriolosclerosis, increased osteosclerosis (length, mm) and articular microfracture with irregular concentric endochondral ossification, not identified in control mice.

Conclusions: Obese, neuropathic animals, when challenged with a controlled exercise regimen designed to induce micro-trauma, develop reliable sensory deficits and radiographic and histopathologic parameters reminiscent of (pre-Charcot) neuroarthropathy in humans. Treadmill running of wild-type obese mice appears to be a viable model for development of histologic vasculopathic-induced neuroarthropathy. Using this model with longer treadmill studies may elucidate our understanding of the progression of microfracture to joint destruction and the underlying pathophysiology of Charcot.

83 Novel Pathologic-Scoring System for Charcot Arthropathy is Reproducible, Correlates with Eichenholtz, and Predicts Need for Amputation

Ben Murie[1], Julie Fanburg-Smith[2], Jesse King[3], Christopher Stauch[4], Michael Aynardi[3]
[1]Penn State Health Milton S. Hershey Medical Center, Palmyra, PA, [2]Penn State Health Milton S. Hershey Medical Center, McLean, VA, [3]Penn State Health Milton S. Hershey Medical Center, Hershey, PA, [4]Penn State College of Medicine, Hershey, PA

Disclosures: Ben Murie: None; Julie Fanburg-Smith: None; Jesse King: None; Christopher Stauch: None; Michael Aynardi: *Consultant*, Stryker Corporation; *Consultant*, Arthrex; *Grant or Research Support*, Arthrex

Background: Charcot arthropathy is a destructive joint disorder in neuropathic diabetic patients. Historically, Charcot is clinicoradiologically classified by the Eichenholtz Stage (E-score). There is no prior histopathologic classification for Charcot. We independently examined histopathologic features to develop a reproducible correlative pathologic scoring system.

Design: Charcot midfoot surgery specimens were analyzed to evaluate vessel, skeletal muscle, nerve, bone, and especially periarticular soft tissue embedded bone and cartilage fragments. Charcot Pathology Score (P-Score) was devised based on our understanding of progression. Afterwards, clinical data and radiology E-score (1-3) were reviewed and compared with P-score.

Results: Forty-eight cases of Charcot, 34M:14 F, mean age 60.3 (Range 28-83) years were included. Clinical risk factors for Charcot included DM2 and longstanding neuropathy. Elevated HbA1C, E-Score, preoperative American Society of Anesthesia score, and Charlson comorbidity index were predictors of amputation. Majority of pathologic specimens examined had superficial ischemic ulceration, dermal fibrosis, cellulitis and half osteomyelitis, skeletal muscle atrophy, and notably intraneural arteriolosclerosis (vasculopathy). Pathology (P)-Scores were classified by observation of pathophysiology. P-Score 1= Large bone fragments without host histiocytic response; P-Score 2= Mixed large and small bone fragments with host histiocytic response; P-Score 3= Small minute spicules to complete absence/resorption of bone fragments with few to absent histiocytes, replaced by reactive fibrosis. Comparisons were 98% accurate with respect to Eichenholtz (one case did not have enough soft tissue to evaluate) and there was 98% interobserver variability on P-scoring by several bone pathologists/trainees, with a single-case discrepancy between score 2 vs 3, though both higher scores correlate with a clinical need for amputation.

Conclusions: This novel Charcot Pathologic (P-score) Scoring System is highly reproducible among pathologists, from trainees to experts, explains the pathophysiology of progression of Charcot, and correlates well with the clinicoradiologic Eichenholtz (E-Score) in all cases with adequate synovial tissue for evaluation. The findings of a high P-score (2 or 3) predicts clinical progression and need for amputation. Distinctive intraneural arteriolosclerosis suggests that vasculopathy plays a role in the development of Charcot.

84 Towards Biomarkers and Therapeutic Targets for Dedifferentiated Chondrosarcoma Discovered by Fourier Transform Mass Spectrometry Proteomics

Makiko Ogawa[1], Atsushi Tanaka[1], Lingxin Zhang[1], Julia Wang[1], Ronald Hendrickson[1], David Klimstra[1], Meera Hameed[1], Michael Roehrl[1]
[1]Memorial Sloan Kettering Cancer Center, New York, NY

Disclosures: Lingxin Zhang: None; David Klimstra: None; Meera Hameed: None; Michael Roehrl: None

Background: Dedifferentiated chondrosarcoma (DDCS) is an aggressive mesenchymal malignancy, associated with early and frequent metastasis and typical 5-year survival below 25%. Thus, novel therapies for DDCS are needed to improve clinical outcomes. DDCS is considered to represent transformation from conventional chondrosarcoma (CCS), but the histogenesis of DDCS remains unclear. Previous molecular studies have primarily focused on genetic mutations in DDCS. Very little is known about the global proteomic landscape that characterizes DDCS. Here, we present our preliminary deep proteome profiling findings.

Design: We collected 20 matched chondrosarcoma cases with both conventional and dedifferentiated components. Total proteins were extracted from formalin-fixed paraffin-embedded (FFPE) tissues and digested by trypsin and lysyl endopeptidase. Protein expression was analyzed by label-free liquid chromatography mass spectrometry. Proteins were identified and quantified by MaxQuant informatics. Differentially expressed protein were analyzed by Perseus. Finally, we performed functional analyses using STRING and the drug-gene interaction database (DGIdb).

Results: Over 4,000 proteins were robustly detected in each tumor sample. In DDCS specifically, we found 190 significantly differentially expressed proteins, including 152 up-regulated and 38 down-regulated proteins (FDR<0.05). Based on a DGIdb search, quantitative proteomic analysis of chondrosarcoma found 367 potential therapeutic vulnerabilities with 179 associated FDA-approved drugs for 1,487 DDCS-specific proteins. A pathway analysis found that the RAS/RAF/MEK/MAPK cascade was enriched in CCS. Furthermore, this pathway was more enriched in DDCS than in CCS. The WNT signaling pathway was also significantly enriched in DDCS (Reactome Pathway).

Conclusions: Global sarcoma proteomics by deep Fourier transform mass spectrometry can find promising biomarkers and new therapeutic candidate targets for high-grade sarcomas such as DDCS. Our proteome-directed experimental and bioinformatics strategy can be applied broadly to many types of sarcomas and may lead to a new paradigm of proteome-based molecular testing.

85 MyoD1 Expression in Fibroepithelial Stromal Polyps

Nicholas Olson[1], Karen Fritchie[1], Jorge Torres-Mora[1], Andrew Folpe[1]
[1]Mayo Clinic, Rochester, MN

Disclosures: Nicholas Olson: None; Karen Fritchie: None; Jorge Torres-Mora: None; Andrew Folpe: None

Background: Fibroepithelial stromal polyps (FESP) are benign polypoid mesenchymal lesions thought to arise from desmin-positive specialized stromal cells of the female genital tract. The presence of such desmin-positive cells in FESP may raise concern for botryoid embryonal rhabdomyosarcoma (ERMS), especially if one is unfamiliar with the typical clinicopathological features of these two entities. Prompted by a recent case of FESP showing limited nuclear immunoreactivity for the skeletal muscle-associated transcription factor MyoD1, we studied MyoD1 and myogenin expression in a well-characterized series of such cases.

Design: Cases of FESPs from our institutional and consultation archives were immunostained for desmin, myogenin and MyoD1, using commercially available antibodies and routine laboratory protocols. Expression of these markers was scored as follows: 0, 0% positive cells; 1+, 1-10%; 2+, 10-49%; 3+ >50%. Only nuclear immunoreactivity was scored for myogenin and MyoD1. Clinical data was recorded. Control cases included ERMS (n=6), mammary-type myofibroblastoma (n=5), deep angiomyxoma (n=2), and angiomyofibroblastoma (n=1).

Results: We identified 25 cases of FESP arising in the vagina (n=24) and vulva (n=1) in patients ranging from 28 to 82 years of age (median 57 years). Desmin expression was seen in 23 FESPs (92%) (1+, n=3, 12%; 2+, n=2, 8%; 3+, 18, 72%). 10 FESP (40%) showed some degree of MyoD1 expression (1+, n=6, 24%; 2+, n=3, 12%; 3+, n=1, 4%); all were myogenin-negative. At least focal myogenin and MyoD1 expression was present in all ERMS (6/6); all other “control” cases were entirely negative. All FESP behaved in a benign fashion, without local recurrence (n=24, 1 to 297 months, median 48 months).

Conclusions: We have found limited MyoD1 expression in 40% of otherwise-typical vulvovaginal FESP, a potentially serious diagnostic pitfall in these routinely desmin-positive lesions. The significance of MyoD1 expression in the stromal cells of FESP is unclear, as skeletal muscle differentiation is not a feature of these benign lesions. Awareness of this potential immunohistochemical pitfall, and careful morphologic evaluation should allow the confident distinction of MyoD1-positive FESP from botyroid ERMS in almost all instances.

86 Fibrous Dysplasia at Unusual Sites: A Series of 36 Cases with Emphasis on Histologic Patterns

Nicholas Olson[1], Carrie Inwards[1], Doris Wenger[1], Karen Fritchie[1]
[1]Mayo Clinic, Rochester, MN

Disclosures: Nicholas Olson: None; Carrie Inwards: None; Doris Wenger: None; Karen Fritchie: None

Background: Fibrous dysplasia (FD) is benign fibro-osseous neoplasm most commonly affecting the skull, ribs and long bones. Imaging features of FD at these sites is characteristic facilitating accurate diagnosis even on biopsy. We have noticed a disproportionate number of FD in our consultation practice when it occurs at less common locations including the spine and short tubular/small bones of hands/feet (STSBHF). Therefore, we sought to study the clinicopathologic features of FD at atypical sites.

Design: Cases of FD arising in the spine/STSBHF were collected from our institutional and consultation archives and assessed for: type of osteoid/bone, stromal cellularity, matrix-poor foci, osteoclast-type giant cells, histiocytes and cartilage. Clinical and radiologic data were collected.

Results: Of 1955 total cases of FD, 128 arose in the spine/STSBHF representing 2% of institutional and 10% of consultation cases, respectively. 36 of those cases (20F, 16 M; 8-72 years) had material available for review and arose in the vertebral bodies (n=17, 47%), sacrum (n=5, 14%), calcaneus/talus (n=6, 17%), metacarpal/tarsal bones (n=5, 14%), and phalanges (n=3, 8%). 3 patients had a polyostotic disease. Radiology was reviewed in 13 cases (7 previously; 6 concurrently) revealing lytic lesions with a narrow zone of transition, peripheral sclerosis and variable osseous expansion. Although the lesions in the STSBHF showed imaging findings classic for

FD, the monostotic cohort generated a broader differential including enchondroma, ABC and giant cell tumor of bone. Histologically, the following patterns were observed at least focally: matrix-poor foci (n=10; 28%), complex/anastomosing bone (n=9, 25%), cementum-like ossicles (n=7, 19%), osteoclast-type giant cells (n=5, 14%), cystic change (n=3, 8%), and increased stromal cellularity (n=2, 6%). Matrix-poor foci occupied 10-90% of tumor in cases with this feature (median 70%). Follow-up (n=8, 22-878 months) revealed no recurrences or malignant transformation.

Conclusions: FD arising in the spine/STSBHF is rare and more frequently results in expert consultation. A significant number of cases at these sites exhibit less commonly recognized pattern of bone formation and stromal changes including osteoclast-type giant cells and large areas devoid of bone formation. Furthermore, imaging features in the STSBHF are often less specific. Awareness of the morphologic spectrum at these locations coupled with radiologic correlation should aid in accurate classification.

87 Desmoplastic Fibroma Is Not Driven by the APC-wnt Pathway and May Have Microscopic Cartilage and ABC-Like Cysts

Nigam Padhiar[1], Julie Fanburg-Smith[2], Mark Murphey[3], Cesar Moran[4]
[1]Penn State College of Medicine, Downingtown, PA, [2]Penn State Health Milton S. Hershey Medical Center, McLean, VA, [3]American Institute for Radiologic Pathology, Silver Spring, MD, [4]The University of Texas MD Anderson Cancer Center, Houston, TX

Disclosures: Nigam Padhiar: None; Julie Fanburg-Smith: None; Mark Murphey: None; Cesar Moran: None

Background: Desmoplastic fibroma (DF) is a rare, benign, locally aggressive bone tumor. Its histopathologic soft tissue counterpart desmoid-fibromatosis is driven by tumor-suppressor APC-wnt pathway, resulting in nuclear accumulation of beta-catenin by immunostain (IHC) and *CTNNB* mutation. ABC-like cystic features have not been previous described in DF.

Design: Cases coded as DF were pulled from our files; several were excluded due to inadequate material, better diagnosis as soft tissue primary or alternate diagnosis as fibrous dysplasia, low grade central osteosarcoma, or undifferentiated pleomorphic sarcoma. Two nuclear beta-catenin positive jaw cases were radiologically reviewed and reclassified as soft-tissue-primary fibromatosis with secondary bone involvement. For included cases, patient data, radiologic imaging, morphologic observations, IHC for beta-catenin or MDM2, and molecular analysis by former pyrosequencing or underway NGS results obtained and FISH mutation reviewed.

Results: Sixty-seven cases included 36 males, 30 females, and 1 patient of unknown sex. Patient ages ranged from 7mo-75 (median 24) years. The most common sites include long bones, followed by the jaw (mandible>maxilla), axial skeleton and distal extremities. Radiology revealed expansile, elongate and lobulated, often metaphyseal, lesions with scalloping, cortical destruction and minimal/no soft tissue extension, 16% cases had pathologic fracture. Notable were distinctive fibrous bands in 75%, of low-to-intermediate signal enhancement on MRI-T2-weighted images, without matrix/mineralization or fluid-fluid levels. Tumor sizes ranged from 2.5-14.8 (median 4.75) cm. Microscopically, DF were bland, fibroblastic proliferations with moderate cellularity, whirling or cartwheel pattern, band like often keloidal collagen, and obscure rather than elongate vessels. 12% cases demonstrated focal chondroid metaplasia, without definite pathologic fracture. Cystic change was focally observed in 8%. No cases of those studied had *MDM2* amplification or *GNAS* or *CTNNB* mutation, nor did these exhibit nuclear beta-catenin or MDM2 IHC.

Conclusions: This large series confirms that DF occurs in a wide age range and anatomic distribution. Its radiologic interpretation with fibrous bands is predictive, and subtle morphological and phenotypical features separate DF from its soft tissue counterpart. Intralesional microscopic cartilage and cystic change may be observed. DF is not driven by *CTNNB* mutation; alternate pathways can be explored.

88 Disentangling Chondroblastoma-like Osteosarcoma from Atypical and Malignant Chondroblastoma and Giant Cell Tumor of Bone

David Papke[1], Yin Hung[2], Gregory Charville[3], John Reith[4], Christopher Fletcher[1], G. Pétur Nielsen[5], Jason Hornick[6]
[1]Brigham and Women's Hospital, Boston, MA, [2]Massachusetts General Hospital, Boston, MA, [3]Stanford University School of Medicine, Stanford, CA, [4]Cleveland Clinic Foundation, Cleveland, OH, [5]Harvard Medical School, Boston, MA, [6]Brigham and Women's Hospital, Harvard Medical School, Boston, MA

Disclosures: David Papke: None; Yin Hung: None; Gregory Charville: None; John Reith: None; Christopher Fletcher: None; G. Pétur Nielsen: None; Jason Hornick: *Consultant*, Eli Lilly; *Consultant*, Epizyme

Background: Chondroblastoma (CB), giant cell tumor of bone (GCTB) and chondroblastoma-like osteosarcoma (CB-OS) are distinguished based on radiologic and histologic findings, although overlapping features are common. Recent studies have identified point mutations in *H3F3A* and *H3F3B*, leading to H3K36M in CB (95%) and H3G34W in GCTB (85%); these alterations are reliably detected by immunohistochemistry (IHC) using mutation-specific antibodies (Abs).

Design: In this study, we investigated 13 cases diagnosed as "atypical CB", "malignant CB" or "CB-OS" retrieved from the archives of 4 academic centers. All cases underwent review to establish diagnostic consensus.

Results: There was striking histologic overlap among tumor types; there were cases initially diagnosed as CB-OS that were found to be positive for H3K36M (clone RM193) or H3G34W (clone RM263). IHC for H3K36M was positive in 6/13 cases, classified as atypical CB (4/6) and malignant CB (2/6) based on cytology, infiltrative growth, tumor size, mitotic activity, and necrosis. One atypical CB and 2 CB-OS contained prominent tenosynovial giant-cell tumor-like epithelioid cells. Osteoclast-like giant cells were rare in 2 atypical CB. In contrast to conventional CB, atypical and malignant cases affected older individuals (median: 52 yr; range: 29–57 yr) and tended to occur in locations unusual for CB: rib (3), scapula (2) and radius (1).

IHC for H3G34W was positive in 2/7 cases negative for H3K36M. On review, these two tumors were classified as malignant GCTB. Both arose in females (19 and 36 yr) in the T7 vertebra and femur. One contained cells with folded nuclei in an eosinophilic matrix, closely mimicking CB. Most cases negative for H3K36M and H3G34W were classified as CB-OS (4/5), while 1/5 was favored to be H3K36M-negative CB. CB-OS mostly occurred in younger patients (median: 21 yr; range: 19–40 yr) than atypical/malignant CB; anatomic locations were rib, scapula, humerus and C7 vertebra.

Follow-up data were available for 8/13 patients overall (median: 14 yr; range: 1–36 yr): 6 experienced local recurrence, and 3 developed widespread metastases (one case from each diagnostic category).

Conclusions: The clinical presentation and course of atypical/malignant CB are distinct from those of conventional CB. Malignant GCTB and atypical/malignant CB show significant histologic overlap with each other and with CB-OS. Ultimately, when considering these tumor types, IHC can be a useful or even critical diagnostic adjunct.

89 Plexiform Myofibroblastoma: Clinicopathologic Analysis of 34 Case of a Distinctive Benign Tumor that Predominantly Occurs in Children and Young Adults

David Papke[1], Christopher Fletcher[1]
[1]Brigham and Women's Hospital, Boston, MA

Disclosures: David Papke: None; Christopher Fletcher: None

Background: The spectrum of benign (myo)fibroblastic cutaneous tumors continues to expand and includes entities such as plexiform fibrohistiocytic tumor, dermatomyofibroma and fibroblastic connective tissue nevus. Here, we describe a previously unrecognized entity: "plexiform myofibroblastoma" (PM). PM is a rare and distinctive superficial mesenchymal tumor of (myo)fibroblastic lineage that occurs in children and young adults.

Design: 34 cases from the consultation archives of one of the authors have been studied to characterize the clinicopathologic characteristics of PM.

Results: 19 patients (56%) were female and 15 were male, with age of presentation ranging from congenital (2 cases) to 57 years of age (median: 11.5 yrs; mean: 15.6 ± 15.5 yrs). Males tended to develop tumors during childhood (median: 2 yrs; range: congenital–37 yrs), while in females the age distribution was relatively uniform from childhood through adulthood (median age: 25 yrs; range: 0.3–50 yrs). Most tumors occurred in the posterior neck (10 patients) and back (10), followed by the anterolateral chest wall (4), axilla (4), abdominal wall (3), occiput (2), inguinal/suprapubic region (2), lower extremity (2) and breast (1). Three male patients, two of whom were siblings, presented around one year of age with several lesions involving the back, occiput and axillae; these lesions spontaneously regressed after being present for 2 years. The average greatest dimension was 2.7 ± 1.9 cm.

Histologically, PM is composed of long plexiform fascicles of (myo)fibroblastic cells that ramify through the subcutis, sometimes with extension into the deep dermis. The bland neoplastic cells have indistinct cell borders, palely eosinophilic cytoplasm and tapered nuclei. There was no histiocytoid component. Immunohistochemical studies were positive for SMA (27/33 specimens), desmin (10/22) and CD34 (13/25) and negative for β-catenin (13/13). An *FGFR2* tyrosine kinase domain mutation was detected in 1/6 sequenced cases, and no somatic alterations were detected in the other 5. Clinical follow up data were available for 12/34 patients (35%; median: 4 yrs; mean: 6.7 ± 6.4 yrs;). Although most excisions had positive margins (10/13), only one patient developed a local recurrence after 4 years. None metastasized.

Conclusions: PM is a benign tumor with characteristic histology, epidemiology and anatomic site predilection. Because PM rarely recurs, a watchful waiting approach would be reasonable when excisions have positive margins.

90 Utility of MYC RNA Chromogenic In Situ Hybridization for the Classification of Post-Radiation Vascular Lesions of the Breast

Travis Rice-Stitt[1], Azfar Neyaz[2], Vikram Deshpande[3], Ivan Chebib[4]
[1]Massachusetts General Hospital, Somerville, MA, [2]Massachusetts General Hospital, Malden, MA, [3]Massachusetts General Hospital, Boston, MA, [4]Massachusetts General Hospital, Harvard Medical School, Boston, MA

Disclosures: Travis Rice-Stitt: None; Azfar Neyaz: None; Vikram Deshpande: *Grant or Research Support*, Advanced Cell Diagnostics; *Advisory Board Member*, Viela; *Grant or Research Support*, Agios Pharmaceuticals; Ivan Chebib: None

Background: Development of cutaneous vascular lesions of the breast is a well-known complication of radiation therapy for breast cancer. Distinguishing between atypical vascular lesions (AVL), which show a benign clinical course, and radiation-associated angiosarcomas (RAAS), which are aggressive and optimally treated with excision of the entire irradiation field, is critical for management and prognostication. Since these lesions can have significant histologic and clinical overlap, the discovery that MYC amplification is present in RAAS and not in AVL has proved a highly valuable diagnostic tool. Current methods for assessing MYC status, including immunohistochemistry (IHC) and fluorescent in situ hybridization (FISH), are hindered by specificity (IHC) and cost / correlation to histology (FISH).

Design: We evaluated 22 vascular lesions of the breast using an automated MYC RNA In Situ Hybridization Assay (RNAscope LS 2.5 Probe Hs-MYC, Advanced Cell Diagnostics). This assay uses a chromogenic RNA probe for MYC (MYC CISH) as a surrogate for DNA amplification and can be interpreted using brightfield microscopy. The cases included 10 AVLs, 6 RAAS, and 6 other vascular lesions absent a history of regional radiation (2 breast hemangiomas, 3 breast primary angiosarcomas, and 1 angiosarcoma secondary to lymphedema).

Results: All 10 (100%) radiation-associated AVLs were negative for MYC CISH. This included four cases which had been classified either as “highly atypical” or “cannot rule out angiosarcoma” based on weak IHC staining for CMYC and/or histologic appearance. All 10 cases have shown a benign clinical course to date. Conversely, 5 of 6 (83%) RAAS showed strong, diffuse staining for MYC CISH and 1 of 6 (17%) showed weak-to-moderate staining for MYC CISH with the caveat that this case had only 5-10 malignant cells present in the material available for testing. All 4 (100%) non-radiation-associated angiosarcomas were negative for MYC CISH (3 primary breast angiosarcomas and 1 arm/axillary angiosarcoma that arose secondary to lymphadenoma). Interestingly, 2 of 2 (100%) histologically benign breast hemangiomas showed weak, scattered staining for MYC CISH.

Conclusions: MYC CISH shows strong potential as a highly sensitive and specific marker for distinguishing RAAS (strong, diffuse staining) from AVL (no staining) and other entities. MYC CISH avoids ambiguity of weak-to-moderate MYC staining by IHC and can be interpreted by ordinary bright field microscopy allowing correlation to histology and inked margins.

91 Osteofibrous Dysplasia (Kempson-Campanacci’s disease): Long Term Follow-up Study on Natural History, Results of Treatment and Relationship with Adamantinoma

Alberto Righi[1], Marco Gambarotti[2], Laura Campanacci[3], Marta Sbaraglia[4], Nicola Fabbri[5], Angelo Dei Tos[6]
[1]IRCCS Istituto Ortopedico Rizzoli, Bologna, Italy, [2]Bologna, Italy, [3]3rd Orthopaedic and Traumatologic Clinic prevalently Oncologic, IRCCS - Istituto Ortopedico Rizzoli, Bologna, Italy, [4]Department of Pathology, Azienda ULSS2 Marca Trevigiana, Treviso, Italy, [5]Memorial Sloan Kettering Cancer Center, New York, NY, [6]University of Padua Medical School, Padua, Padua, Italy

Disclosures: Alberto Righi: None; Marco Gambarotti: None; Laura Campanacci: None; Marta Sbaraglia: None; Nicola Fabbri: *Speaker*, Onkos Surgical; *Consultant*, Onkos Surgical; Angelo Dei Tos: None

Background: Osteofibrous dysplasia, also called Kempson-Campanacci disease, is a rare benign fibro-osseous lesion usually diagnosed during early childhood or pre-adolescence. Consensus has not been reached on the histologic criteria differentiating osteofibrous dysplasia, osteofibrous dysplasia-like adamantinoma and adamantinoma. Moreover, progression to adamantinoma has not been convincingly documented so far.

Design: To assess the natural history of the disease and late results of treatment, we reviewed all patients with histologically and immunohistochemical proven osteofibrous dysplasia treated at our institution with an available follow-up.

Results: Forty-three cases of osteofibrous dysplasia were retrieved with an immunohistochemical confirmation of the presence of isolated/scattered cells or very small clusters of cytokeratin-positive cells. All cases involve the tibial diaphysis with an eccentric and well margined intra-cortical osteolysis. Variable amounts of pan-cytokeratin AE1/AE3 were observed in all but one case (42/43, 97.7%), whereas pan-cytokeratin 34 beta-E12 and MNF116 immunopositivity were present in 15 (34.9%) and in 7 % (16.3%) cases, respectively. The single case not showing cytokeratin AE1/AE3 positive cells, featured however scattered positive cells for cytokeratin 34 beta-E12. The epithelial cells in the fibrous stroma were always negative for the mast-cells marker CD117. Age ranged from 10 months to 17 years (median 7 years) with a slight female prevalence (22 females and 21 males). Musculoskeletal tumor society functional result was 27-30 points in 100% of patients that received a single biopsy or curettage for treatment, 75% of patients that had repeated curettage and only

20% of patients that underwent multiple resections and osteotomies. During follow-up (mean: 24 years, range 4-63 years), no patients featured symptoms, radiographic features or sequential radiographic changes suggesting progression to adamantinoma.

Conclusions: 1. Osteofibrous dysplasia is a benign condition with mild to moderate consequence at skeletal maturity in most cases. 2. Non-operative management may be adequate in the majority of patients. 3. There was no evidence of adamantinoma development in this long-term study.

92 Synovial Chondrosarcoma: A Monocentric Retrospective Analysis of 9 Patients

Alberto Righi[1], Poosit Ruengwanichayakun[2], Marco Gambarotti[3], Marta Sbaraglia[4], Angelo Dei Tos[5]
[1]IRCCS Istituto Ortopedico Rizzoli, Bologna, Italy, [2]Sawankhalok, Sukhothai, Thailand, [3]Bologna, Italy, [4]Department of Pathology, Azienda ULSS2 Marca Trevigiana, Treviso, Italy, [5]University of Padua Medical School, Padua, Padua, Italy

Disclosures: Alberto Righi: None; Poosit Ruengwanichayakun: None; Marco Gambarotti: None; Marta Sbaraglia: None; Angelo Dei Tos: None

Background: Synovial chondrosarcoma is an exceedingly rare disease which can arise either primarily or secondarily from preexisting synovial chondromatosis. Accurate diagnosis is challenging and most often needs clinical, radiological, and pathological correlation.

Design: To evaluate histologic criteria to differentiate synovial chondrosarcoma from synovial chondromatosis, all cases of synovial chondrosarcoma treated at our institution were retrieved and reevaluated morphologically and radiologically. Molecular analysis of *IDH1/2* gene was performed.

Results: Nine cases of synovial chondrosarcoma were identified. Age ranged from 23 to 74 years (median 54 years) with a slight male prevalence (5 males and 4 females). Five cases (56%) involved knee joints, two (22%) hip joints, and one each (11%) scapula and ankle, respectively. Seven patients had history of preexisting synovial chondromatosis and morphologic evidence of malignant transformation showing both areas of synovial chondromatosis and chondrosarcoma. The mean time to malignant transformation was 57 months (range: 14-140 months). Five patients underwent surgical excision with wide margins and four patients were amputated following excision or wide resection. Macroscopically, all cases appeared as a cartilaginous mass on the articular surface with invasion into adjacent periarticular soft tissues or underlying bone; tumor size ranged from 3 to 17 cm (mean 9 cm). Microscopically, all 9 cases showed areas of hypercellularity with focal spindling of tumor cells. Loss of clustering pattern was seen in 7 cases (77%) and 6 cases (66%) showed myxoid change of the stroma. Five tumors (55%) showed “filling-up” pattern of marrow space invasion. No *IDH1/2* mutations were found. The follow-up (mean: 77 months, range 3 - 156 months) was available for 6 patients. Two patients developed lung metastases (6 months and 10 years from diagnosis of malignancy) and one of these patients developed recurrence 7 years after wide resection. At last follow-up, one patient died of disease, one was alive with disease and 4 were alive without evidence of disease.

Conclusions: 1. Histologic criteria in correlation with clinical and radiological features allow recognition of synovial chondrosarcoma. 2. *IDH1/2* mutations are not presented in synovial chondrosarcoma. 3. Clinical behavior overlaps that of central counterpart. 4. Complete resection is crucial for optimal disease control.

93 Characterization of PAX7 Expression in Synovial Sarcoma

Jason Scapa[1], Gregory Charville[2], Alexander Lazar[3]
[1]Stanford University Medical Center, Menlo Park, CA, [2]Stanford University School of Medicine, Stanford, CA, [3]The University of Texas MD Anderson Cancer Center, Houston, TX

Disclosures: Jason Scapa: None; Gregory Charville: None; Alexander Lazar: None

Background: Accounting for 5-10% of soft tissue sarcomas, synovial sarcoma (SS) is defined by an SS18-SSX fusion oncoprotein. Previous studies have demonstrated that SS18-SSX drives a distinctive transcriptional signature characterized by activation of PRC2-repressed genes, such as *PAX7*, a paired box transcription factor implicated in myogenesis. Given this association between the SS18-SSX fusion and *PAX7* transcriptional activation, we sought to examine the clinicopathologic characteristics of PAX7 expression in SS.

Design: Publicly available gene expression microarray data from human bone marrow-derived mesenchymal stem cells expressing SS18-SSX2 (GSE26563) were analyzed. Whole tissue sections from 30 cases of SS with evidence of *SS18* rearrangement were assessed by immunohistochemistry (IHC) using monoclonal antibodies against PAX7 (DSHB), cytokeratin (AE1/3, CAM5.2), and epithelial membrane antigen (E29). PAX7 expression was also analyzed on a previously published tissue microarray containing 188 cases represented as duplicate 1-mm cores.

Results: Analysis of gene expression data revealed enrichment of genetic loci associated with “muscle structure development” (GO:0061061; N = 47 genes; P = 2.7×10^{-9}), including *PAX7*, among those genes that were activated by overexpression of an SS18-SSX2 fusion in mesenchymal stem cells. *PAX7* expression was induced by SS18-SSX2 at a level (4.2-fold, P = 0.0016) similar to that

of *TLE1* (4.1-fold, P = 0.0007). PAX7 was expressed in 77% (23/30) of cases by IHC analysis of whole tissue sections. This observation correlated with identification of PAX7 in 74% (139/188) of tissue microarray cases. Overall, PAX7 was expressed in 94% (17/18) of biphasic and 73% (146/200) of monophasic tumors (P = 0.048). In whole sections, 59% (13/22) of PAX7-positive cases expressed an epithelial marker in >10% of cells, while none (0/8) of the PAX7-negative cases did (P < 0.004; Figure 1). Among 17 cases involving the trunk/extremities with available follow-up, there was local recurrence in 9.1% (1/11) of PAX7-positive cases and 33.3% (2/6) of PAX7-negative cases after margin-negative resection.

Figure 1 - 93

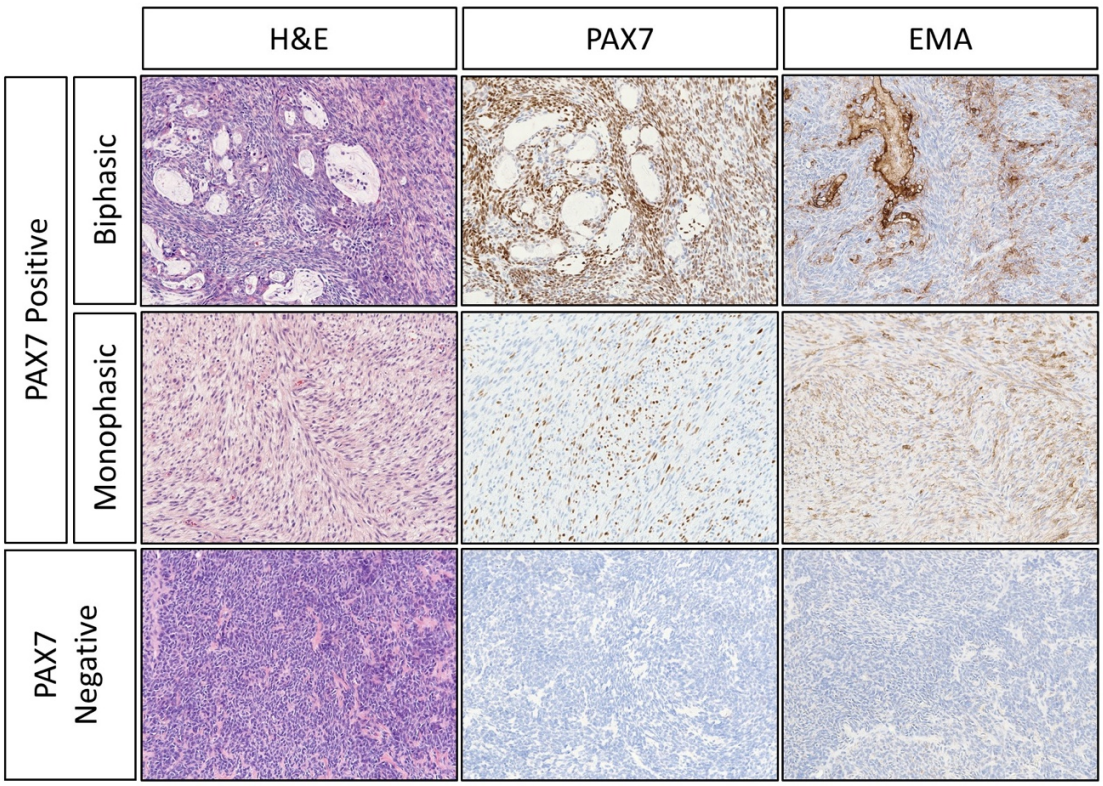

Conclusions: We demonstrate PAX7 expression in a cohort of SS cases, finding that PAX7 expression is associated with epithelial differentiation. Our data suggest that analysis of PAX7 expression may be used in a panel of markers to aid classification of SS. Future studies of PAX7 expression may help to understand the developmental origins and clinicopathologic heterogeneity of SS.

94 Significance of NGS in Diagnosis and Therapy Guidance of Bone and Soft Tissue Sarcomas

Xiaoliang Shi[1], Angen Liu[2], Kai Wang[3], Bo Zhang[4], Jian Wang[5]
[1]Shanghai, China, [2]Origimed, Shanghai, China, [3]OrigiMed Inc., Zhejiang University International Hospital, China, [4]Peking University Third Hospital, Beijing, China, [5]Fudan University Shanghai Cancer Center, Shanghai, China

Disclosures: Xiaoliang Shi: None

Background: Sarcoma has a poor prognosis and targeted therapy options are limited. Accurate diagnosis and classification of sarcoma is needed. Next-generation sequencing (NGS) technology has been able to meet the need for more accurate and efficient molecular characterization.

Design: A total of 199 sarcoma patients were enrolled. Immunohistochemistry (IHC) and NGS based deep sequencing targeting 450 cancer genes were performed for further diagnosis. Correlation analysis between mutated genes/clinical characteristics and specific sarcoma subtypes compared to the other subtypes was performed.

Results: Among 199 sarcoma samples, 131 were classified based on IHC results, 14 sarcomas, including 3 liposarcoma (LPS) with *MDM2* and *CDK4* amplifications, 3 Ewing's sarcoma (ES) with *EWSR1* fusion, 3 dermatofibrosarcoma protuberans (DFSP) with a *COL1A1-PDGFB* fusion, 2 leiomyosarcomas (LMS) with *RB1* and *TP53* mutations, 2 infantile fibrosarcoma with a *ETV6-NTRK3* fusion, and 1 gastrointestinal stromal tumor (GIST) with a *PDGFRA* mutation were defined by NGS testing (Figure 1). Statistical analysis showed

that *TP53*, *AKT2*, *FAM135B*, *CDKN2A*, *JUN*, *CDKN2B*, *ROS1*, *AXL*, *SETD2*, and *CCNE1* mutations were significantly associated with myxofibrosarcoma; *KIT* and *TP53* mutations were significantly associated with GIST; *NCOR1*, *GID4*, *LRP1B*, *RB1*, *AURKB*, *GLI2*, *RICTOR*, *MAP2K4*, *STK24*, *TNFSF13B*, *CCNE1*, *PRKDC*, *PTEN*, *CCND3*, *FGF10*, *BRD4*, *PRKACA*, *RET*, and *IL7R* mutations were significantly associated with osteosarcoma; *CDK4*, *MDM2*, *FRS2*, *FUS*, *LRP1*, *MYB*, *PTPN11*, and *TYK2* mutations were significantly associated with LPS; *MAP2K4*, *TP53*, and *KDM6A* mutations were significantly associated with LMS; mutated *SS18* and *EWSR1* significantly occurred in synovial sarcoma (SS) and ES, respectively (Table 1). *TP53* mutations were significantly negatively correlated with SS and GIST. In addition, *LMNA-NTRK1, ETV6-NTRK3, IRF2BP2-NTRK1*, *MEF2A-NTRK3*, and *ITFG1-NTRK3* fusions were detected in 6 sarcomas, which is important for NTRK inhibitor therapy. Notably, osteosarcoma, LPS, GIST, ES, and SS were associated with the patients' age (Figure 2A), LMS was associated with gender (Figure 2B), and angiosarcoma was associated with high tumor mutational burden (Figure 2C).

Sarcoma Subtype	Mutated Gene	Mutation Frequency in Specific Subtype	Mutation Frequency in Other Subtypes	p-value
Osteosarcoma	NCOR1	36.36%	1.69%	8.14E-07
	GID4	22.73%	1.13%	0.000192
	LRP1B	22.73%	1.69%	0.000475
	RB1	31.82%	6.21%	0.001115
	AURKB	13.64%	0.00%	0.00119
	GLI2	13.64%	0.00%	0.00119
	RICTOR	18.18%	1.13%	0.001485
	MAP2K4	18.18%	2.82%	0.009901
	STK24	9.09%	0.00%	0.011725
	TNFSF13B	9.09%	0.00%	0.011725
	CCNE1	13.64%	1.69%	0.018989
	PRKDC	13.64%	1.69%	0.018989
	PTEN	22.73%	6.21%	0.020035
	CCND3	18.18%	3.95%	0.022231
	FGF10	13.64%	2.26%	0.030825
	BRD4	9.09%	0.56%	0.032795
	PRKACA	9.09%	0.56%	0.032795
	RET	9.09%	0.56%	0.032795
	IL7R	13.64%	2.82%	0.045756
Myxofibrosarcoma	TP53	91.67%	31.02%	4.28E-05
	AKT2	25.00%	0.53%	0.000657
	FAM135B	33.33%	2.67%	0.000832
	CDKN2A	58.33%	16.04%	0.001768
	JUN	25.00%	1.60%	0.003061
	CDKN2B	50.00%	12.83%	0.003479
	ROS1	16.67%	1.07%	0.018763
	AXL	16.67%	1.60%	0.030216
	SETD2	16.67%	1.60%	0.030216
	CCNE1	16.67%	2.14%	0.043793
Leiomyosarcomas	MAP2K4	30.77%	2.69%	0.001176
	TP53	69.23%	32.26%	0.012635
	KDM6A	15.38%	1.08%	0.02202
	KIT	91.30%	1.70%	4.00E-23

Gastrointestinal stromal tumors	TP53	0.00%	39.20%	3.36E-05
Liposarcomas	CDK4	64.29%	3.78%	1.72E-08
	MDM2	64.29%	4.86%	6.96E-08
	FRS2	50.00%	4.32%	7.70E-06
	FUS	21.43%	0.00%	0.000281
	LRP1	28.57%	3.24%	0.002575
	MYB	14.29%	0.00%	0.004619
	PTPN11	14.29%	0.54%	0.013294
	TYK2	14.29%	1.62%	0.040797
Synovial sarcomas	SS18	77.78%	0.00%	1.63E-11
	TP53	0.00%	36.32%	0.028691
	CREB3L1	11.11%	0.00%	0.045226
	PDK1	11.11%	0.00%	0.045226
	TET1	11.11%	0.00%	0.045226
Ewing's sarcomas	EWSR1	71.43%	1.04%	1.75E-07
	EPHB1	14.29%	0.00%	0.035176
	FEV	14.29%	0.00%	0.035176
	VGLL3	14.29%	0.00%	0.035176
NTRK fusion sarcomas	NTRK1	33.33%	2.01%	0.001131
	NTRK3	66.66%	1.51%	5.55E-14

Figure 1 - 94

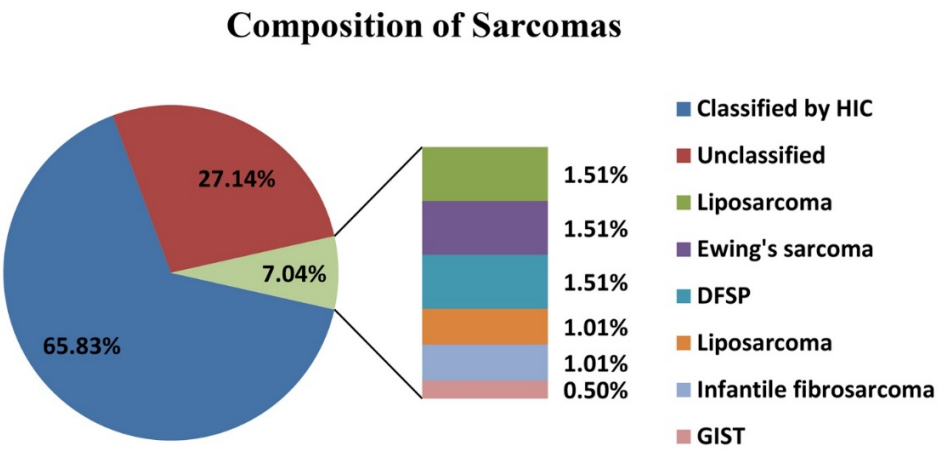

Figure 2 - 94

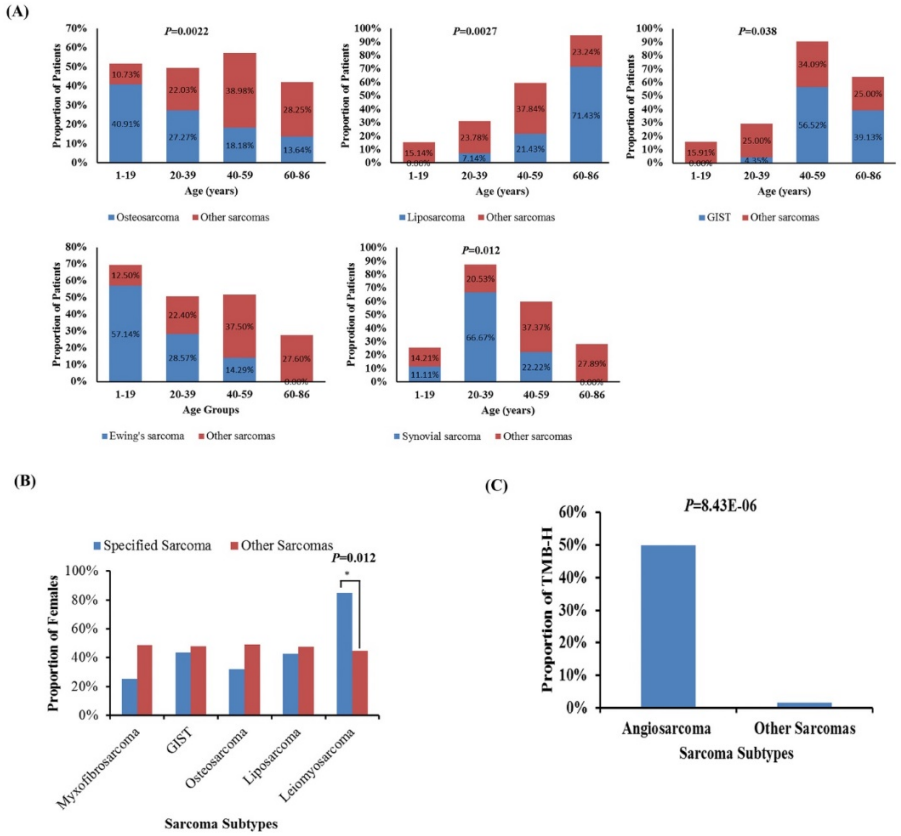

Conclusions: Our results suggest that NGS technology provides comprehensive and accurate information of GAs, which provides insight into new biomarkers for sarcoma diagnosis that may guide precise therapeutic strategies for patients with bone and soft tissue sarcomas.

95 Pseudocarcinomatous Epithelial Hyperplasia of Bone: A Diagnostic Pitfall Mimicking Squamous Cell Carcinoma

Smiljana Spasic[1], Oleksandr Kryvenko[2], Darcy Kerr[3], G. Pétur Nielsen[4], Andrew Rosenberg[2]
[1]University of Miami/Jackson Memorial Hospital, Miami, FL, [2]University of Miami Miller School of Medicine, Miami, FL, [3]Dartmouth-Hitchcock Medical Center and Geisel School of Medicine at Dartmouth, Lebanon, NH, [4]Harvard Medical School, Boston, MA

Disclosures: Smiljana Spasic: None; Oleksandr Kryvenko: None; Darcy Kerr: None; G. Pétur Nielsen: None; Andrew Rosenberg: None

Background: Pseudocarcinomatous epithelial hyperplasia (PEH) within bone is an uncommon complication of osteomyelitis and an important diagnostic pitfall. It is defined as a benign reactive proliferation of squamous epithelium arising from a cutaneous or mucosal surface that grows directly into the medullary cavity of adjacent bone. The epithelium accesses the bone through ulcers or sinus tracts. Histologically, PEH mimics well-differentiated squamous cell carcinoma (SCC) because of its location in bone, infiltration, and cytological changes. Its distinction from SCC is important because of the differences in treatment and prognosis.

Design: Cases were identified from the surgical pathology files of the participating institutions between the years 1985 - 2019.

Results: 30 cases were identified that exhibited the features of PEH from 21 males, 8 females, 1 unknown; 28 patients were 20-87, average 58 years. Sites: 17 - mandible, 5 - phalanges, 4 - maxilla, and 1 case each in femur, tibia, ischium and unknown. 14 patients had history of SCC treated with resection and chemoradiation, 3 had peripheral vascular disease and diabetes mellitus, 3 had previous trauma, 3 had drug-associated osteomyelitis, 2 had hematologic malignancy, 1 had osteomyelitis, 1 had history of cherubism and 3 patients had unknown medical histories. All cases exhibited severe acute and chronic osteomyelitis. Each case showed reactive keratinizing squamous epithelium that originated from ulcerated oral mucosa or ulcer/draining sinus tract of skin that permeated the medullary cavity and abutted or encompassed preexisting, often necrotic bone trabeculae. The keratinizing surface of the epithelium was often located adjacent to the bone surface and there was no significant pleomorphism, hyperchromasia, or mitotic activity. Acute and chronic inflammation was abundant. Patients with history of SCC developed PEH after 10 months - 10 years, av. 3.6 years. 11 of 30 patients had follow-up that

ranged from 1 month - 4 years, av. 21 months. 7 patients experienced repeated debridements over a period of 2 months - 2 years. No patient developed SCC.

Conclusions: PEH involving bone is an infrequent process that mimics well-differentiated SCC. It occurs in the setting of severe osteomyelitis and many patients (~50%) have history of previously treated SCC. Its recognition is important to avoid inappropriate treatment.

96 Epithelioid Sarcoma of the Peripheral Nerve: Clinicopathologic Analysis of 4 Cases

Smiljana Spasic[1], Julio Diaz-Perez[2], Edward Mccarthy[3], Jaylou Velez Torres[2], Andrew Rosenberg[2]
[1]University of Miami/Jackson Memorial Hospital, Miami, FL, [2]University of Miami Miller School of Medicine, Miami, FL, [3]Baltimore, MD

Disclosures: Smiljana Spasic: None; Julio Diaz-Perez: None; Edward Mccarthy: None

Background: Epithelioid Sarcoma (ES) is a rare distinct sarcoma of uncertain lineage. Two histological subtypes of ES are recognized, distal (classical or conventional) and proximal-types. ES usually arises in the superficial soft tissues of the distal extremities and has a propensity for local recurrence and dissemination via lymphatic spread. ES rarely arises in peripheral nerve and in this study, we present the clinicopathological features of ES arising in the peripheral nerve in 4 patients.

Design: The pathology files of the institutions including consultation files of the authors were searched for ES of the peripheral nerve. The clinical, radiological, histological and immunohistochemical were reviewed and tabulated.

Results: Four patients were identified including 3 men and 1 woman who ranged in age from 21-52 years; median, 24.5. 2 cases originated in the sciatic nerve, 1 radial nerve and 1 ulnar nerve. All patients presented with numbness, weakness in 2 cases, electric pain in 2 cases and foot drop in 1 case. Tumor size ranged from 2.4-5.8 cm (mean, 3.9). 3 tumors were avid on PET CT and showed increased signal intensity on T2-weighted MR images. Histologically, 3 tumors arose within the nerve and were confined to the epi-, peri- and endo-neurium of the nerve fascicles; 1 tumor invaded the epineurium into the adjacent soft tissues. All cases had conventional morphology with tumor cells enmeshed in a sclerotic stroma (4/4) and showed diffuse strong expression of keratin (4/4), and CD34 (3/3) and loss of INI1 (3/3). 1 case focally stained with S100, and all 3 tumors tested for SOX-10 were negative. The tumors had low mitotic activity (1-2/10 hpf) and exhibited focal necrosis. All tumors were treated with wide resection and one developed local recurrence that required amputation. Metastases were documented to lymph node (2), lung (2), pleura (1) and skin (1). 1 patient died of disease after 53.7 months, 1 patient is disease free, and 2 are alive with disease after a median follow-up of 2 months.

Conclusions: This is the first case series on ES of nerve. This aggressive neoplasm should be distinguished from other neoplasms arising in nerve including epithelioid schwannoma, epithelioid malignant peripheral nerve sheath tumor, meningioma, synovial sarcoma, angiosarcoma, and perineurial invasion by carcinoma or melanoma. Diagnosis of ES can be confirmed by expression of keratin and loss of INI1 and treatment should include wide excision.

97 Variant WWTR1-Related Gene Fusions in Epithelioid Hemangioendothelioma – A Genetic Subset Associated with Cardiac Involvement

Albert Suurmeijer[1], Brendan Dickson[2], David Swanson[3], Lei Zhang[4], Cristina Antonescu[4]
[1]University Medical Center Groningen, Groningen, Netherlands, [2]Mount Sinai Health System, Toronto, ON, [3]Mount Sinai Hospital, Toronto, ON, [4]Memorial Sloan Kettering Cancer Center, New York, NY

Disclosures: Albert Suurmeijer: None; Brendan Dickson: None; David Swanson: None; Lei Zhang: None; Cristina Antonescu: None

Background: Epithelioid hemangioendothelioma (EHE) is a malignant vascular neoplasm, arising at various anatomic sites and showing significant heterogeneity in clinical presentation and prognosis. The large majority of EHE (>90%) harbor unique *WWTR1-CAMTA1* fusions and CAMTA1 immunostaining may assist in diagnosing these cases. A small subset of EHE with distinct morphology but overlapping clinical features harbor instead *YAP1-TFE3* fusions and show TFE3 overexpression. However, a small group of tumors with otherwise typical histologic features lack these canonical fusions and remain unclassified.

Design: Triggered by an index case of a cardiac EHE with a variant *WWTR1-MAML2* fusion detected by RNA sequencing, we studied five additional EHE cases identified from our molecular files that lacked the common *WWTR1-CAMTA1* and *YAP1-TFE3* fusions. Fluorescence in situ hybridization and targeted RNA sequencing were applied to detect possible variant fusions. IHC for endothelial markers (ERG, CD31) was performed and confirmed positive in all cases.

Results: A group of 6 EHE cases lacking the canonical translocations were found to have variant *WWTR1* gene fusions (see Table). Two tumors had *WWTR1-MAML2* fusions, 1 harbored *WWTR1-ACTL6A* and 3 showed *WWTR1* rearrangements by FISH (and were negative for *MAML2* and *CAMTA1* abnormalities). All tumors occurred in adult patients. Remarkably, 4/6 cases presented as cardiac tumors (3

atrial, 1 ventricular). Four tumors had typical EHE histology and 2 showed malignant features. Clinical follow-up was limited and is under investigation.

Case 1	*WWTR1-MAML2*	EHE	76/F	Heart, left atrial mass
Case 2	*WWTR1-MAML2*	EHE	21/M	Bone, vertebra T11
Case 3	*WWTR1-ACTL6A*	Malignant EHE	73/F	Heart, right ventricle
Case 4	*WWTR1* rearrangement	EHE	72/F	Heart, atrium
Case 5	*WWTR1* rearrangement	EHE	67/M	Heart, atrium, and lungs
Case 6	*WWTR1* rearrangement	Malignant EHE	65/M	Pelvic mass

Conclusions: With the advent of targeted RNA sequencing the molecular subclassification of vascular tumors, including EHE is evolving. Our results identify yet another molecular subset involving *WWTR1*-related fusions, with *MAML2* and *ACTL6A* gene partners, which showed a striking predilection for cardiac presentation, in 4/6 patients. This anatomic location is rarely encountered among EHE with the more typical fusions. Clearly, larger series of EHE with variant *WWTR1* fusions are needed for more definitive clinicopathological correlations.

98 A Proposed Staging System for Improved Prognostication of MDM2-Amplified Liposarcoma

Jonathan Tucci[1], Nooshin K. Dashti[1], Justin Cates[1]
[1]*Vanderbilt University Medical Center, Nashville, TN*

Disclosures: Jonathan Tucci: None; Nooshin K. Dashti: None; Justin Cates: None

Background: Despite release of anatomic site-specific staging systems for soft tissue sarcomas in the AJCC 8th edition, there is only one minor difference between the algorithms for the extremities/trunk and retroperitoneum. Retroperitoneal localization of sarcomas, particularly liposarcomas, not only provides a larger potential space for tumor growth prior to clinical presentation, but the anatomic complexities of the retroperitoneum can complicate effective surgical resection, and subsequently disease-free survival, compared to sarcomas of the extremities/trunk. Here, we propose a new staging system for *MDM2*-amplified liposarcomas that properly emphasizes retroperitoneal localization, in addition to degree of differentiation and presence of distant metastasis.

Design: A retrospective cohort of 4,769 adult patients with surgically resected liposarcomas was extracted from the SEER database to compare the natural history of *MDM2*-amplified liposarcomas arising in the extremities/trunk or retroperitoneum. Cox-proportional hazard regression, non-linear regression, and nomographic analyses were performed to determine the most significant parameters in predicting cancer-specific death. A new staging system was derived and its predictive accuracy was compared to the AJCC 8th edition system by comparing areas under receiver-operating characteristic curves. Pairwise comparisons were performed to assess discriminatory ability.

Results: Multivariable Cox regression models revealed that dedifferentiation (HR: 5.0±0.5; p<0.001), retroperitoneal localization (HR: 3.6±0.4; p<0.001), and distant metastasis (HR: 2.6±0.4; p<0.001) had the largest effects on cancer-specific survival. Nomograms confirmed that categorized tumor size had a minimal impact on outcomes. A new staging system for *MDM2*-amplified liposarcoma was derived based on histologic subtype, anatomic location, and metastasis (Table). The proposed system showed better discrimination, higher concordance with clinical outcomes (0.73 vs 0.68; p<0.001), and greater predictive accuracy than the AJCC 8th edition staging system (0.84±0.01 vs. 0.81±0.01; p<0.001).

Table: Proposed staging system for *MDM2*-amplified liposarcoma

Stage	Criteria	N	5-yr survival (95% CI)
Stage I	WD, Extr/trunk, pM0	2,272	98% (97%-99%)
Stage II	WD, RP, M0 DD, Extr/trunk, pM0	1,575	86% (84%-88%)
Stage III	DD, RP, M0	783	64% (59%-68%)
Stage IV	M1	139	39% (28%-49%)

Abbreviations: CI, confidence interval; DD, dedifferentiated; Extr, extremity; M0, no metastasis; M1, distant metastasis; RP, retroperitoneal; WD, well differentiated

Figure 1 - 98

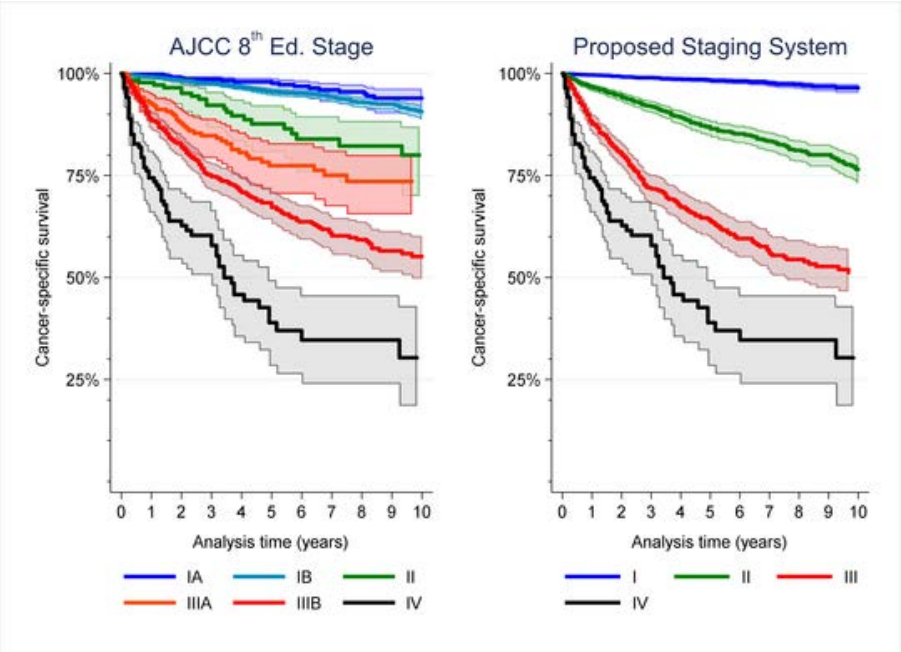

Conclusions: Statistical analysis of a large national cohort fails to confirm that categorized tumor size is a significant prognostic factor in staging *MDM2*-amplified liposarcoma. We propose a new simplified staging system that classifies liposarcomas, regardless of tumor size, by differentiation, anatomic location, and metastasis that outperforms the AJCC staging system.

99 Correlation Between FNCLCC Grading and Clinical Outcomes in Malignant Peripheral Nerve Sheath Tumors (MPNST)

Kristina Wakeman[1], Robert Ricciotti[2], Jose Mantilla[2]
[1]University of Washington-Seattle, Seattle, WA, [2]University of Washington, Seattle, WA

Disclosures: Kristina Wakeman: None; Robert Ricciotti: None; Jose Mantilla: None

Background: Malignant peripheral nerve sheath tumors (MPNST) may occur sporadically, in the setting of neurofibromatosis-1 (NF1), or in association with radiation exposure. In clinical practice, predictive factors and histologic grading criteria for MPNST have not been universally accepted. In this study we evaluate a cohort of patients with MPNST and correlate histologic tumor grade as well as other parameters with clinical outcomes.

Design: We searched our institutional pathology archives for tumors diagnosed as MPNST between 1990 and 2018. All available histologic slides were reviewed and tumors were graded using the Fédération Nationale des Centres de Lutte Contre Le Cancer (FNCLCC) criteria. Demographic characteristics, clinical history, and outcomes, including death of disease, local recurrence and metastasis, were recorded.

Results: We reviewed 90 examples of MPNST. Patients included 50 men and 40 women, with age ranging from 10 to 84 years (mean 45 years). Mean length of follow-up was 34 months (range 0-200). 48 cases were sporadic (53%), 34 occurred in the setting of NF1 (38%), and 8 were radiation associated (9%). FNCLCC grading resulted in 13 grade 1 (14%), 9 grade 2 (10%), and 68 grade 3 tumors (76%). No patients with grade 1 MPNST died of disease, while 3 with grade 2 (33%) and 30 with grade 3 (44%) died of disease. Metastatic disease was seen in 1 (7.7%) grade 1, 3 (33%) grade 2, and 26 (38%) grade 3 tumors (P=0.053). Local recurrence was seen in 1 grade 1 (7.7%), 2 (22%) grade 2, and 23 (33.8%) tumors (P=0.10). These findings are summarized in Table 1. Log-rank analysis demonstrated a significant difference in overall (P=0.002) and progression free survival (P=0.0007) when comparing all cases of MPNST by FNCLCC grade, as well as when comparing sporadic MPNST by grade (P=0.003) as a separate cohort. In NF1 associated cases, there was a significant difference in progression-free survival between grade 1 and grade 2/3 tumors (P=0.036). We found no significant difference in survival outcome when comparing sporadic, NF-1 associated, and radiation associated MPNST (Figure 1).

	All MPNST	Grade 1	Grade 2	Grade 3	M	F
n	90	13 (14%)	9 (10%)	68 (76%)	50 (56%)	40 (44%)
Recurrence	25 (28%)	1 (7.7%)	2 (22%)	23 (34%)		
Metastasis	30 (33%)	1 (7.7%)	3 (33%)	26 (38%)		
DOD	33 (37%)	0	3 (33%)	30 (44%)		
	Sporadic	**Grade 1**	**Grade 2**	**Grade 3**	**M**	**F**
n	48	9 (19%)	7 (15%)	32 (67%)	26 (54%)	22 (46%)
Recurrence	13 (27%)	0	0	13 (41%)		
Metastasis	18 (38%)	1 (11%)	3 (43%)	14 (44%)		
DOD	14 (29%)	0	2 (29%)	12 (38%)		
	NF-1	**Grade 1**	**Grade 2**	**Grade 3**	**M**	**F**
n	34	3 (8.8%)	1 (2.9%)	30 (88%)	19 (56%)	15 (44%)
Recurrence	14 (41%)	0	0	14 (47%)		
Metastasis	12 (35%)	0	0	12 (40%)		
DOD	16 (47%)	0	0	16 (53%)		
	Radiation	**Grade 1**	**Grade 2**	**Grade 3**	**M**	**F**
n	8	1 (13%)	1 (13%)	6 (75%)	5 (63%)	3 (38%)
Recurrence	1 (12.5%)	1 (100%)	0	0		
Metastasis	0	0	0	0		
DOD	3 (38%)	0	1 (100%)	2 (33%)		

Figure 1 - 99

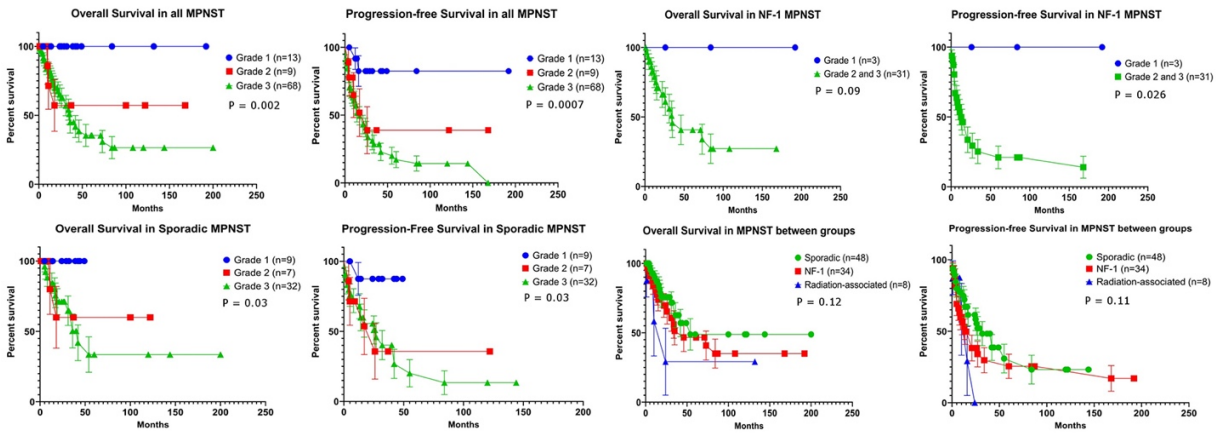

Conclusions: We found a correlation between FNCLCC grade and survival outcomes when comparing all MPNST, as well as within separate cohorts of sporadic and NF1-associated lesions. FNCLCC grading of these tumors may be helpful in the clinical setting to predict biological behavior.

100 Malignant Melanotic Xp11 Neoplasm Exhibit a Clinicopathological Spectrum and Gene Expression Profiling Akin to Alveolar Soft Part Sarcoma, with a Proposal for the Reclassification

Xiaotong Wang[1], Ru Fang[2], Qiuyuan Xia[2], Qiu Rao[3]
[1]Nanjing, Jiangsu, China, [2]Department of Pathology, Jinling Hospital, Nanjing University School of Medicine, Nanjing, Jiangsu, China, [3]Jinling Hospital, Nanjing, Jiangsu, China

Disclosures: Xiaotong Wang: None; Ru Fang: None; Qiuyuan Xia: None; Qiu Rao: None

Background: Recently, a group of distinct mesenchymal neoplasms corresponding to Xp11 translocation RCCs have attracted increasingly attention. The classification of these distinctive neoplasms, first described as "Xp11 translocation PEComa" and for which recently the term "melanotic Xp11 neoplasm" or "Xp11 neoplasm with melanocytic differentiation" has been proposed, remains challenging and controversial. It is limited by overlapping histopathologic features, inconsistent terminology, and uncertain clinical behavior.

Design: We collected 27 cases of melanotic Xp11 neoplasm, the largest series to date, for a comprehensive evaluation. Fourteen of the cases, along with 8 alveolar soft part sarcomas, 9 conventional PEComas, and a control group of 7 normal renal tissues were submitted to RNA sequencing. The gene expression profile data were used for subsequent clustering analysis, combined with previously obtained data from Xp11 translocation RCCs and *PRCC-MITF* RCC.

Results: The distinctive clinical, morphology and immunophenotype were still the clues to the diagnosis of melanotic Xp11 neoplasms. Follow-up available in 22 patients showed 5-year OS and 5-year DFS of 47.6% and 35.7% respectively, which was similar to ASPS, and significantly worse than conventional PEComa. Univariate analysis of location, infiltrative growth pattern, nuclear pleomorphism, mitotic activity ≥ 2/50 HPF, necrosis, and lymphovascular invasion were found to be associated with OS and/or DFS. Multivariate analysis identified that location was the only factor found to independently correlate with DFS. More importantly, RNAseq-based unsupervised clustering analysis segregated melanotic Xp11 neoplasm and ASPS, clearly from other tumor entities including conventional PEComa and Xp11 translocation RCC, and formed a compact cluster representative of the largely similar expression signature.

Figure 1 - 100

A

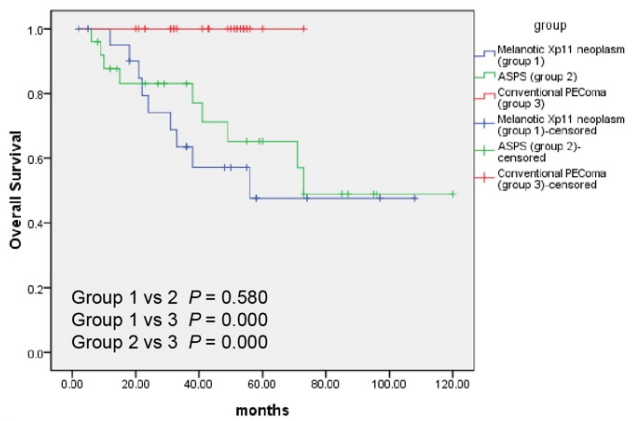

B

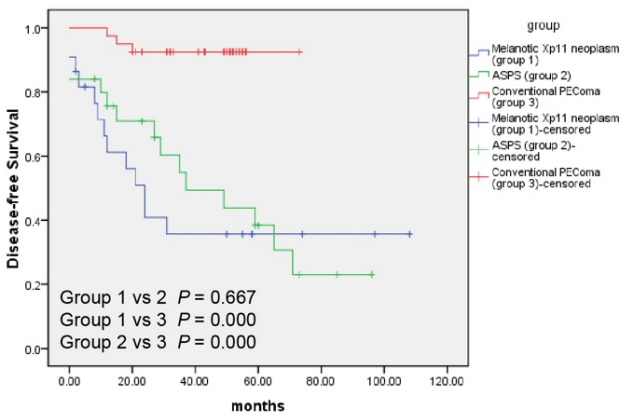

C

	Overall Survival			Disease-free Survival		
	Median survival (month)	3-year survival (%)	5-year survival (%)	Median survival (month)	3-year survival (%)	5-year survival (%)
Melanotic Xp11 neoplasm (n=22)	50	63.5	47.6	24	35.7	35.7
ASPS (n=25)	72	77.3	57.2	37	52.1	30.7
Conventional PEComa (n=40)	-	100	100	-	92.5	92.5

Figure 2 - 100

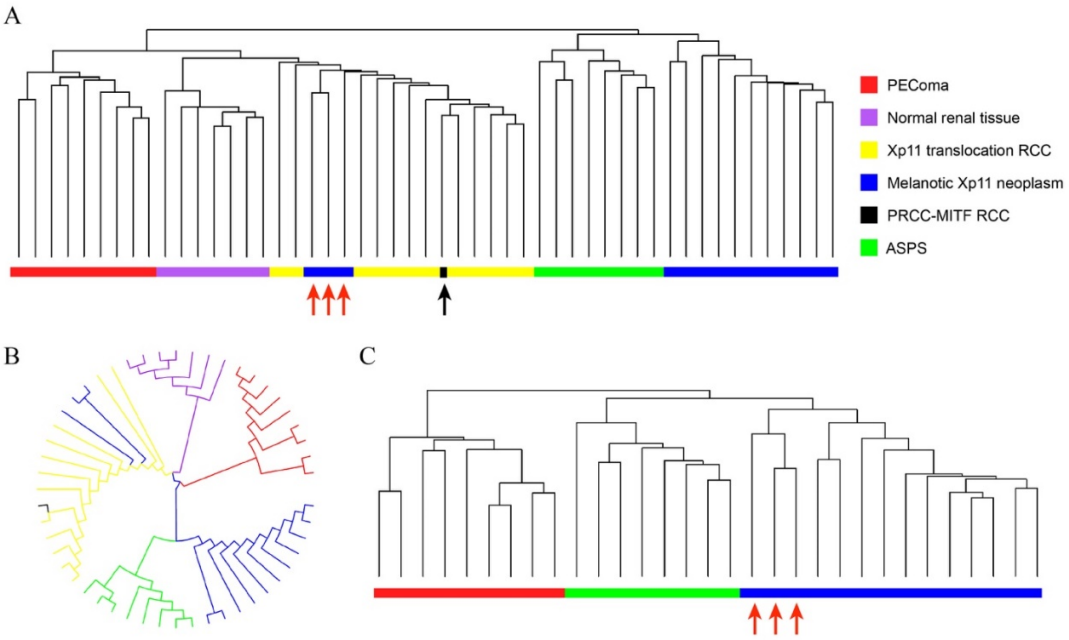

Conclusions: We first clearly define the true biologic nature that melanotic Xp11 neoplasms are distinctive malignant mesenchymal tumor, rather than a simply PEComa variant with occasionally unpredictable behavior. Meanwhile, melanotic Xp11 neoplasm and ASPS more likely represent phenotypic variants of the same entity, which is distinct from conventional PEComa and Xp11 translocation RCC. Based on these important findings, melanotic Xp11 neoplasm can be reclassified into a distinctive entity together with ASPS, independent from PEComa, in the future revisions of the current World Health Organization categories of tumors of soft tissue and bone.

101 Chondroblastoma in Adults: Clinicopathologic Study of 14 Cases

Sintawat Wangsiricharoen[1], Stefano Negri[1], Edward Mccarthy[2], Aaron James[1]
[1]Johns Hopkins University School of Medicine, Baltimore, MD, [2]Baltimore, MD

Disclosures: Sintawat Wangsiricharoen: None; Stefano Negri: None; Edward Mccarthy: None; Aaron James: None

Background: Chondroblastoma is a rare benign tumor of immature cartilage cells that generally occurs in an epiphyseal location of skeletally immature individuals. They are most commonly diagnosed in the second decade of life; however, a few studies have reported cases in older patients. The purpose of this study was to evaluate the clinical and pathologic features of chondroblastoma in adults.

Design: The pathology archives of our institution were searched for chondroblastoma in patients ≥ 25 years of age. Hematoxylin and eosin slides were reviewed. Clinical information was obtained.

Results: Of the 14 patients, eight were male and six were female with a median age of 34 years (range 29-54 years). Most lesions occurred in short bones of hands and feet (N=7, 50%: 3 calcaneus, 2 phalanx, 1 metacarpal, 1 cuboid), followed by long tubular bones (N=4, 28%: 2 fibula, 1 femur, 1 humerus), flat bones (N=2, 14%: 1 scapula, 1 rib), and vertebra (N=1, 7%: thoracic). All were composed of chondroblasts associated with chondroid matrix. Osteoclast-like giant cells were present in all cases, but sparse in three cases. Twelve cases (86%) had calcifications in various patterns, including chicken wire, serpiginous, punctate, and nodular patterns. Six (43%) showed focal to extensive necrosis. Secondary aneurysmal bone cyst formation and hemosiderin deposition were identified in approximately half of the cases. One case (7%) showed mitotic activity without atypical mitosis (7/10 HPFs). Some overlapping histologic features of chondromyxoid fibroma were seen in two cases (14%). One case (7%) demonstrated a pulmonary edema-like pattern. Other features include woven bone formation (14%), foamy macrophages (14%), hyalinized vascular spaces (14%), mature hyaline cartilage formation (35%), cortical breakthrough (14%), soft tissue invasion (14%), and spindle cell changes (21%). At follow-up (N=12, median 73.5 months, range 1-278 months), two patients (16%, thoracic vertebra and calcaneus) had a local recurrence. None had metastasis.

Conclusions: Chondroblastoma in adults tends to involve the short bones of hands and feet more than the long tubular bones. More extensive calcification may be seen over and beyond typical ‘chicken wire’ calcification. Some demonstrate features associated with degenerative changes and necrosis, implying this may be a longstanding process. Finally, tumors involving the vertebrae and the short bones of hands and feet may behave more aggressively than those in the long tubular bones.

102 INSM1 Can Be Expressed in Angiosarcoma

Laura Warmke[1], Emma Tinkham[2], Davis Ingram[3], Alexander Lazar[1], Gauri Panse[4], Wei-Lien Billy Wang[1]
[1]The University of Texas MD Anderson Cancer Center, Houston, TX, [2]Department of Translational Molecular Pathology, UT MD Anderson Cancer Center, Houston, TX, [3]Houston, TX, [4]Yale University, New Haven, CT

Disclosures: Laura Warmke: None; Emma Tinkham: None; Davis Ingram: None; Alexander Lazar: None; Gauri Panse: None; Wei-Lien Billy Wang: None

Background: Insulin-associated protein 1 (INSM1) is a zinc-finger transcription factor important in neuroendocrine differentiation and employed as a specific immunohistochemical marker for neuroendocrine carcinoma, including small cell lung carcinoma (SCLC). Neuroendocrine expression has also been described in mesenchymal tumors including some vascular tumors. We investigated INSM1 expression in a large series of angiosarcomas and also surveyed a variety of other sarcomas including those with round cell morphology which can overlap with SCLC.

Design: Unstained slides were prepared from tissue microarrays constructed from formalin-fixed paraffin-embedded tissue of angiosarcoma (n = 149), Ewing sarcoma (n = 148), DSRCT (n = 63), clear cell sarcoma (n = 17), synovial sarcoma (n = 192), soft tissue leiomyosarcoma (n = 66), uterine leiomyosarcoma (n = 65), alveolar soft part sarcoma (n = 31), epithelioid sarcoma (n = 35), and UPS (n = 107). Immunohistochemical study was performed with an anti-INSM1 antibody (clone A8, Santa Cruz Biotechnology) using a Leica Bond autostainer (Leica Biosystems, Buffalo Grove, IL). Labeling was examined for extent (percentage of tumoral nuclear labeling) and intensity (weak, moderate or strong). Any tumoral labeling was considered to be positive. Diffuse labeling was defined as >50%, while focal <10%.

Results: INSM1 expression was seen in a subset of analyzable angiosarcomas (n=27/122; 22%), the majority (n=18) with diffuse tumoral labeling and predominantly weak to moderate intensity. Focal INSM1 was also detected in DRSCT (n=7/62, 11%) and synovial sarcoma (n=3/176, 2%). None of analyzable Ewing sarcoma (n=131), clear cell sarcoma (n=14), epithelioid sarcoma (n=30), soft tissue leiomyosarcoma (n=59), uterine leimyosarcoma (n=65), alveolar soft part sarcoma (n=29), and UPS (n=100) showed expression for INSM1.

Conclusions: Angiosarcomas can occasionally express INSM1, sometimes diffusely. Given that these tumors can also express keratins, this could be a potential diagnostic pitfall particularly in solid areas and small biopsies. In addition, INSM1 was found to be expressed in a small subset of sarcomas including desmoplastic small round cell tumor and synovial sarcoma, both of which can harbor round cell morphology and overlap with small cell lung carcinoma. However, expression was only focal in these tumors in contrast to SCLC. The significance of INSM1 expression in these tumors needs to be further investigated.

103 SATB2 Expression in Undifferentiated Sarcomas of Bone

Laura Warmke[1], Alexander Lazar[1], Wei-Lien Billy Wang[1]
[1]The University of Texas MD Anderson Cancer Center, Houston, TX

Disclosures: Laura Warmke: None; Alexander Lazar: None; Wei-Lien Billy Wang: None

Background: Undifferentiated sarcomas of bone are rare. Some theorize these may be osteosarcomas with minimal osteoid formation. SATB2 (SATB Homeobox 2) is a DNA binding protein involved in regulating transcription and chromatin remodeling and has been suggested to be a marker of osteogenic differentiation. We investigated the prevalence of SATB2 and significance of expression in undifferentiated primary bone tumors. For comparison, we also examined the prevalence of SATB2 expression in soft tissue undifferentiated plemorphic sarcomas.

Design: Pathology archives (2014-2018) were examined for undifferentiated sarcomas involving bone with no evidence of osteoid. Unstained slides were prepared and immunohistochemical study was performed using an anti-SATB2 (1:50, clone CL0276, Sigma Prestige) with autostainer. Slides were evaluated for extent. Any labeling was considered positive. Clinical follow-up was obtained. For comparison, unstained slides were prepared from a tissue microarray consisting of 46 formalin-fixed paraffin-embedded primary soft tissue undifferentiated pleomorphic sarcomas and stained with SATB2.

Results: Sixteen cases primary undifferentiated bone sarcomas were identified. The median age was 43 years (range:16-83) with slight female predominance (7M:9F). Sites involved include pelvis (5), femur (4), skull (3), tibia (2), and scapula (2). SATB2 expression was seen in 10/16 cases (63%), with three focal. The median follow up was 16.5 months (range:6-57). At last follow up, n=10 alive and well(AW), n=2 alive with disease(AWD) and n=4 dead of disease(DOD). All patients AW or DOD had metastases. 3/10 patients with tumors with SATB2 DOD, while 1/6 patients without SATB2 DOD. 5/46 (11%) primary soft tissue undifferentiated plemorphic sarcomas exhibited any SATB2 labeling (2 localized to giant cells only.)

Conclusions: SATB2 expression can be seen in undifferentiated sarcomas of bone without evident osteoid production and was found at a higher prevalence than primary undifferentiated plemorphic sarcoma of soft tissue. Regardless of SATB2 status, undifferentiated pleomorphic sarcomas of bone can metastasize and be aggressive. Additional studies to further expand this series are on-going to better understand if tumors with SATB2 behave more aggressively than those without.

104 SWI/SNF Family Protein Expression and Myoepithelial Phenotype in Breast Carcinomas with Rhabdoid Morphology

Jin Xu[1], Paul Weisman[2], William Rehrauer[3], Molly Accola[4], Kristen Karasiewicz[1], Rebecca Baus[5], Stephanie McGregor[2], Darya Buehler[6]
[1]University of Wisconsin-Madison, Madison, WI, [2]University of Wisconsin, Madison, WI, [3]University of Wisconsin School of Medicine and Public Health, Madison, WI, [4]University of Wisconsin Hospital, Madison, WI, [5]Madison, WI, [6]University of Wisconsin, Madison, Madison, WI

Disclosures: Jin Xu: None; Paul Weisman: None; William Rehrauer: None; Molly Accola: None; Kristen Karasiewicz: None; Rebecca Baus: None; Stephanie McGregor: None; Darya Buehler: None

Background: In addition to adult and pediatric sarcomas, SWI/SNF (SWItch/Sucrose Non-Fermentable) deficiency is being reported in an increasing number of adult carcinomas. Common features include rhabdoid/plasmacytoid morphology, an aggressive clinical course, loss of expression of site-specific markers or acquisition of a myoepithelial phenotype. Both pleomorphic lobular carcinomas (PLC) of the breast and matrix-producing metaplastic breast carcinomas (MPMBC) exhibit many of the above features. Despite these similarities to SWI/SNF-deficient tumors, to the best of our knowledge, SWI/SNF protein expression has not been specifically investigated in PLC or MPMBC. In addition, even though MPMBC show myoepithelial features by immunohistochemistry (IHC), the molecular basis for this phenotype and its relationship to primary fusion-associated myoepithelial tumors remain poorly understood.

Design: Thirty breast carcinomas with rhabdoid features (19 invasive PLC, 5 PLC in situ and 6 MPMBC) were stained with IHC for SWI/SNF family proteins: SMARCB1, SMARCA4 and other SWI/SNF family proteins implicated in breast cancer pathogenesis including ARID1A, ARID1B, ARID2, SMARCD1, PBRM1 and SMARCD3. Loss of expression was defined as no nuclear expression in the setting of retained nuclear expression in the internal normal controls. Myoepithelial differentiation was evaluated by IHC for SOX10, SMA and p40. Gene fusions were probed by targeted RNA-based next generation sequencing (NGS) using Archer FusionPlex® Sarcoma Panel according to the kit-specific protocol. Illumina® specific adapters were used and NGS was performed on the Illumina® MiSeq.

Results: At least one myoepithelial marker was positive in all 6 cases of MPMBC: SOX10(5/6); SMA(2/6); p40(0/6); 1/6 cases co-expressed more than one marker. None of these six cases demonstrated *EWSR*, *FUS*, *PLAG1, HMGA2* or other gene fusions reported in primary myoepithelial tumors. None of the 19 PLC or 5 PLC in situ cases showed myoepithelial marker positivity. All eight SWI/SNF family proteins showed retained nuclear expression by IHC in all 30 cases.

Conclusions: The means by which breast carcinomas acquire rhabdoid morphology appears to involve mechanisms other than SWI/SNF deficiency. In the MPMBC subset, rhabdoid morphology could be explained by the myoepithelial immunophenotype but not by gene fusions commonly reported in primary myoepithelial tumors.

105 Integrated Bioinformatics Analyses Identify a Novel HDGF/ALCAM/GTPases Axis in Metastasis of Ewing Sarcoma

Yang Yang[1], Anjia Han[1]
[1]Guangzhou, Guangdong, China

Disclosures: Yang Yang: None; Yang Yang: None

Background: Metastatic spread is the most powerful predictor of poor outcome in Ewing sarcoma (ES), but the specific molecular mechanisms underlying ES metastasis have not been fully elucidated. The transcription factor hepatoma-derived growth factor (HDGF) regulates ES growth and its expression in tumor predicts poor prognosis in ES patients. However, whether and how HDGF is involved in ES metastasis remain largely unknown.

Design: HDGF ChIP-seq was performed in human ES cell line RD-ES, while gene expression profiling was performed in HDGF-silenced RD-ES cells. Immunofluorescence staining, cell adhesion assay, scratch assay, transwell migration and invasion assays, as well as *in vivo* tumor metastasis assay were employed to test the metastasis-related functions of ES cell lines RD-ES and A673 with over-expression or silencing of target genes.

Results: In this study, we confirmed the putative pro-metastatic function of HDGF in ES in vitro and in vivo, and further demonstrated in human ES samples that high HDGF expression levels correlated significantly with poor metastasis-free survival. Based on the ChIP-seq data and our previous GEP data, we identified a genome-wide binding signature for HDGF, comprehensively dissected the spectrum of HDGF-regulated genes and pathways in ES cells, and validated the regulation of HDGF on some metastasis-associated genes, including activated leukocyte cell adhesion molecule (ALCAM, also known as CD166). Our data demonstrated that ALCAM played a metastasis-suppressor role in ES probably through decreasing the expression and activity of small G proteins Rac1 and Cdc42. Notably, we showed that ALCAM was a critical downstream effector of HDGF and ALCAM inhibition was indispensable for HDGF-driven migration and invasion of ES cells in vitro.

Conclusions: Our study establishes a novel link between HDGF overexpression and ALCAM inhibition in the ES pathogenesis. To our knowledge, this is the first report demonstrating the role of ALCAM as a metastasis suppressor in the context of ES. More importantly, we demonstrated that ALCAM signaling was directly repressed by HDGF, and suppression of ALCAM was functionally required for HDGF-driven cell migration and invasion. Therefore, we propose that targeting of the HDGF/ALCAM/GTPases axis may represent a potentially effective strategy in anti-metastasis therapy for ES patients.

106 TERT Rearrangements are Present in a Subset of Chordomas

Ju-Yoon Yoon[1], Mitul Modi[2], Sharon Song[3], Raghunath Puthiyaveettil[3], John Brooks[4], Chase Rushton[3], Christopher Orr[3], Jason Rosenbaum[5], Paul Zhang[6]
[1]Perelman School of Medicine at the University of Pennsylvania, Philadelphia, PA, [2]Pennsylvania Hospital of University of Pennsylvania Health System, Philadelphia, PA, [3]Hospital of the University of Pennsylvania, Philadelphia, PA, [4]University of Pennsylvania Perelman School of Medicine, Swarthmore, PA, [5]UPenn, Center for Personalized Diagnostics, Philadelphia, PA, [6]Hospital of the University of Pennsylvania, Media, PA

Disclosures: Ju-Yoon Yoon: None; Mitul Modi: None; Sharon Song: None; Raghunath Puthiyaveettil: None; John Brooks: None; Christopher Orr: None; Jason Rosenbaum: None; Paul Zhang: None

Background: Chordomas are rare, slow-growing neoplasms thought to arise from the fetal notochord remnant. A limited number of studies that examined the mutational profiles in chordomas identified potential driver mutations, including duplication in the *TBXT* gene (encoding brachyury), mutations in the PI3K/Akt signaling pathway, and loss of *CDKN2A*. Most chordomas remain without clear driver mutations, and no fusion genes have been identified thus far.

Design: 7 cases of chordomas underwent targeted sequencing of cancer-related genes for single nucleotide variants (SNVs) and insertions/deletions (indels), with 4/7 cases examined with a laboratory-developed 152-gene panel. A custom fusion transcript panel examining 55 fusion partners was performed on 2 cases. Fluorescent in-situ hybridization (FISH) for *TERT* rearrangements using break-apart *TERT* probes was performed on 5 cases.

Results: 1/2 cases examined for gene fusions harbored an in-frame fusion transcript involving *RPH3AL* (exon 5) and *TERT* (exon 2), and the transcript-positive case was also positive for *TERT* rearrangement by FISH. 4 additional chordomas were examined by FISH, with *TERT* rearrangement present in 1 case for which the fusion panel was not done (total of 2/5 FISH-positive cases). The number of disease-associated SNVs and indels was limited, but variants in a number of tumor suppressor genes were identified, including *ARID2*, *PBRM1*, *TSC2*, and *VHL*. Alterations in *IGF1R* and *MTOR* were also found.

Conclusions: In accord with previous studies, the mutational spectrum of chordomas is limited, with driver mutations generally absent. However, we identified a case with a novel TERT fusion transcript, and TERT rearrangement was present in 2/5 cases by FISH. Additional studies are underway to better examine the frequency of TERT rearrangement in chordomas and to examine clinico-pathological features of those cases.

107 Myoepithelioma-like Tumor of the Vulvar Region: A Clinicopathological Study of 14 Additional Cases Supporting a Distinctive Group of SMARCB1（INI-1）Deficient Neoplasms

Lin Yu[1], I Weng Lao[1], Meng Sun[2], Jian Wang[1]
[1]Department of Pathology, Fudan University Shanghai Cancer Center, Fudan University, Shanghai, China, [2]Fudan University Shanghai Cancer Center, Fudan University, Shanghai, China

Disclosures: Lin Yu: None; Meng Sun: None

Background: Myoepithelioma-like tumor of the vulvar region (MELTVR) recently has been proposed as a rare mesenchymal neoplasm of the vulvar area. We describe an additional series of 14 cases of MELTVR in order to enhance the recognition of this emerging novel group of SMARCB1（INI-1）deficient neoplasms.

Design: The clinicopathological data of 14 cases of MELTVR were collected; morphological observation, immunohistochemical staining and interphase fluorescence in situ hybridization (FISH) were performed, and the literatures were also reviewed.

Results: The tumors all occurred in the subcutis of the vulva and surrounding regions of adult women aged 26 to 54 years, with a mean and median age of 39.6 and 40 years, respectively. Preoperative duration ranged from 2 months to 3 years. Clinically, 12 tumors presented as a slowly growing painless mass, and 2 tumors were detected accidentally. The tumor size ranged from 1 to 8cm (mean, 3.2cm). Histologically, the tumor was well circumscribed, focally encapsulated, and lobulated by incomplete fibrous septa. The tumor was mainly composed of hypocellular myxoid areas and hypercellular non-myxoid areas, with relatively abundant vascular networks in the stroma. In myxoid areas, tumor cells grew singly or in a loosely reticular manner with cords, chains, or clusters. In the non-myxoid region, tumor cells were arranged in diffuse sheets, fascicular or storiform pattern. The tumor cells were epithelioid to spindle shaped, with fine amphophilic

cytoplasm, and relatively uniform nuclei with vesicular chromatin and prominent nucleoli. The mitotic figures were rare. Immunohistochemically, the positive rates of AE1/AE3, EMA, calponin, ER and PR were 85.7% (12/14), 80% (8/10), 100% (14/14), 90.9% (10/11) and 75% (9/12), respectively. 4 cases expressed SMA (28.6%, 4/14). S-100 protein, SOX10, P63, GFAP and CD34 were all negative. SMARCB1(INI-1) expression was deficient in all cases. Ki-67 proliferation index is 5 ~ 40% (mean, 25%). 5 cases

Figure 1 - 107

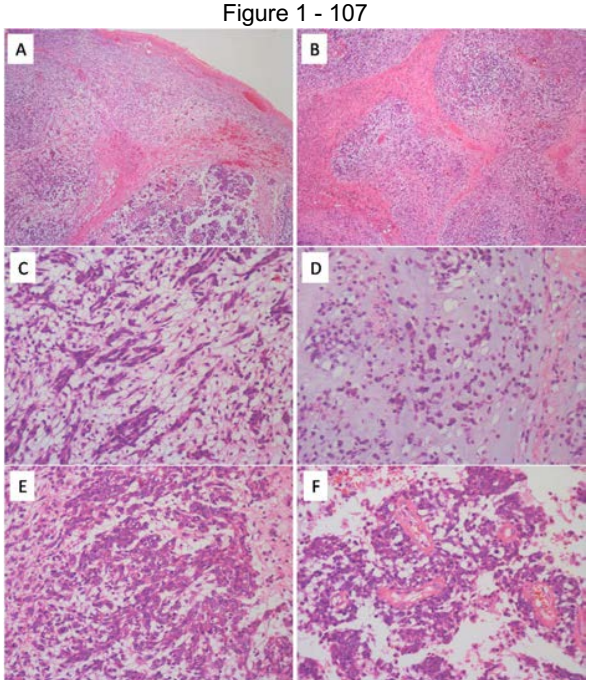

Figure 2 - 107

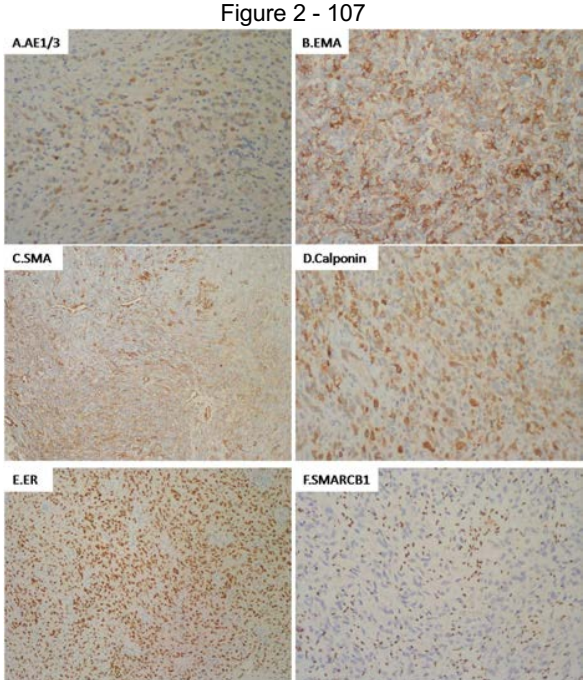

Conclusions: Myoepithelioma-like tumor of the vulvar region represents a new member of the family of SMARCB1 (INI-1) deficient neoplasms. It shows unique clinical presentation, characteristic histology and distinguishing immunoprofile which do not fit perfectly into soft tissue myoepithelioma. MELTVR may follow an indolent clinical course, and a few cases can develop local recurrence. Familiarity with its clinicopathological characteristics is helpful in avoiding confusion with a variety of vulval mesenchymal tumours with overlapping features.

108 A Next-Generation Sequencing Study of Seven Primary Central Chondrosarcomas in the Pediatric Population Showed Recurrent IDH Mutations and a Novel EWSR1-SMAD3 Fusion

Lingxin Zhang[1], Gord Guo Zhu[2], Khedoudja Nafa[1], Abhinita Mohanty[1], Satshil Rana[3], John Healey[1], Nicola Fabbri[1], Meera Hameed[1]

[1]Memorial Sloan Kettering Cancer Center, New York, NY, [2]Cooper University Hospital, Camden, NJ, [3]Memorial Sloan Kettering Cancer Center, New York City, NY

Disclosures: Lingxin Zhang: None; Gord Guo Zhu: None; Khedoudja Nafa: *Speaker*, Biocartis; Abhinita Mohanty: None; Satshil Rana: None; John Healey: None; Nicola Fabbri: *Speaker*, Onkos Surgical; *Consultant*, Onkos Surgical; Meera Hameed: None

Background: Primary central chondrosarcoma mostly affects older adults (peak age in the 5th to 7th decades of life) and *IDH1/2* mutations are the most common genetic alteration. The occurrence of chondrosarcoma in patients 16 years or younger is rare. There has not been a systemic study to analyze the genetic alteration profile of primary central chondrosarcomas in this young age group.

Design: A search for primary central chondrosarcoma diagnosed from 2001 to 2018 in patients 16 years old and younger was performed. After the diagnoses were confirmed by histologic review, suitable material was submitted for next-generation sequencing (NGS) analysis using a hybridization capture-based large panel NGS assay.

Results: Seven patients diagnosed with primary central chondrosarcomas between 10 and 16 years old were identified. Six chondrosarcomas were located in the diaphysis, metaphysis and epiphysis of long bones while one case occurred in the pelvis with extensive bone destruction and extraosseous extension (see Table). One patient had biopsy-proven lymph node metastasis. Analysis of the genomic data from the seven cases showed mutations in *IDH1* (p.R132) and *IDH2* (p.R172) in four cases, all of which arose in the diaphysis of long bones. Two cases showed *IDH1* p.R132H, one case showed *IDH1* p.R132C, and one case showed *IDH2* p.R172G

mutation. In one of the three cases without *IDH1/2* mutation, a novel *EWSR1-SMAD3* fusion was detected by NGS and further confirmed by targeted RNA sequencing analysis. The same fusion has been previously reported in superficial acral fibroblastic tumor.

Case No.	Age/ gender	Tumor location	Pathologic Diagnosis	Genetic findings	Treatment	Follow up
1	11/M	Humerus, metaphysis	Chondrosarcoma, grade II	No *IDH1/2* mutation	Curettage, then en bloc resection	Recurrence and LN metastasis s/p surgical resection, DF at 180 mo
2	10/M	Humerus, diaphysis	Chondrosarcoma, WHO grade I	*IDH1* p.R132C	Curettage	DF at 63 mo
3	10/M	Femur, diaphysis	Chondrosarcoma, WHO grade I-II	*IDH1* p.R132H	En bloc resection	DF at 52 mo
4	14/M	Tibia, diaphysis	Chondrosarcoma, WHO grade I	*IDH2* p.R172G	Curettage and ablation	DF at 47 mo
5	14/F	Humerus, epiphysis	Chondrosarcoma, WHO grade I-II	No *IDH1/2* mutation	Curettage and ablation	DF at 20 mo
6	13/F	Femur, diaphysis	Chondrosarcoma, WHO grade I-II	*IDH1* p.R132H	Curettage and ablation	Pulmonary nodules on surveillance (not biopsied), no recurrence at 16 mo
7	16/M	Pelvis	Chondrosarcoma, WHO grade I	No *IDH1/2* mutation; *EWSR1-SMAD3* fusion (in-frame)	En bloc resection	DF at 8 mo

Abbreviations: DF – disease free; mo – months; s/p – status post

Conclusions: *IDH1/2* hot spot mutations were found in four of seven primary central chondrosarcomas in young patients. The finding mirrors the genetic alteration profile in central chondrosarcomas of adulthood. A novel *EWSR1-SMAD3* fusion was identified in a chondrosarcoma arising in the pelvis, suggesting that an alternative pathogenetic mechanism exists.

109 Superficial CD34-Positive Fibroblastic Tumor: Reporting Five Cases of a Newly Described and Potentially Underrecognized Mesenchymal Neoplasm with Molecular Analyses of PRDM10 Rearrangement and MGEA5-TGFBR3 Fusion

Ming Zhao[1], Jianguo Wei[2], Xianglei He[3]
[1]Hangzhou, Zhejiang, China, [2]Department of Pathology, Shaoxing People's Hospital, Shaoxing, Zhejiang, China, [3]Department of Pathology, Zhejiang Provincial People's Hospital, People's Hospital of Hangzhou Medical College, Hangzhou, Zhejiang, China

Disclosures: Ming Zhao: None

Background: Superficial CD34-positive fibroblastic tumor (SCD34FT) is a rare and newly identified mesenchymal neoplasm which often cause significant diagnostic challenges. Most recently, a novel *PRDM10* rearrangement was identified in a subset of low-grade undifferentiated pleomorphic sarcoma (UPS) which exhibits morphologic spectrum overlapping with SCD34FT. However, the underlying molecular mechanism of SCD34FT is largely unknown and the genetic relationships of SCD34FT to UPS and myxoinflammatory fibroblastic sarcoma(MIFS), are undetermined.

Design: We described 5 additional cases of SCD34FT. Paraffin-embedded blocks and slides were retrieved from the files of the authors. Immunohistochemistry was performed using the EnVision method, and all cases were studied by fluorescence in-situ hybridization (FISH) for *PRDM10* rearrangement and *MGEA5-TGFBR3* fusion.

Results: There were three male and two female patients (age range: 30 to 60years). The tumors were located in thigh (3 cases) and button(2 cases) and were subcutaneous-based in 4 cases and dermal-based in 1 case. Tumor size ranged from 1.5 to 5.8 cm (mean: 3.4 cm). The tumor cells were spindled to epithelioid with abundant eosinophilic often granular cytoplasm and displayed marked nuclear pleomorphism with hyperchromasia and multiple large inclusion-like nucleoli as well as cytoplasmic nuclear pseudoinclusions. Xanthomatous foamy tumor cells are commonly seen, and mixed inflammation is often present. Mitotic figures were very rare. By immunohistochemistry, all tumors showed strong and diffuse CD34 positivity. All lacked expression of cytokeratin, EMA, S100 protein, desmin, SMA and ERG proteins and showed retained expression of INI-1. The Ki67-labeling index was extremely low. By FISH analysis, 3 of the 5 cases (60%) showed *PRDM10* rearrangement and none demonstrated *MGEA5-TGFBR3* fusion. There were no clinicopatholigc differences between the *PRDM10*-rearrangement positive and negative cases. There were no recurrences or metastases reported in all the 5 patients with follow-up (range: 2-46mo).

Conclusions: SCD34FT is characterized by pleomorphic morphology and a low mitotic count, as well as CD34 positivity. Clinical features of this small series suggest an indolent behavior of SCD34FT. Despite small series, *PRDM10* rearrangement was present in 60% of the tumors suggesting demonstration of this rearrangement may help for its diagnosis and differential diagnosis. Negative for *MGEA5-TGFBR3* fusion supports no genetic relationship to MIFS.